UNIVERSITY OF PISA

MSc THESIS IN NUCLEAR ENGINEERING

NUCLEAR PLANT HIGH ENERGY PIPING:
PIPE BREAK AND PIPE WHIP RESTRAINT DESIGN AND VERIFICATION METHODOLOGICAL APPROACH

CANDIDATE

Lorenzo CAMPINOTI

SUPERVISORS

Prof. Donato AQUARO

Dott.ssa Rosa LO FRANO

Ing. Eugenio RIVARA

Summary

Restraints design is conceived in order to protect structures, systems and components from the anticipated rupture and whipping phenomena of high energy lines in nuclear power plants and guarantee the safe shutdown itself. It is therefore compelling for the plant safety to investigate these topics accurately. Various research programs have been conducted in many countries to develop analytical methods and to verify the validity of these methods.

The reference regulation is the ANSI/ANS-58.2, which deals with postulated rupture locations and configurations, protection requirements and evaluation of consequences.

First part of this work will cope with the regulation following those main steps of High Energy Pipe Break (HEPB) analysis to restraint design. A nonlinear dynamic Finite Element Analysis (FEA) is then conducted using ANSYS-LS DYNA program in order to simulate the smashing of a whipping pipe against its own restraint. Break locations will be identified, the thrust force will be computed, plastic hinge formation evaluated, stress-strain curve outlined.

The task reproduces two JAERI tests performed between 1979 and 1982 under BWR LOCA conditions for a 6” and 4” pipe.

Modelling High Energy Pipe Break phenomena covers deep accuracy in sizing components and structures involved; their stiffness and mass, thicknesses and mostly material properties. The study analyzes different material behaviours under impact starting from ANS 58.2 recommendations, and furtherly exploiting different properties embedded within ANSYS LS-DYNA.

The other important aspect is that of inputting to the Code a well-defined thrust force trend; this has been done following the regulations and later on with a transient blowdown analysis using RELAP5 Code.

A procedure to deal with HEPB phenomena has been built and tested and has been practiced for a real case analysis.

Table of Contents

List of Figures

List of Tables

Chapter I: Postulated Pipe Rupture

NOMENCLATURE

HEPB	High Energy Pipe Break
ANS	American Nuclear Society
D	Pipe Diameter
LBB	Leak Before Break
ASME	American Society of Mechanical Engineers
S_m	Allowable Stress-Intensity Value as specified in Sec. III of the ASME BPV Code
U	Cumulative Usage Factor as specified in Sec. III of the ASME BPV Code
S_h	Stress Calculated by the rules of NC-3600 and ND-3600 for Class 2 and 3 Components, respectively, of the ASME Code, Section III
S_A	Allowable stress range for expansion stress calculated by the rules of NC-3600 of the ASME Code, Sec. III
SSC	Safety-Related Systems and Components
NRC	Nuclear Regulatory Commission
BTP	Branch Technical Position
GDC	General Design Criterion
CFR	Code of Federal Regulation
SSE	Safe Shutdown Earthquake
A_f	Break Flow Area
ANSI	American National Standard Institute

I.1 Introduction

The pipe whip assessment belongs to HEPB phenomena; present Chapter deals with this kind of argument, which is properly treated in ANSI/ANS-58.2-1988 [Ref. 2]. The reference legislation examine those three main steps of pipe rupture practical implementation, which are:

- Postulation of pipe rupture locations;
- Assessment of break consequences;
- Providing of safety measures.

Main concepts and fundamental criteria are introduced in this Chapter: distinction between high and moderate energy piping is made; ruptures configurations, locations and characterization are outlined together with the main consequences and those countermeasures necessary for safety purposes.

I.2 High and Moderate Energy Piping

As stated in ANS Standard 58.2: *"Postulated pipe ruptures shall be considered in all plant piping systems and the associated potential for damage to required systems and components evaluated on the basis of the energy in the system."*

Piping systems are thus classified as high energy or moderate energy fluid systems.

A high energy fluid system is a fluid system that, during normal plant conditions, is either in operation or maintained pressurized under conditions where either or both of the following are met:

- Maximum operating temperature exceeds 95°C (200 ° F);
- Maximum operating pressure exceeds 1900 kPa (275 psig).

A moderate energy fluid system is a fluid system that, during normal plant conditions, is either in operation or maintained pressurized under conditions where both of the following are met:

- Maximum operating temperature is 95°C (200 ° F) or less;
- Maximum operating pressure is 1900 kPa (275 psig) or less.

Normal Plant Conditions are those plant operating conditions during reactor startup, operation at power, hot standby, or reactor cooldown to cold shutdown conditions.

I.3 Ruptures Configurations

Still according to ANS standard 58.2 [Ref. 2] we know that: "*[...]postulated ruptures shall be classified as circumferential breaks, longitudinal breaks, leakage cracks, or through-wall cracks. Each postulated rupture shall be considered separately as a single postulated initiating event.*"

In more detail:

- Circumferential breaks result in pipe severance with full separation of the two pipe ends;
- Longitudinal breaks result in a split of the pipe wall along the pipe longitudinal axis, but without severance. The break has to be circular in shape or elliptical (2DxD/2) with its long axis parallel to the pipe axis;
- Leakage cracks are assumed to be crack through the pipe wall where the size of the crack and the corresponding flow rate are determined by analysis (LBB) and a leak detection system;
- Through-wall cracks are assumed to be circular orifices through the pipe wall of cross sectional area equal to the product of one half the pipe inside diameter and one half the pipe wall thickness.

A detailed description of each rupture is reported in Sec. I.5.

I.4 Ruptures Locations

It is paramount to distinguish between breaks and cracks. Each postulated break will be evaluated to determine the effect of pipe whip and blowdown jet forces on all equipment and structures essential for a safe shutdown, and on the containment vessel; each postulated crack will be evaluated to determine the environmental effects on equipment essential for a safe shutdown (as reported in Section I.6).

Wherever these pipe break and crack effects may impair the required function of essential equipment, structures, or the containment, protection will be provided to assure proper function (see Section I.7).

I.4.1 Pipe breaks locations

Pipe breaks are postulated to occur in high energy piping systems, or portion of systems, in accordance with appropriate criteria reported below:

- For **Class 1 piping** (as defined in ASME Code Sec. III, see Ref. 13), inside and outside of the containment, breaks are postulated to occur at the following locations in each piping or branch run:
  - ❖ At terminal ends of the pressurized portions of the runs, and
  - ❖ At intermediate locations between terminal ends selected by either of the following criteria:
    - i. At each fitting (e.g. elbow, tee, cross, flange, and non-standard fitting), welded attachment, and valve; or
    - ii. At locations where the maximum stress ranges for normal and upset plant conditions and for an operating basis earthquake (OBE) exceed 2.4 S_m, calculated by either Eq. (12) or Eq. (13) in NB-3653 of the ASME Code, Section III, and
    - iii. At locations where the cumulative usage factor U, derived from the piping fatigue analysis, under the loadings associated with OBE and operational plant conditions, exceed 0.1;
    - iv. Where no breaks are required to be postulated by application of the above stress and usage factor criteria, at least two breaks will be postulated at separated locations selected on the basis of highest cumulative usage factor or stress intensity.
- For **Class 2 and 3 piping** (ASME Code Sec. III, see Ref. 13), inside and outside the containment, breaks are postulated to occur at the following locations in each piping or branch run:
  - ❖ At terminal ends of the pressurized portions of the runs, and
  - ❖ At intermediate locations between terminal ends selected by either of the following criteria:
    - i. At each pipe fitting (e.g. , elbow, tee, cross, flange, and non-standard fitting), welded attachment, and valve; or

ii. At each location where the stresses associated with normal and upset plant conditions and an OBE event, calculated by Eq. (9) plus Eq. (10) in NC-3652 of the ASME Code, Section III, exceed 0.8 (1.2 S_h + S_A) but not less than two separated locations chosen on the basis of highest stress. Where the piping consist of a straight run without fittings, welded attachments, or valves, and all stresses are below 0.8 (1.2 S_h + S_A), a minimum of one location chosen on the basis of highest stress.

- For **non-nuclear class piping** (outside the containment) breaks are postulated at the following locations in each piping or branch run:
  - ❖ At terminal ends of the pressurized portion of the run;
  - ❖ At intermediate locations selected by either of the following criteria:
    i. At each pipe fitting, welded attachment, and valve, or
    ii. At each location where the thermal expansion stress exceed 0.8 S_A but at not less than two separated locations chosen on the basis of highest stress. In the case of a straight pipe run without any pipe fittings or welded attachments and stresses below 0.8 S_A, a minimum of one location chosen on the basis of highest stress.

Otherwise in high energy piping at locations that are isolated or physically remote from essential equipment, structures, and the containment, breaks are not postulated. For locations that are marginal, breaks are assumed for the purpose of establishing separation.

Moreover several exclusion criteria are outlined:

- Between the containment penetration and the containment isolation valves, outside and inside the containment.
- Between the isolation valve and the first restraint or group of restraints designed to protect these portions of piping from breaks outboard of the break exclusion area, both outside and inside containment.
- Between the containment penetration and the restraint(s) inside containment designed to protect the penetration with no isolation valve inside containment.

I.4.2 Pipe cracks locations

Through-wall leakage cracks are postulated (in accordance with the criteria below) for moderate energy piping systems outside of the containment that are operated or pressurized during normal plant operation.

Criteria for through wall leakage cracks in moderate energy systems outside the containment are following reported.

- Cracks are not postulated at locations that are isolated or physically remote from essential systems and components.
- Crack are not postulated in pipes of nominal pipe size of 1 in. and less.
- Cracks are not postulated in area in which break in high energy piping is postulated except where a postulated leakage crack results in more limiting environmental conditions than the high energy piping break.
- Cracks are not postulated in ASME Code, Section III, Class II or Class III piping, where the maximum stress range does not exceed 0.4 ($1.2\ S_h + S_A$) and in non-nuclear piping where the thermal expansion stress is less than $0.4\ S_A$.
- Cracks are postulated to occur individually, at locations not excluded above, that result in the maximum effects from fluid spraying and flooding. Only environmental effects that develop from these cracks are considered.
- Crack instead of breaks are postulated in the piping of those fluid systems that qualify as high energy fluid systems for only short operational periods, but qualify as moderate energy fluid systems for the major operational period.

An operational period is considered short if the fraction of time that the system operates within the pressure-temperature conditions specified for high energy fluid systems is less than 2 percent of the time that the system operates as a moderate energy fluid system.

Appendix A reports mentioned ASME equations and a flow-chart for postulation of ruptures in high energy lines.

I.5 Ruptures characterization

I.5.1 Circumferential Breaks

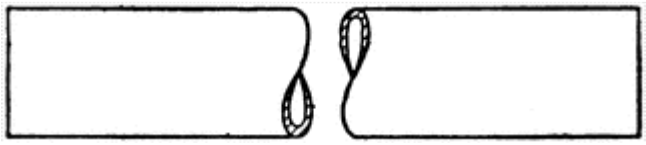

Figure I-1. Circumferential Type Rupture

Figure I-1 reports a circumferential pipe severance. Circumferential breaks are postulated in high energy piping at the locations previously specified except:

1. For nominal pipe sizes of 1 in. and less.
2. Where it is determined by detailed stress analysis that the stress in the circumferential direction is at least 1.5 times that in the axial direction.

Where break locations are selected at pipe fittings without the benefit of stress calculations, breaks are postulated at piping weld to each fitting, valve, or welded attachment. If detailed stress analysis (e.g., finite element analyses) or test are performed, the maximum stressed location in the fitting may be selected instead of the pipe-to-fitting weld.

For purposes of calculating jet impingement forces, circumferential breaks are assumed to result in pipe severance and initial separation amounting to a one-diameter lateral displacement of the ruptured piping sections unless physically limited by piping restraints, structural members, or piping stiffness as may be demonstrated by inelastic analysis; a more detailed description of jet impingement is reported in Section I.6.2.2.

The dynamic force of the jet discharge at the break location is based on the effective cross-sectional flow area of the pipe and on a calculated fluid pressure as modified by an analytically or experimentally determined thrust coefficient. Limited pipe displacement at the break location, line restrictions, flow limiters, positive pump controlled flow, and the absence of energy reservoirs have to be taken into account, as applicable, in the reduction of jet discharge.

Pipe whipping is assumed to occur in the directions defined by the stiffness of the piping configuration and jet reaction forces, unless limited by structural members, piping restraints, or piping stiffness (e.g., a plastic hinge in the piping is not developed under loading).

I.5.2 Longitudinal Breaks

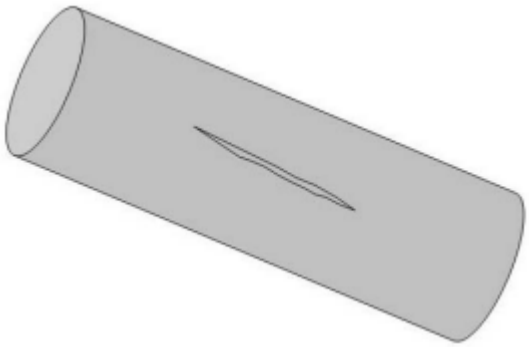

Figure I-2. Longitudinal Type of Break

Figure I-2 reports a longitudinal break. Longitudinal breaks are postulated in high energy piping at the locations previously specified except:

1) For nominal pipe sizes smaller than 4 in.
2) Where it is determined by detailed stress analysis that the stress in the axial direction is at least 1.5 times that in the circumferential direction .
3) At terminal ends.
4) At intermediate locations where the criterion for a minimum number of break locations must be satisfied; except where it is determined by detailed stress analysis that the stress in the circumferential direction is at least 1.5 times that in the axial direction.

Longitudinal breaks are assumed to result in an axial split without pipe severance. Splits are located (but not concurrently) at two diametrically opposed points on the piping circumference such that a jet reaction causing out-of-plane bending of the piping configuration results. Alternately, a single split may be assumed at the section of highest stress as determined by detailed stress analysis, as finite element analysis.

The dynamic force of the fluid jet discharge is based on a circular break area equal to the effective cross-sectional flow area of the pipe at the break location and on a

calculated fluid pressure modified by analytically or experimentally determined thrust coefficient as determined for a circumferential break at the same location. Line restrictions, flow limiters, positive pump controlled flow, and the absence of energy reservoirs are taken into account, as applicable, in the reduction of jet discharge.

Pipe deflection is assumed to occur in the directions defined by the stiffness of the piping configuration and jet reaction forces, unless limited by structural members or pipe restraints.

I.5.3 Through-Wall Leakage Cracks (outside of containment only)

Cracks are postulated in moderate energy piping at the locations previously specified. Fluid flow from a crack is based on a circular opening of area equal to that of a rectangle one-half pipe diameter in length and one half pipe wall thickness in width. The flow from the crack is assumed to result in an environment that wets all unprotected components within the compartment, with consequent flooding in compartment and communicating compartments. Flooding effects are determined on the basis of conservatively estimated time period required to effect corrective actions. Figure I-3 reports a sketch for this kind of rupture.

Figure I-3.Through-Wall Leakage Crack

I.5.4 Leakage Cracks, the LBB Approach

Figure I-4 represent a leakage crack.

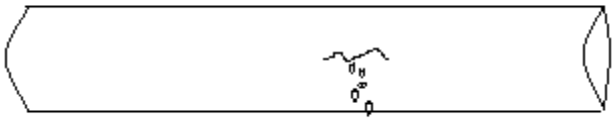

Figure I-4. Leakage Crack

The “leak-before-break” (LBB) or “mechanistic pipe break” methodology may be used on a location-by-location basis to justify postulating a leakage crack instead of a circumferential break, longitudinal break, or through-wall crack at a postulated pipe rupture location; this means not planning to set up a constraint or a jet impingement shield for this specific rupture. In this way, a particular pipe could have both large pipe ruptures postulated at some locations, and leakage cracks justified at other locations. However, application of LBB approach is limited to piping where operating experience, test, or analysis indicate little or no susceptibility to failure from mechanisms such as intergranular stress corrosion cracking, extreme or repetitive loads (e.g. water hammer or fatigue), cleavage type failure, or indirect causes.

In accordance with GDC 4 of 10 CFR 50 Appendix A [Ref. 14], the mechanistic leak-before-break approach, justified by appropriate fracture mechanics techniques, is recognized as an acceptable procedure under certain conditions to exclude design against the dynamic effects from postulation of breaks in high-energy piping. However the following effects from each postulated leakage crack are to be considered: static pressurization effects, environmental effects, flooding effects.

The procedure thus consists of two steps:

I. Screening: to demonstrate that the candidate piping is not susceptible to failure from cited degradation mechanisms, the operating history and measures to prevent or mitigate this degradation must be reviewed.

II. Fracture mechanics: after LBB candidate piping has been reviewed for degradation mechanisms and found to be acceptable, it is subjected to a rigorous fracture mechanics evaluation. The purpose of this evaluation is to show that there is flaw stability and the resulting leakage will be detected in the unlikely event that a flaw should develop.

Summarizing the first step in the application of LBB concept is to screen the candidate systems for susceptibility to known degradation mechanisms. Next, for systems that potentially qualify for LBB, data on the fracture and material properties, piping loads, weld procedures and locations, and leak detection capabilities are gathered. At those locations in each system which have the least favorable combinations of material

properties and stress, a crack is postulated. Calculations, including fluid mechanics, are performed to determine leak rate values and fracture mechanics analysis is used to demonstrate corresponding size flaw stability.

I.6 Consequences of a postulated rupture

As previously mentioned all postulated breaks (inside the containment) are systematically analyzed for potential damage to the containment and to systems and structures required for safe shutdown resulting from pipe whip, jet impingement, and cubicle pressurization.

The flow from leakage cracks is assumed to result in an environment that wets all unprotected components within the compartment, with consequent flooding in the compartment and communicating compartments. Flooding effects are determined on the basis of a conservatively estimated time period required to effect corrective action.

The following part of the present Section comes from [Ref. 2]:

I.6.1 "Evaluation of Pipe Whip and Pipe Internal Load Effects

The release of fluid from a circumferential or longitudinal break in high energy piping could result in significant changes in flow characteristics within the piping system, creating reaction forces which could dynamically excite the piping. If these forces are sufficient to cause pipe whip, nearby required systems and components must be protected or designed to withstand the results of the pipe impact. In addition, required components, if any, within or bounding the broken piping fluid system, must be designed to withstand the pipe break loads. Therefore, as specified, an evaluation has to be made of potential pipe whip and pipe internal loads from postulated break locations to ensure protection requirements are met. A ruptured pipe which creates unacceptable effects due to pipe motion will be provided with pipe whip restraints or barriers or some other method of protection to prevent unacceptable damage, or separated from the required system or component affected.

Pipe whipping phenomenon and his features will be deeply analyzed in Chapter II.

I.6.2 Evaluation of Jet Impingement Effects

A circumferential or longitudinal break in a high energy line could result in a jet of fluid emanating from the break point. Required systems and components should be

protected or designed to withstand the results of the impingement of this jet. Therefore, as previously specified, an evaluation shall be made at each postulated break location of the potential effects of a fluid jet impinging on nearby structures and components.

The evaluation has to consider the effects of jet loading, fluid temperature and moisture on the targets impinged upon. The jet shape and direction, the jet loading, temperature and moisture effects follow.

Where unacceptable effects due to jet impingement have been identified, barriers or some other method of protection will be provided to prevent damage, or the pipe separated from the required system or component.

Jet parameters are influenced by the transient fluid conditions within the pipe. Accordingly the most severe impingement conditions may vary with time depending on which effect is being evaluated. An acceptable approach is to use multiple sets of time dependent fluid and environmental parameters.

The fluid conditions assumed within the pipe immediately prior to the postulated break are those specified in Chapter II (II.2.4) for the whipping pipe, and the same apply for the break discharge rate (consistently with the type of break).

I.6.2.1 Jet shape and direction

Schematics of jets discharging from a pipe break are shown in Figure I-5*. In I-1 (A) the assumption of non-expansion into the surrounding environment is made while I-1 (B) includes the effects of expansion into the surrounding environment.*

For subcooled high energy lines where the fluid temperature is less than its saturation temperature at the surrounding environmental pressure, the discharge jet is characterized by a nearly constant diameter jet approximately equal to the break diameter (as in Figure I-5 *(A)). Since the fluid temperature is below saturation it will not flash but instead will form an incompressible fluid jet. Generally, however experimental data show that the defined high energy line breaks result in a two-phase choked (critical) flow at the break exit plane. Fluid pressure at the exit plane is in general at some pressure greater then ambient. As the fluid leaves the pipe break area, it expands*

as the jet pressure decreases from the higher exit (break) plane pressure to the atmospheric pressure surrounding the jet (see Figure I-5 *(B)).*

A jet discharging from a saturated steam line will accelerate and expand due to the pressure differential, and it will partially condense to a low-moisture wet steam with the liquid phase in the form of dispersed, entrained water droplets. A jet discharging from a subcooled or saturated hot water line (greater than 100°C) will flash to a low quality wet steam. The flashing will cause the jet diameter to expand very rapidly since in almost all instances of interest, highly under-expanded jets are considered.

To establish those structures and components which would be subject to fluid jet impingement effects due to a postulated pipe break, an analytical model to define jet geometry and direction shall be defined. Any such model shall consider jet fluid conditions at the break exit plane, and initial free expansion of the jet to the local ambient pressure.

Regardless of the fluid jet model used to determine affected structures and components, engineering judgment is needed in determining whether the jet will impinge upon a given target. The geometry of the jet cannot be perfectly defined for all of the various fluid conditions. Only representative models can be defined as a basis for design. Neither can the movement of the ruptured pipe, thus the jet centerline, be defined with complete accuracy. The following assumptions are applied:

a) *For circumferential breaks where the two separated ends are not physically restrained, the ends shall be assumed to move clear of each other such that no interference with the jet issuing from each severed end will occur, and the centerline of each jet at the break is assumed to be coincident with the pipe centerline at the postulated break, as shown in* Figure I-6*(A).*
b) *For circumferential breaks in piping which is physically restrained from significant separation (axial pipe movement equal to or less than ½ pipe diameter and lateral pipe movement less than pipe wall thickness) following the break, the jet centerline has to be assumed normal to the pipe centerline and extend 360 degrees around the circumference of the pipe as shown in* Figure I-6*(b).*

c) *For longitudinal breaks circular jet shapes identical to those for circumferential breaks are assumed, and the jet to issue from the break opening with its centerline normal to the opening areas and the pipe centerline as shown in* Figure I-6 *(c) .*

I.6.2.2 Jet impingement load

The jet impingement load is defined as the force exerted by the jet impinging upon a target and being turned or diverted to a different direction. It is a function of the jet properties of quality, velocity, pressure, temperature and cross-sectional area at the point of interaction with the target (impingement plane) and the shape of the target itself. The jet impingement load may be calculated by establishing the pressure distribution on the component and integrating the pressure over the target surface or by calculating the momentum change of the jet caused by the target.

The movement of the jet centerline due to pipe whip is taken into account in the characterization of jet impingement loads on a target. For example, the jet impingement load on a target located between the initial and the final resting position of a whipping pipe can be characterized as an impulse load with a time width equal to the time of jet/target interaction and an amplitude equal to the load average of the time interval.

The jet impingement loading rate is important and proper considerations are necessary in the evaluation of jet impingement loads on target equipment and structures. The response of the target is a function of the stiffness characteristics of the target and the jet impingement loading rate. This response is determined from a dynamic analysis utilizing the actual impingement force loading rate, or from an equivalent static analysis with the use of a dynamic load factor as follows:

$$F_s = DLF\ (F_{imp,max}) \qquad \text{Eq. 1.1}$$

Where

F_s *= Equivalent static impingement force*

DLF = Dynamic load factor

$F_{imp,max}$ *= Maximum value of the jet impingement force*

For a target which can be represented as essentially an elastic one degree of freedom system, the impingement force may conservatively be assumed to occur instantaneously and a dynamic load factor of 2.0 used. There is no simple formula for inelastic, or multi-degree-of-freedom systems, or both. Analysis must be performed to determine the dynamic response of the system or to justify a DLF.

A fluid jet will develop during and immediately following a pipe break. A conservative bounding of the minimum time associated with jet development corresponds to the minimum time to reach the maximum break flow area (A_f). actual jet development time is governed by fluid acceleration time after the break. A certain time is required for establishing the quasi-steady state condition. This delay has been evaluated by Moody and may be used in determining the loading rate of the jet.

I.6.2.3 Jet impingement temperature

When a free jet is slowed or stopped by a target, the kinetic energy is converted into thermal energy, thereby heating the target. This effect on a target may be established based upon the jet temperature at the impingement plane, with appropriate consideration given to the heat transfer from the fluid jet to the target and conduction within the target. Heat transfer coefficients and models used have to be justified through experimental data or analysis, or both. The most severe condition occurs when the jet is stagnated (stopped), resulting in a jet temperature on the target surface which is equal or higher than the static temperature.

Stagnation, however, can occur only at a point on the target. Also, fluid conditions in the turbulent region at the target are more realistically represented by static fluid conditions.

If heat transfer to the target is not considered, the target surface temperature will be assumed equal to the jet temperature.

I.6.2.4 Jet impingement moisture

Depending upon jet fluid conditions, target temperature and target shape, a thin film of liquid could coat the target. The liquid film will. In most instances, be continually swept away and replaced by the jet flow around the target. This is a very complex phenomenon which is very difficult to predict accurately. Therefore in the evaluation of

jet effects is assumed that a thin film of liquid at the jet temperature and pressure coats the target unless other conditions can be justified through experimental data or analysis.

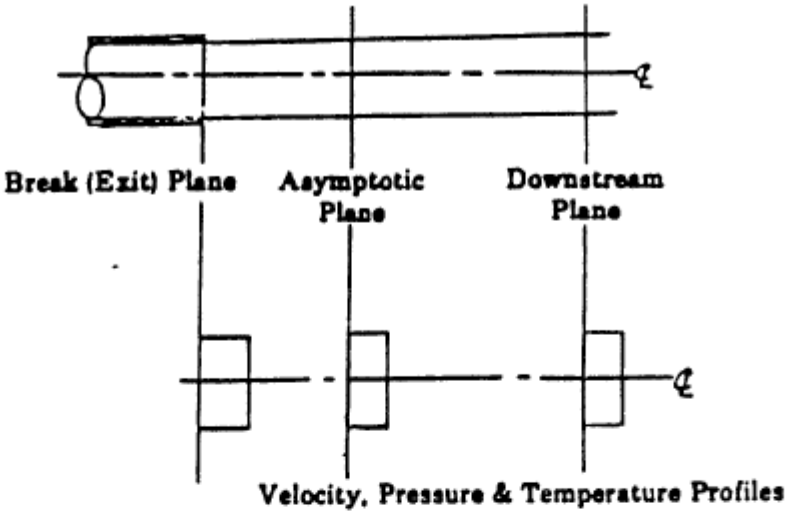

(A) Non-expanding Jet

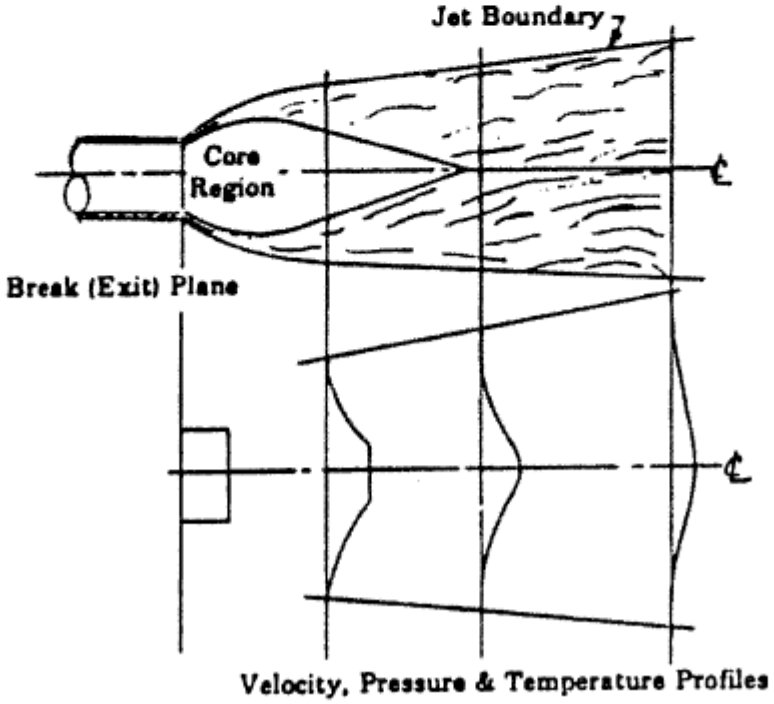

(B) Expanding Jet

Figure I-5. Fluid Jet Models (a)

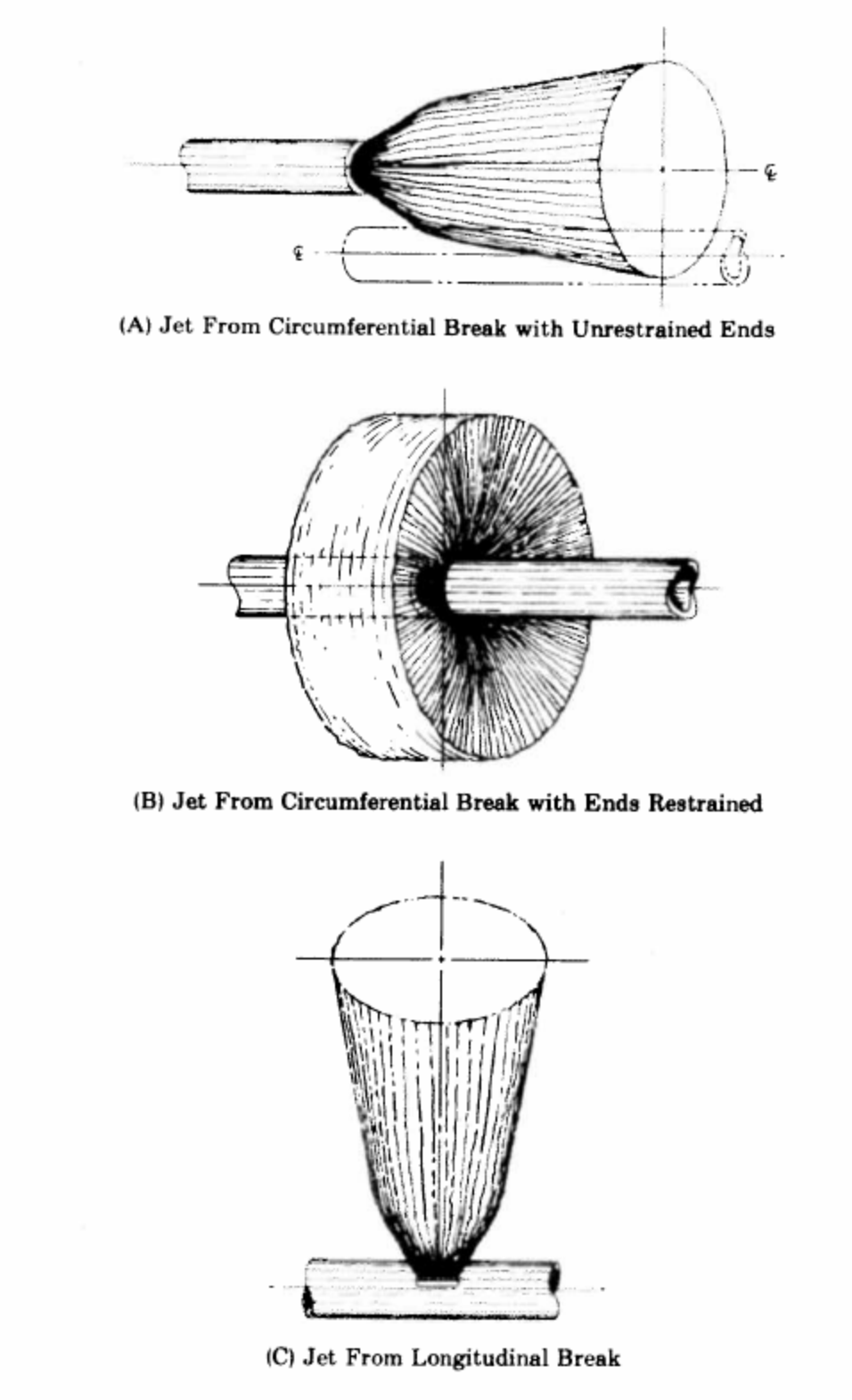

(A) Jet From Circumferential Break with Unrestrained Ends

(B) Jet From Circumferential Break with Ends Restrained

(C) Jet From Longitudinal Break

Figure I-6. Fluid Jet Models (b)

I.6.3 Evaluation of Compartment Pressurization Effects

As mentioned an evaluation has to be made for each postulated pipe break and leakage crack of the effect of compartment pressurization on required systems and components. For postulated breaks, both dynamic and static effects are considered; however, for leakage cracks, only the static effects need be considered.

Steam from postulated steam or flashing water piping ruptures, or gas from postulated gas piping ruptures, are the causative agents of pressurization. For this reason, liquid water lines with fluid temperatures less than the boiling point of water need not be regarded as capable of generating pressurization, regardless of the line pressure, and thus need not be considered in the compartment pressurization evaluation.

For postulated breaks compartment pressurization includes a short term transient, occurring in a few seconds or less, and its effects are born chiefly by structural elements of a compartment, e.g. walls, floors, barriers, etc. As such this effect interacts closely with other effects associated with the postulated pipe rupture. Jet impingement, for example, can introduce additional loads on structural elements. Such effects, when applicable, are to be evaluated in conjunction with pressurization.

Opening through barriers such as walls or floors near the postulated pipe break may be provided to reduce pressure loads.

The normal plant operating conditions defined in Chapter II are to be used in these evaluations*.*

Criteria for mass and energy release source terms, pressure and temperature transient analysis, and asymmetric pressure analysis are provided in ANSI/ANS-56.10-1987. Pipe rupture characteristics have been previously defined.

Evaluation of Environmental Effects

A rupture in high energy piping or moderate energy piping will release fluid into a building region and could over a period of time affect the environmental conditions (e.g. temperature, pressure, radiation and humidity) surrounding required systems and components. As the discharge continues, adjacent regions can be affected by flow through doors, windows, penetrations, and heating ventilation and air conditioning ducting. These environmental changes could damage affected required systems and components. Therefore as specified earlier in this chapter, an evaluation has to be

made for each postulated rupture of the effect of environmental changes on required systems and components. The criteria to be applied in this evaluation are given below for the general regional environment. The local environmental effects from circumferential or longitudinal breaks in high energy piping are governed by local effects of jet impingement (I.6.2.3 and I.6.2.4). To account for the local environmental effects from through-wall and leakage cracks, the flow from the cracks is assumed to spray all structures and components in the vicinity.

A component may be considered capable of withstanding the environmental effects if:

a. *Each individual part can withstand the effects of physical, chemical or other properties relating to its nuclear safety function, and*
b. *The change in physical characteristics of any part is not sufficient to prevent the performance of its nuclear safety function (e.g. excessive thermal expansion of metal components could prevent the performance of the nuclear safety function of a system even though individual components comprising that system could structurally withstand the temperature).*

In evaluating required systems and components, the time duration for which the nuclear safety function is required following the break initiation has to be established , and should be demonstrated that the nuclear safety function is not impaired during that full duration under the influence of the pipe break environmental effects.

The normal plant condition is used in the evaluation and mass and energy releases from ruptured pipe into local area are provided in ANSI/ANS-56.10-1987.

Openings which vent a room, enclosure or region of the plant, including any appropriate time delay effects, may be included in the evaluation. Flow from the room with the ruptured pipe to other areas of the plant is included in the evaluation of required systems and components in those other areas. The discharge coefficients defined in ANSI/ANS-56.10-1987 are to be used.

The environmental changes resulting from the mass and energy releases from the ruptured pipe are typically determined with the use of a computer code. The methods and assumptions utilized in the code are to be justified and demonstrated to result in upper-bound values for the magnitude and time duration of the temperature,

pressure, radiation, and humidity environmental parameters. Credit can be taken for the heat loss of walls, ceilings, floors and equipment within a region if fully justified.

Evaluation of Flooding Effects

A rupture in high energy piping or moderate energy piping could result in water falling to the floor and draining to adjacent regions. Therefore, an evaluation shall be made for each postulated rupture which traces the water drainage and resulting water levels, and evaluates the effects on required systems and components. Guidance is provided by American National Standard Design Criteria for Protection Against the Effects of Compartment Flooding in Light Water Reactor Plants, ANSI/ANS-56.11-1988.

In agreement with what is said some systems which have a potential for causing flooding are:

- *Circulating water system*
- *Main feedwater systems*
- *Essential service water system*
- *Turbine building cooling water system*
- *Demineralized water system*
- *Reactor makeup water system heating*
- *Heating and auxiliary steam boiler feed-water water*
- *Fire protection system*
- *Component cooling water system*
- *Reactor water cleanup system*
- *Steam generator blowdown*
- *Residual heat removal*
- *Chemical and volume control system*
- *Containment spray*

The normal plant operating conditions outlined sizing pipe whip in chapter two are to be used in the evaluation.

The requirements used to establish the mass release from the ruptured pipe into the local area are those reported in ANSI/ANS-56.10-1987.

Guidance on the criteria to accommodate flooding has been formulated and exists in ANSI/ANS-56.11-1988."[Ref. 2].

I.7 Countermeasures

If the resulting damage to SSCs is unacceptable in terms of relevant protection criteria, protective measures are taken such as rerouting piping, relocation of equipment, or providing additional enclosures. Pipe whip restraints and jet impingement shields are installed, if required.

Pipe whip restraints will be deeper analyzed in Chapter III and a steel U-bars restraint for a reference whipping pipe will be modelled (Chapter IV).

A logic diagram for pipe rupture evaluation is reported from ANS 58.2 [Ref. 2]:

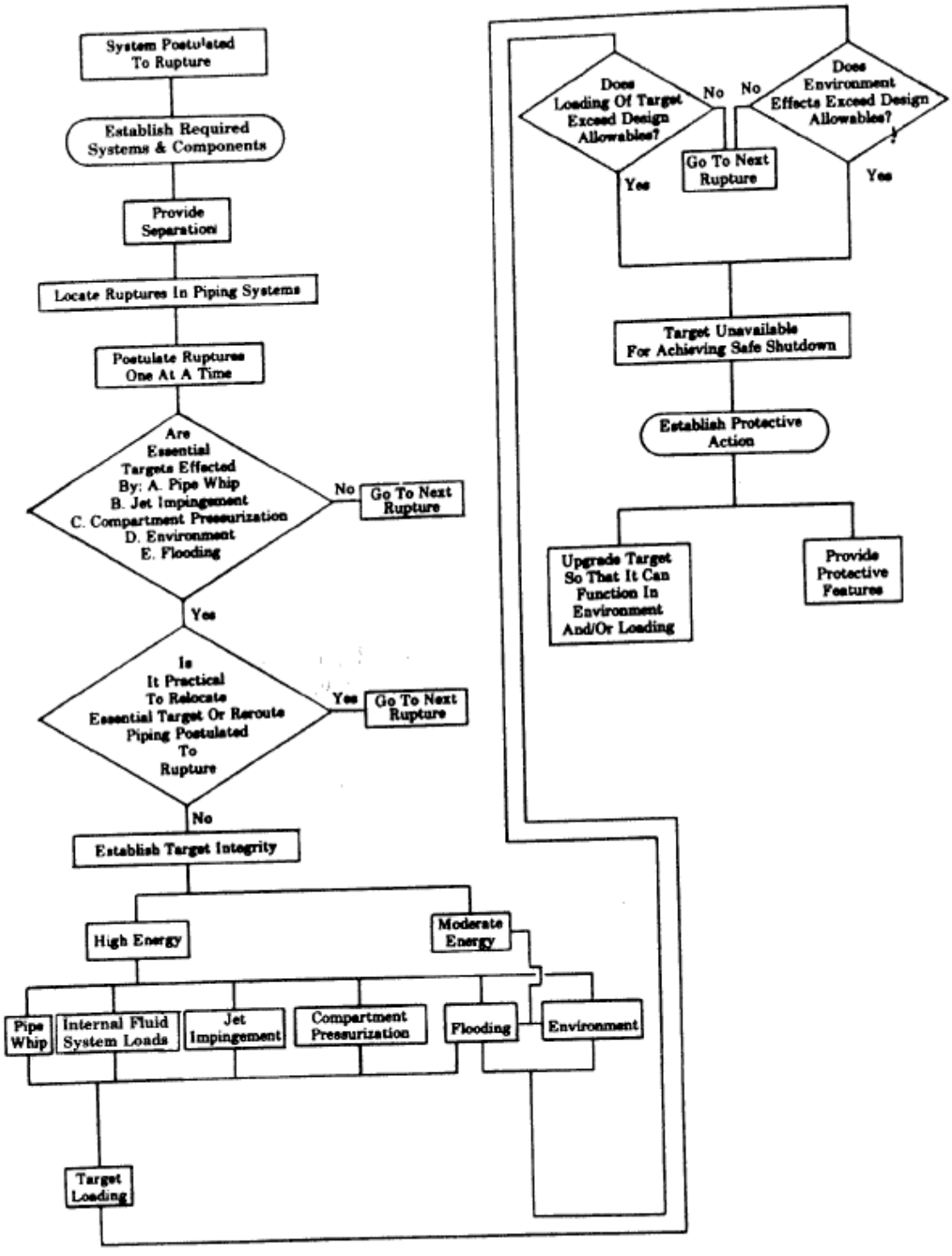

Figure I-7. Logic Diagram for Pipe Rupture Evaluation

Chapter II: Pipe whip characteristics

II.1 Introduction

Studying the free whip phenomenon mainly concerns the evaluation of fluid forces acting on ruptured pipe besides to the formation of one or more plastic hinge along pipe route itself, so generating a mechanism. These and few other characteristics are presented in this Chapter in order to clarify the concepts for further analysis.

II.2 Fluid Forces

The fluid forces acting on the ruptured pipe are a function of time and space, and depend upon the fluid state within the pipe prior to rupture, the break flow area, frictional losses, plant system characteristics, piping system geometric design, and other factors.

II.2.1 Force Calculations Methods

The generalized equation which describes the fluid forces acting on a ruptured pipe reported in ANS 58.2 is:

$$\vec{T} = -\left[\int_{c.v.} \frac{d}{dt}(\overrightarrow{\rho u})dV + \int_{c.s.} \overrightarrow{\rho u}\,(\vec{u} - \overrightarrow{dA}) + \int_{A_m} Pd\,\overrightarrow{A_{in}} + \int_{A_{out}} Pd\overrightarrow{A_{out}} - \int_{A_{pipe}} P_a d\overrightarrow{A_{pipe}}\right] \qquad Eq.2.1$$

Where:

$\vec{T}$= dynamic fluid thrust force vector on pipe

$c.v.$ = control volume

c.s. = control surface

V = volume

$\vec{A}$ = surface area

ρ = mass density

u = fluid velocity vector

P = local pressure at center of elemental area (dA or dS)

$\overrightarrow{A_{in}}$ = area of flow into control volume

$\overrightarrow{A_{out}}$ = area of flow out of control volume

P_a = ambient pressure around pipe

A_{pipe} = pipe external surface area

For longitudinal breaks or circumferential breaks of branch lines at branch connections, both represented in Figure II-1 (B), or a circumferential break in constant area pipe just downstream of a 90° elbow, such as shown in Figure II-1 (A), the generalized equation may be simplified to the following:

$$T_x = -\int_{c.v.} \frac{d}{dt}(\rho u_x)dV - \rho u_e^2 A_e - P_e A_e + P_a A_e \qquad Eq.2.2$$

Where:

$T_x =$ dynamic fluid thrust force acting on pipe in the x direction

$u_x =$ control volume fluid velocity in the x direction

$u_e =$ fluid velocity at break plane area

$P_e =$ fluid pressure at break plane area

$A_e =$ control volume area at plane of break or break plane area

The first term of this second equation is the acceleration term; for steady state flow conditions, the acceleration term is zero and the remaining three terms define the steady state fluid force.

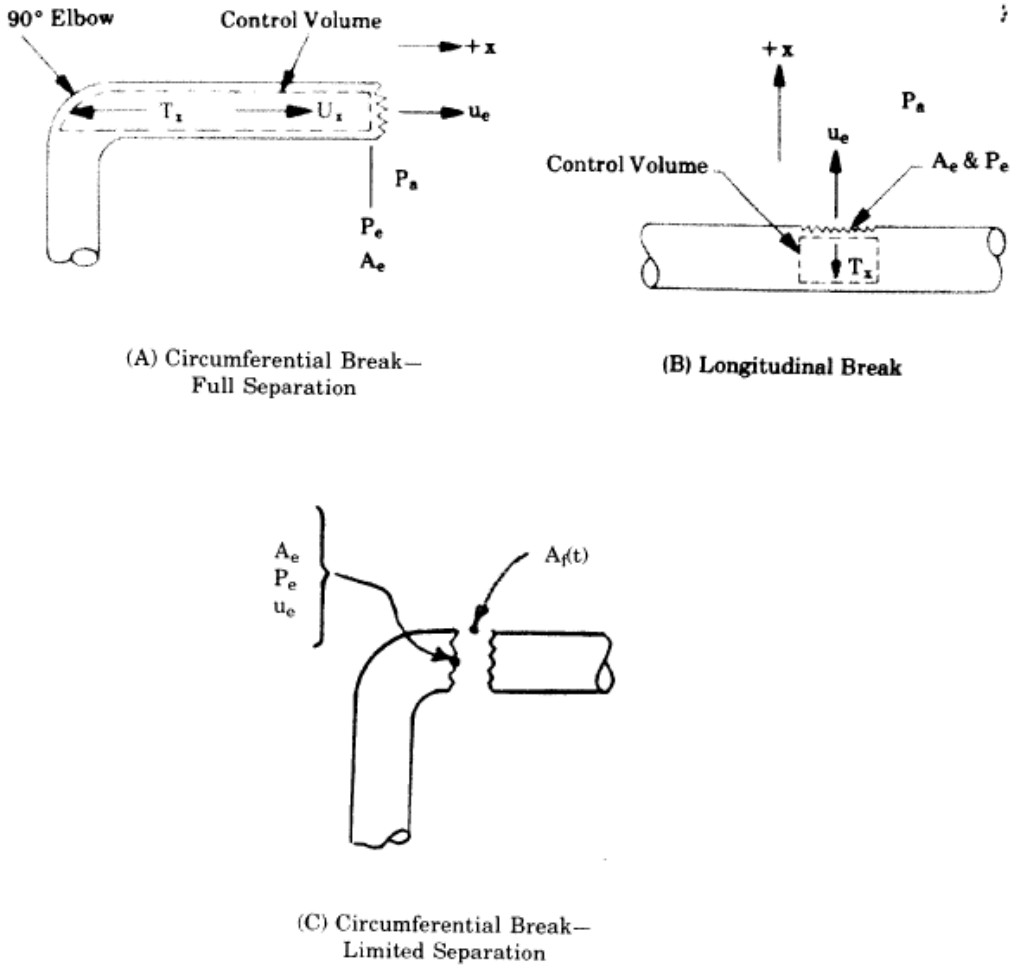

Figure II-1. Control Volume Models

In order to solve for the reaction thrust force, the various fluid transient characteristics in the piping system must first be established. This is done by means of computer programs which calculate one or more of the following balances as a function of time: flow, mass, energy and momentum. Simplified methods may also be used for determining fluid forces where demonstrated to be conservative.

The simplified method given in Appendix B of ANS 58.2 [Ref. 2] that will be applied later on during the analysis follows.

The initial force is the initial pressure times the break plane area; as the time rate of change in fluid momentum decreases, the acceleration term in Eq. 2.2 approaches

zero. The momentum flux term (second term) generally increases with time until it reaches its maximum at steady state.

Knowing the initial and steady state forces, a conservative approximation for the time dependent thrust force can be made. When the steady state thrust is greater than the initial thrust, as shown in Figure II-2, the time dependent thrust shall be assumed to rise to the steady state thrust force in one millisecond and remain constant with time for the pipe whip analysis. If the steady state force is less than the initial force, as shown in Figure II-3, the initial thrust shall be assumed until the time to steady state thrust is reached, and the steady state thrust assumed to occur thereafter. An instantaneous step change of thrust from initial to steady state need not be assumed. Following the time to reach steady state t_{ss}, a time interval sufficient to avoid calculation instabilities may be assumed. Shown in Figure II-2 and Figure II-3 are typical thrust force transients for frictionless and friction-limited flow from a constant pressure source.

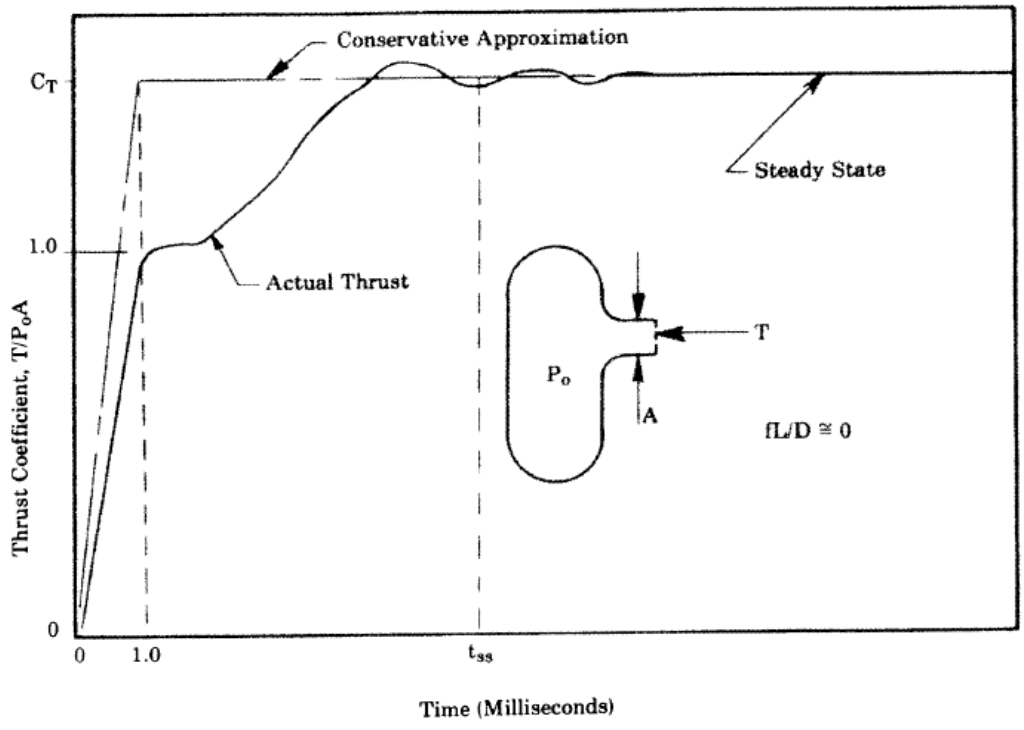

Figure II-2. Thrust Force Transient, Very Low Friction Flow

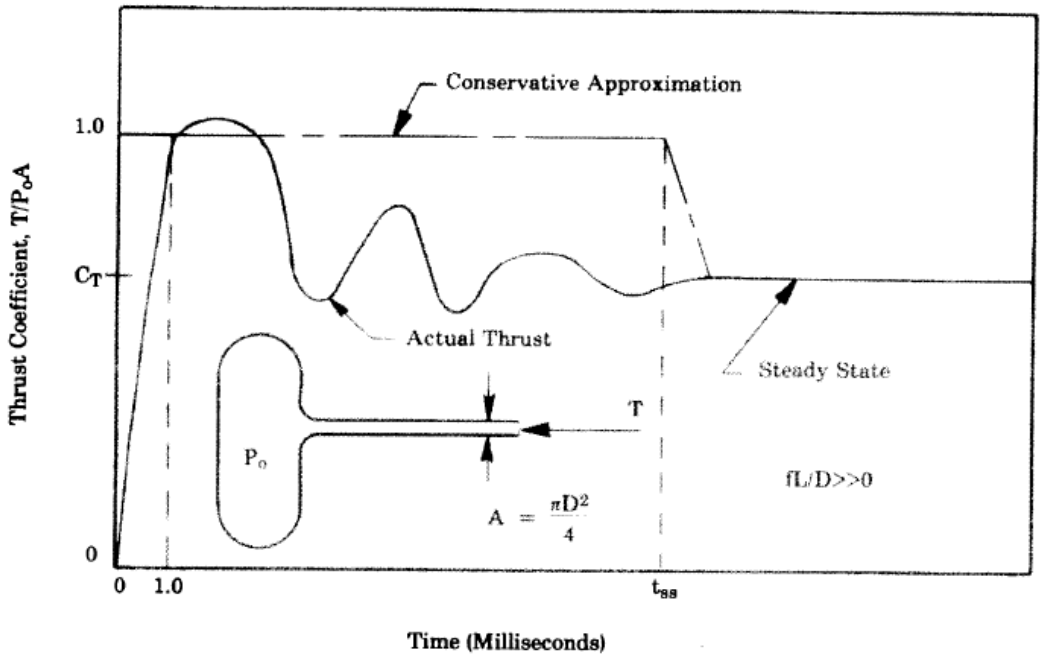

Figure II-3. Thrust Force Transient, Friction Flow

II.2.2 Initial thrust force

The initial thrust force is simply the break plane area times the initial pressure within the pipe,

$T_{INT} = P_{0,pipe}A$ Eq.2.3

Where

T_{INT} = initial thrust force, where $T = T_x$

$A = A_e$

$P_{0,pipe}$ = initial total (stagnation) pressure in the pipe

The initial thrust force for a circumferential break is equal to $P_{0,pipe}A$ regardless of the resultant break flow area because of the initial unbalanced longitudinal tensile stress across the broken pipe section. The initial thrust force for a longitudinal break is also equal to $P_{0,pipe}A$.

II.2.3 Steady State Thrust Force

When steady state flow conditions are reached, the transient wave force (first term of Equation 2.2 due to fluid acceleration) vanishes and only the steady state blowdown

force continues to act. To apply the simplified approach, the steady state thrust force can be written as:

$T_{ss} = C_T P_0 A_e$ Eq. 2.4

Where:

T_{ss} = steady state thrust force at time, t_{ss}

t_{ss} = time to reach steady state

C_T = steady state thrust coefficient

P_0 = initial pressure in the source

The steady state thrust coefficient is dependent on the fluid and the frictional loss terms. The steady state thrust coefficient for frictionless flow is typically assumed equal to 1.26 for saturated or superheated steam, and equal to 2 for non-flashing subcooled water.

II.2.4 Operating Conditions

For the purpose of design, ruptures are postulated to occur only during normal plant conditions, and the following assumptions are used to determine the thermodynamic state in the pipe and the attached reservoirs (vessels, heat exchanger, pressurizers, etc.) for the calculation of the fluid reaction forces:

a) For those portions of piping systems which are normally pressurized during operation, the thermodynamic state in the pipe and the associated reservoirs is that corresponding to 100 percent power.

b) For those portions of high energy piping systems which are normally pressurized only during plant conditions other than 100 percent power, the thermodynamic state and associated operating conditions are determined using the most severe mode.

II.2.5 Break Opening Time

For the purpose of the analysis, circumferential and longitudinal break plane areas (A_e) are assumed to develop within one millisecond after break initiation (conservative time), unless otherwise analytically or experimentally substantiated. When circumferential breaks are postulated, it can be assumed that it takes up to ten milliseconds for the broken pipe segments to move sufficiently to achieve a break flow

area (A_f) equal to the sum of the upstream and downstream break plane areas ($2A_e$). Partial area breaks should instead be assumed to take proportionally less time to achieve maximum break flow area.

II.2.6 Pipe Geometry Effects

In calculating forces acting on the piping system, credit can be taken from flow resistance losses between the break and the pressure reservoir(s). Typical components which may be considered are: orifices, nozzles, valves, reduced cross-sections, spargers, elbows, bends and straight pipe.

II.2.7 Critical Flow Model

The critical flow model used to establish the maximum flow through breaks and restricted regions of the piping will directly affect the calculated reaction force. For flashing or steam-water mixtures with quality greater than zero percent at stagnation conditions at the discharge plane, Moody's critical flow model or the homogeneous equilibrium model (HEM) are acceptable. For the subcooled region, the Henry-Fauske model is acceptable. Other critical flow models can be used if they are justified through experimental data or analysis.

II.3 Hinge location and deformation

The pipe whip phenomenon involves rotational motion due to a propulsion force and the subsequent formation of plastic hinges in the pipe sections.

The location of a plastic hinge is related to the effective mass of the whipping pipe and to existing pipe supports. Occurrence of a pipe whip is dependent on formation of a sufficient number of hinges to make up a mechanism and result in plastic deformation. Piping which has a complex configuration may lead to the creation of a torsion hinge, with a whip motion outside the main bending plane; conservative assumptions are then to be made to estimate maximum potential displacements around the hinge.

Two commonly encountered simple mechanisms (reported in Figure II-4) are:

a. Cantilever pipe with end load: $T_{whip} = \frac{M_p}{L}$

b. Pipe restrained at both ends with lateral load: $T_{whip} = 2M_p(\frac{1}{L_1} + \frac{1}{L_2})$

Where:

T_{whip} = minimum thrust force required to cause pipe whip

M_p = plastic moment = $\frac{4}{3}\sigma_y(r_o^3 - r_i^3)$

σ_y = yield stress at maximum operating temperature

r_o = pipe outside radius

r_i = pipe inside radius

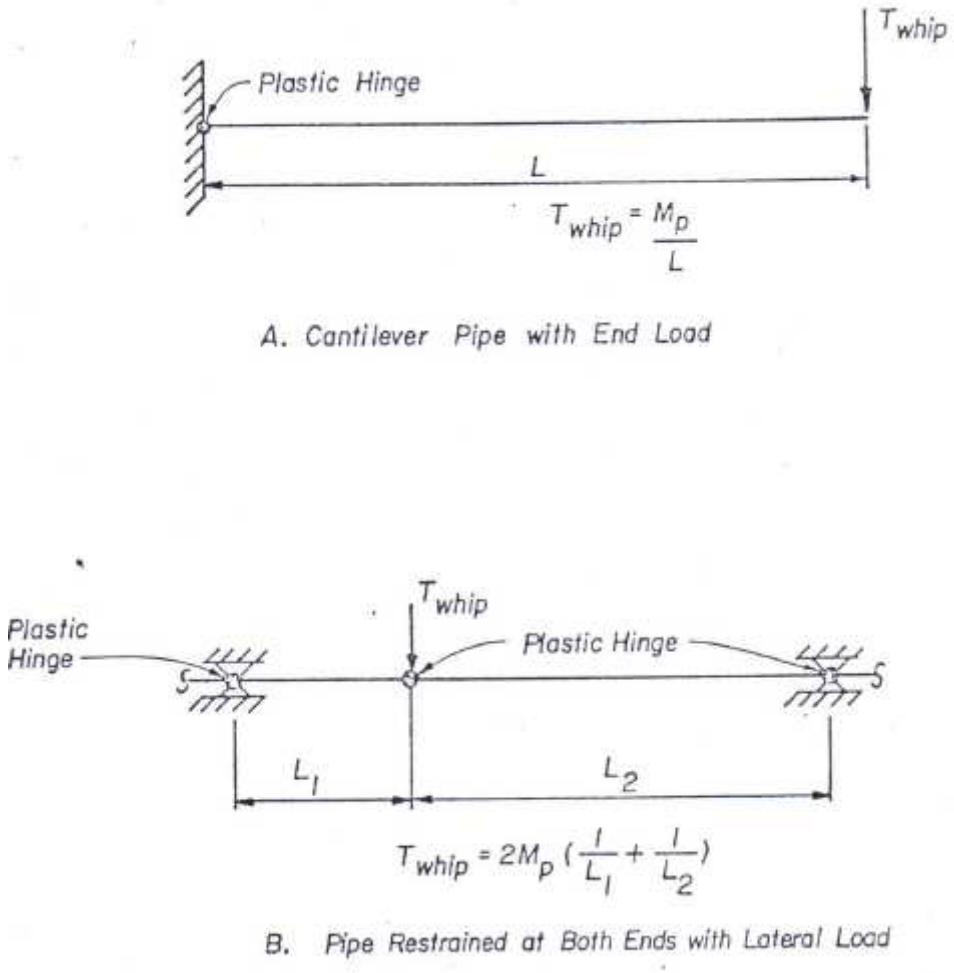

Figure II-4. Common Pipe whip Mechanisms

Pipe whip is thus assumed to occur in the plane defined by the piping geometry and configuration and results in pipe movement in the direction of the jet thrust. Secondary failures in the whipping pipe are not assumed to occur, i.e., the pipe at the point where plastic hinges form is assumed to remain intact.

A plastic hinge will absorb a portion of the energy by rotational resistance. For a small angular rotation the pipe should retain its circular geometry and its rotational resistance will be large.

A large angular rotation may result in some collapse of the pipe at the hinge. A collapsed pipe may act as a valve to restrict flow, limit the thrust, and may reduce the hinge rotational resistance. A relatively incompressible fluid may have a retarding effect on the collapse rate.

For large hinge rotation it may be feasible to base resistance on ultimate moment rather than plastic moment; it is:

$$M_{ult} = \sigma_y Z_p + (\sigma_u - \sigma_y) Z_e \qquad \text{Eq. 2.5}$$

where:

$Z_p =$ plastic bending section modulus = $\frac{4}{3}(r_o^3 - r_i^3)$

$Z_e =$ elastic bending section modulus = = $\frac{\pi}{4r_o}(r_o^4 - r_i^4)$

$\sigma_u =$ tensile stress corresponding to the strain at maximum deformation, sometimes taken as the ultimate tensile strength.

The above formulations, which are commonly used in static analysis, neglect any influence of the pipe length from the break to the first elbow, as well as any restraint effect. That allows a conservative estimation of the minimum unrestrained length of pipe inducing the formation of a plastic hinge, but it may lead to unrealistically short hinge lengths. On the other hand, for the assessment of the aggressive PBL (Pipe Break Location), the envelope of the whipping pipe should assume a pivotal motion around a plastic hinge located at the maximum distance from the break point. For this reason, the following, more realistic, formulation for L_h is often used in restraint design based on energy balance analysis (see III.2.2III.2):

$$L_h = \frac{3M_p}{2T_{whip}}\left(1 + \sqrt{1 + \frac{8LT_{whip}}{3M_p}}\right)$$

The above equation takes into account the inertial effect of the length from pipe end to first elbow (L).

II.4 Mass

The effective mass of a whipping pipe is a function of pipe length, geometry, and stiffness. Pipe stiffness is dependent upon the pipe section properties, the pipe operating temperature and its effect on material properties, and the pipe internal pressure.

In general, the effective mass of the whipping pipe is assumed to be one-third of the mass between adjacent hinges making up the pipe whip mechanism for sections of pipe impacting side-on and full mass for sections of pipe impacting end-on. In accordance with the simplified pipe whip mechanism of Figure II-5 the effective mass is approximately given by relationship:

$$M_i = M_1/3 + M_2 \qquad \text{Eq.2.6}$$

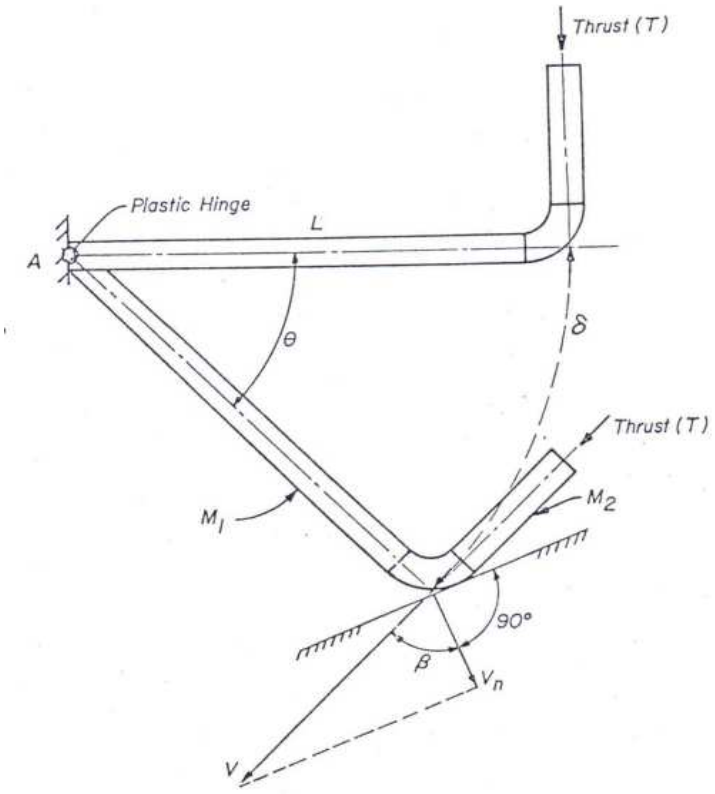

Figure II-5. Simplified Pipe Whip Mechanism

II.5 Velocity and impact force

Kinetic energy increases as the square of the velocity; minimizing impact velocity is a prime concern, along with accurate determination of its value. Conservation of energy method is the approach used to calculate velocity. For example, assuming a pivotal

motion around the plastic hinge as shown in Figure II-5, the kinetic energy (E_{kin}), which results from the jet thrust work, may be evaluated by equation:

$$E_{kin} = T\delta - M_p\theta = (TL - M_p)\theta \qquad \text{Eq.2.7}$$

The impact velocity (V) of the whipping pipe may then be estimated by means of equation:

$$E_{kin} = \frac{1}{2} I_{AR}\omega^2 = \frac{1}{2} I_{AR}(\frac{V}{L})^2 \qquad \text{Eq.2.8}$$

Finally, an estimation of the maximum impact force (F_{max}) on a potential target can be given by equation [Ref. 7]:

$$F_{max} = V\sqrt{M_i K} \qquad \text{Eq.2.9}$$

Where:

δ = free-end displacement

θ = rotation of the whipping pipe

I_{AR} = moment of inertia around the plastic hinge

ω = V/L =angular velocity around the hinge

K = stiffness of impacted structure or component

II.6 Insulation

The energy absorption capacity of insulation is dependent on its crush strength, thickness, and impact area. Insulation may act to soften the impact by increasing the load application time, but to date this property has not been considered, since it is felt that the crush strength is very small with respect to the thrust loading. Also, the crush strength of insulation is a property that is not normally defined by the vendor.

II.7 Impact area

The impact area is directly related to the shape and properties of the pipe and target. The ability of the pipe and target to deform to increase contact bearing area is desirable. The pressurized contents of a pipe may reduce pipe collapse. Lateral loads could be generated by liquid contents due to deceleration at impact which would cause an increase in impact area. Insulation is anticipated to increase impact area. The impact area is a somewhat indeterminate value.

II.8 Rebound

Rebound is influenced by elastic strain, hysteresis, stiffness, mass, contents, target damage, and pipe damage. The thrust force will often oppose rebound.

The NRC in their discussion of any energy balance model states that: ”For applications where pipe rebound may occur upon impact on the restraint an amplification factor of 1.2 should be used to establish the magnitude of the forcing function in order to determine the maximum reaction force of the restraint. Amplification factors other than 1.2 may be used if justified by more detailed dynamic analysis.”

Chapter III: Pipe Whip Restraints

III.1 Introduction

Pipe rupture restraints are designed to mitigate the consequences of one postulated pipe rupture at a time. The pipe is assumed to be in a normal plant operating condition prior to rupture.

The pipe whip restraints required, except for anchors and supports used as restraints, are nonintegral with the piping. The gap between the pipe and restraint must account for all operating conditions including seismic excursions; to minimize the gap and the kinetic energy, pipe insulation is sometimes locally thinned.

Pipe rupture restraints are normally linear type structures such as columns, beams, frames, or rings which are designed with or without energy absorbing elements. Design allowable stresses are increased to account for the pipe rupture event; strain hardening of the material; and strain rate effects.

Elastic pipe rupture restraints which have no discrete energy absorbing element are usually designed elastically to resist the pipe thrust, and energy absorption by the restraint is not considered.

Pipe rupture restraints with energy absorption structural elements dissipate the kinetic energy of the whipping pipe by buckling, elongation or crushing. For a given energy absorbing material, the material area is sized to limit the maximum load on the support structure, embedments, and building structure; to limit the deformation of the restraint thus limiting pipe motion; and to resist the steady-state blowdown thrust without further deformation.

Lateral forces perpendicular to the thrust force are probably low in magnitude. Secondary restraints to prevent lateral movement are sometimes used.

Pipe supports (rigid supports, seismic snubbers, spring hangers, and constant load hangers) are used to mitigate the effects of pipe rupture when their load ratings are large enough. If the load rating of the pipe support is exceeded, it is assumed to fail completely and no load resisting or energy absorbing capability is considered in the

event of a pipe rupture. The assumed zero energy absorption and load resistance of a support is inherently conservative.

III.2 Analysis methods

The evaluation of piping response following a break should assess the capability of the overall system(piping, restraints and support structures) to dissipate the total energy accumulated during the dynamic event and to withstand the steady state fluid forces (i.e. when motion ceases). Among the acceptable alternatives for the pipe whip evaluation, the following methods [Ref.7] are the most commonly retained for pipe break analysis of high-energy systems.

III.2.1 "Static Analysis Approach

In this approach, a conservative amplification factor (the Dynamic Load Factor) is used in the restraint design to establish the magnitude of the forcing function induced by the jet thrust force following the postulated pipe break, and the ruptured system is analyzed statically. A conservative value is used for this amplification factor, as drawn from detailed dynamic analyses of comparable systems; a commonly accepted DLF for a preliminary design is 2.

III.2.2 Energy Balance Analysis

This method is based on the main hypothesis that the kinetic energy generated during the first quarter cycle movement of the ruptured pipe (initial and final pipe velocities equal to zero) and imparted to the piping and restraint system through impact is converted into equivalent strain energy. The energy absorbed by the pipe deformation can be deducted from the total energy imparted to the system. As with a dynamic analysis, the input energy shall be conservatively evaluated taking into account the maximum possible initial gap at restraints.

Since energy balance cannot account for any time dependence, a constant jet thrust force will be conservatively assumed (Eq.4). For applications where pipe rebound can occur, an amplification factor of at least 1.1 is recommended to account for the potential occurrence of the maximum stress or strain in the pipe whip restraint after the first quarter cycle of response. A simple collapse mechanism is generally assumed to predict the pipe behavior and conservative laws to assess the span distance between

break and primary plastic hinge, as well as the maximum impact load on any nearby structure. The length to the main plastic hinge is evaluated taking into account the influence of restraint location (if any) and of the energy absorbed by pipe bending, as well as of the mass of the attached pipe.

The energy balance method is well suited for the design of energy absorbing restraints, which is based on the evaluation of pipe and target post-impact deformation through the extrapolation of experimental pipe crash data.

III.2.3 Dynamic Time History

A dynamic time history analysis, being often time-consuming, could be a "last resource" method, to be used only if conservatism of simplified models results in too large calculated loads on structures or restraints. The model of piping and pipe whip restraints shall adequately reflect its dynamic characteristics, taking into account inertia and stiffness properties of the complete system, as well as the effects of material inelastic behavior and large deformations. The maximum initial clearance at restraints (the "acceleration gap") is used in calculations, to account for the most adverse dynamic effects of pipe whip. The time history forcing function will be applied at each pipe break end, and the time history response, in terms of restraint loads , pipe deformation, etc., computed by numerical integration.

In a simplified approach, a limited portion of the piping system may be modelled in the analysis instead of the complete system; proper consideration should be given in this case to dynamic coupling between the portion to be analyzed and the remainder of the system. Conservative assumptions may also regard the time history forcing functions and the representation of the dynamic characteristics of the pipe whip restraint system." [Ref. 7].

III.3 Gap determination

Increasing the gap between the restraint and the pipe has a direct effect on the energy absorption requirements of the restraint system because the blowdown force serves to accelerate the pipe through the distance of the gap.

In general, the physical gap distance (G) can be calculated as follows:

G = tolerance ± thermal movement ± seismic movement + installation + insulation (if required)

The physical gap is the gap at 100% operating condition. For U-bars an effective gap (G_e) is considered and is determined as the summation of the physical gap (G) stated above and the geometric gap (G_g). The geometric gap is defined as the increase in travel distance due to the U-bar bend radius conforming to tangential contacts with the pipe until significant resistance to movement as demonstrated in Figure III-1 below:

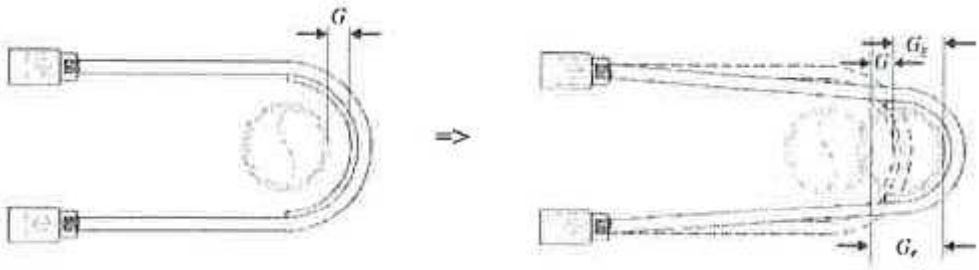

Figure III-1. Geometric Gap Consideration

III.4 Secondary Hinge

A secondary hinge check has also to be performed to ensure that a plastic hinge does not form between the line of action of the fluid thrust force and the edge of the restraint to pipe contact; since it is recognized that this is a dynamic event and plastic deformation of the process pipe is probable upon impact with the restraint, Figure III-2.

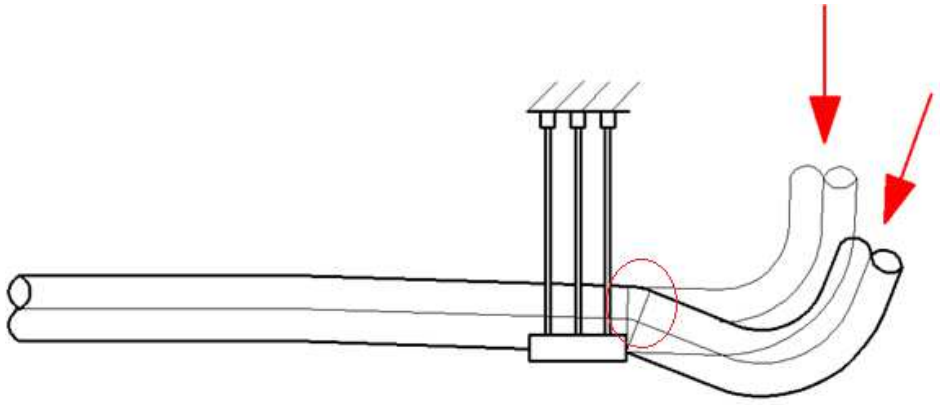

Figure III-2. Secondary Hinge Formation

III.5 Materials

All PWR materials in the load path of the pipe whip restraint are classified as safety-related material.

AISC N690 details acceptable materials for pipe whip restraints. It has to be noted that since PWRs experience impact loadings, material used for PWRs require a Charpy V-Notch impact test, using procedures described in ASTM 20 [Ref. 15]. The Charpy V-Notch test has to be conducted at a temperature not less than 30°F below the Lowest Service Temperature of the structural component.

The acceptance criteria for the Charpy V-Notch test is that the material withstand not less than the energy (average of three samples) indicated in the Table III-1 below and with any individual specimen withstanding not less than the energy (one sample minimum) indicated in the Table below.

Specified Minimum Yield Stress	Charpy V-Notch Energy Value	
	Average of Three Specimens, Minimum	One Individual Specimen, Minimum
Equal to or less than 36 ksi (250 MPa)	15 ft-lb (21 J)	10 ft-lb (14 J)
Greater than 36 ksi (250 MPa), less than 44 ksi (300 MPa)	20 ft-lb (27 J)	15 ft-lb (21 J)
Equal to or greater than 44 ksi (300 MPa)	30 ft-lb (41 J)	25 ft-lb (34 J)

Table III-1. Charpy V-Notch Test Conditions

It's important to remind that for dual function structures (structures that function as pipe supports and as PWRs), the material procured for these supports has to meet both the pipe support requirements as well as the PWR requirements. In most cases, this means that a Charpy V-Notch test is required.

Materials procured in accordance with ASME Section II (SA materials) [Ref. 13] can be substituted for ASTM (A materials), provided that the Charpy V-Notch impact test has been conducted.

Due to the susceptibility of high strength materials to brittle fracture and stress corrosion cracking, the maximum measured ultimate tensile strength of component support material has not to exceed 170 ksi (1172 MPa).

All materials are to be provided with a Certified Mill Report or Certified reports of test made by the fabricator or a qualified testing laboratory.

III.5.1 Dynamic Versus Static Mechanical Properties

Absorption of energy via plastic deformation is an acceptable and typically the most desirable method in the design of piping and restraints for protection against pipe whip effects. When applying such design methods, careful consideration has to be given to the material properties throughout the range of the stress-strain curve at the applicable temperature. Also, as pipe rupture is a dynamic event, careful consideration is also given to the effects of impact loading and high strain rates on the material properties. During the dynamic pipe rupture event average strain rates expected are approximately 10^5 times higher than the rates encountered in typical tensile tests. Impact velocities for pipe whip restraints are generally between 5 fps and 100 fps.

Materials used in the design of nuclear power plant piping, pipe whip restraints, and structures are to be ductile metals having good impact properties. These types of metals have been extensively evaluated, both under slowly applied (static) and impact loading conditions.

Numerous tests ([Ref. 16] for example) have been conducted which demonstrate that ductile behavior rather than brittle fracture will occur under dynamic loading rates typical during a pipe rupture event. Direct application of results of such tests, on a general basis, might not be valid since the survey primarily covers impact testing with the final force being zero, whereas pipe rupture events generally have relatively high remaining steady state forces. The general trend for material property changes in these typical ductile metals under both static and dynamic loading is shown in Figure III-3.

The effects of the strain hardening behavior changes on the design under dynamic loading has to be considered in establishing material design limits under the rules of ANS 58.2-6.22 since such potential changes can reduce energy absorption capacity and increase resultant pipe whip restraint and structural loadings, even though the mechanical strength properties of the material are higher than those for slowly applied (static) loading.

Also shown in Figure III-3 is the general, but not always true, trend that ductile metals exhibit a lower strength at elevated temperatures. Therefore, care should be taken to ensure the material properties used in design correspond to actual temperature of the material during the pipe rupture occurrence.

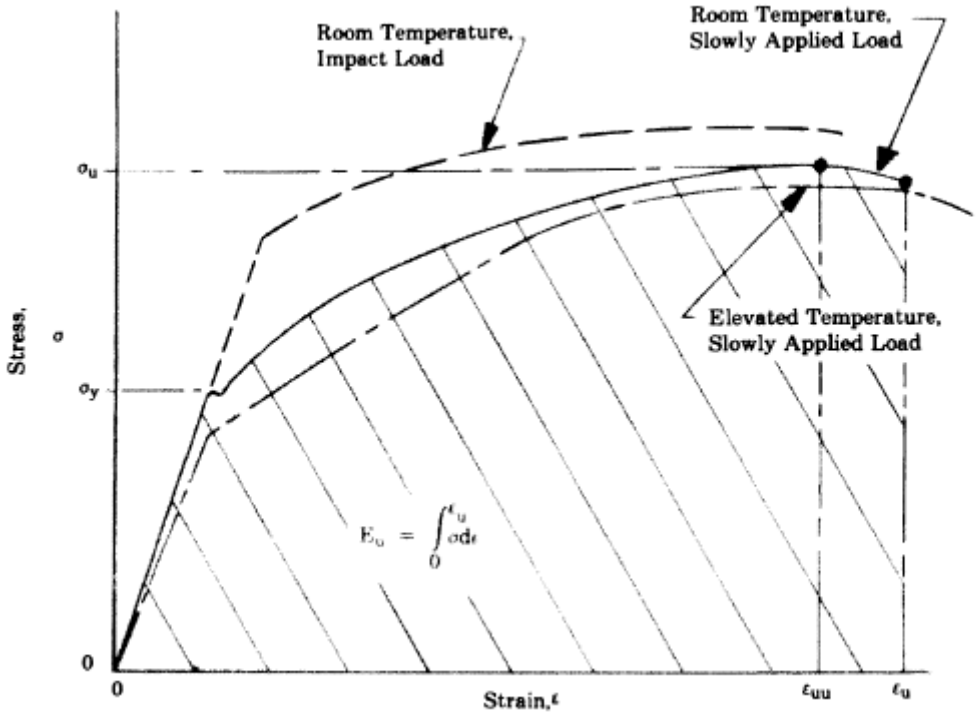

where

σ_y = yield strength

σ_u = ultimate strength

ε_{uu} = ultimate uniform strain

ε_u = ultimate fracture strain

E_u = ultimate energy absorption

Figure III-3. Typical Ductile Metal Engineering Stress-Strain Behaviour

III.6 Types of restraints

The restraints that have been used and/or proposed till today can be categorized in two broad groups.

III.6.1 Inelastic Restraints

These are the restraints which are intended to absorb the energy associated with the break by the yielding or crushing of a part of the restraint system. The gap between the pipe and the restraint is relatively large and after the pipe impacts the restraint, large displacement results. Minimum and maximum capacity of the yielding element of the restraint are to be well-defined so that the yielding element can be designed using the minimum capacity and the supporting element can be designed for the maximum capacity. Some of the most common inelastic PWR are described below.

III.6.1.1 Stainless Steel U-bar Restraints

One of the simpler restraints is that of stainless steel U-bars as reported in Figure III-4. This design has several advantages:

- Stainless steel is a very ductile material. Therefore, this type of restraint has a large energy absorbing capability
- Stress-strain characteristics are fairly uniform, thus the forces transmitted to the supports can be calculated with accuracy which simplifies the support design.
- It is a flexible system and can be fitted around the pipe in crowded areas.
- It has a built-in lateral load capability since the restraint conforms to the geometry dictated by the direction of the force. However, the capability may be limited due to geometry (e.g., if the pipe is too close to the supporting structure, such as a wall).
- Installation and removal is relatively easier which improves in service inspection capability.

Disadvantages of this type of restraint include the following:

- Resulting displacements are large (due to geometric and inelastic deformation); thus increasing the possible target areas of the impinging jet
- Lateral load capability is smaller than the axial load capability. This create difficulty if the jet thrust can be in any direction.

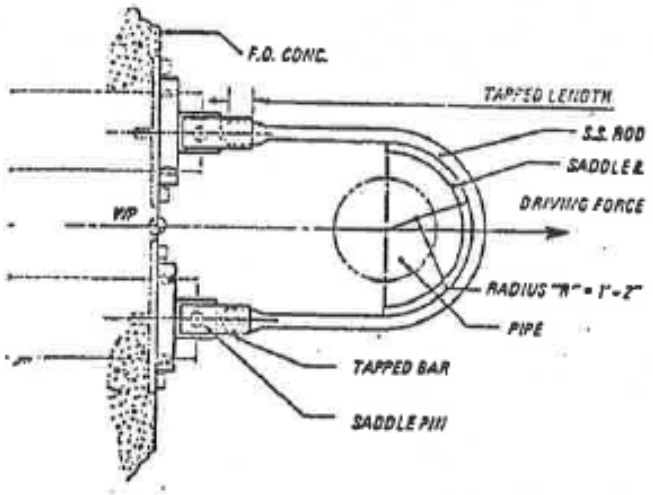

Fig III-3 (a)

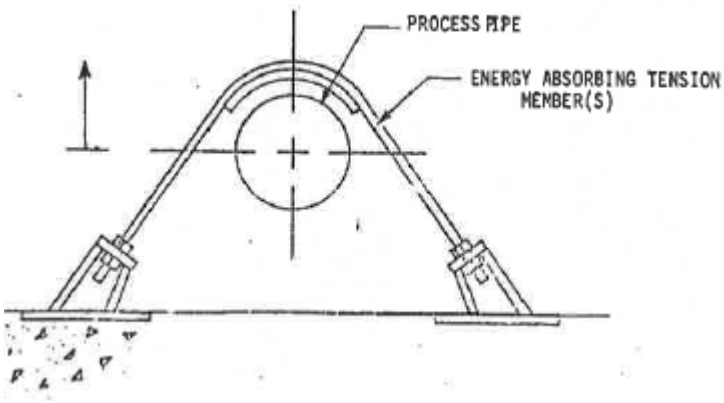

Fig III-3 (b)

Figure III-4. Typical Stainless Steel U-Bar Restraint

III.6.1.2 Mild Steel U-bar Restraints

Similar to the stainless steel U-bar restraints discussed above, mild steel U-bar restraints are considered. Since the energy absorption is directly related to the usable area under the stress-strain diagram, more restraints are needed if the steel used has lower ductility. As a result, the support design forces are greater, requiring a larger support system. Also, the stress-strain characteristics of mild steel are less uniform and thus necessitate more testing and more conservative design criteria.

III.6.1.3 Restraints with Crushable Material

In past years, restraints incorporating a crushable pad have been widely used. The crushable pad is the energy-absorbing element in the restraint system. The restraint may be of any geometry and material. Several types of restraints with crushable pad are shown in Figure III-5 to Figure III-8.

Advantages of the use of crushable pad include the following:

- The crushable pad has a large energy-absorbing capacity, since it can compress up to 50 percent of its original thickness.
- Load-deformation characteristic of the pad is well-defined; thus, the loads transmitted to the supporting system can be established accurately.
- Installation and removal is simple.

Among the disadvantages of this type of restraint the following are worth noting:

- Lateral load capability is practically non-existent. Thus, a pad must be provided in every direction in which jet thrust may occur.
- The result restraint system may be large and costly, especially if the restraint location is away from a convenient support structure.
- Resulting displacements are relatively large (but less than U-bar restraint displacements).

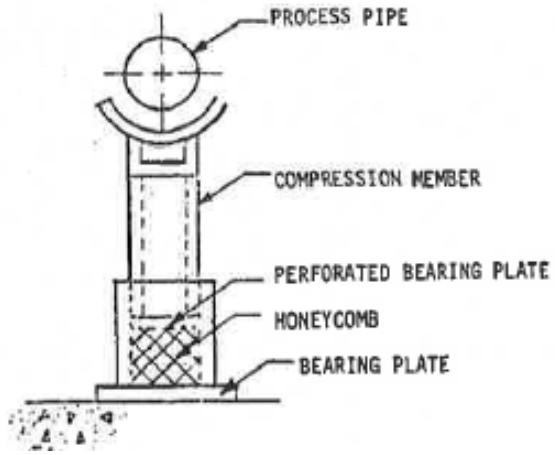

Figure III-5. Crush Block with Compression Member

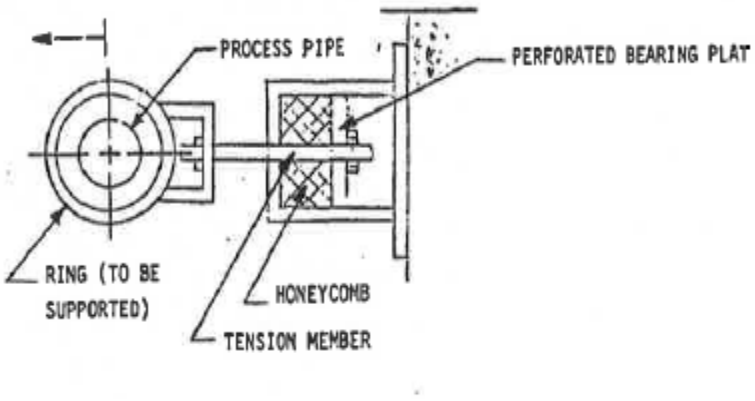

Figure III-6. Crush Block with Tension Members

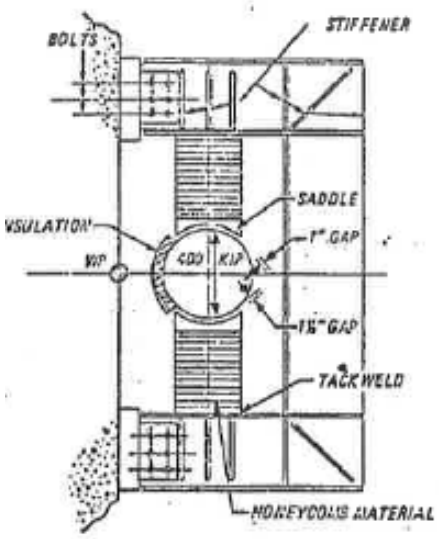

Fig III-6 (a)

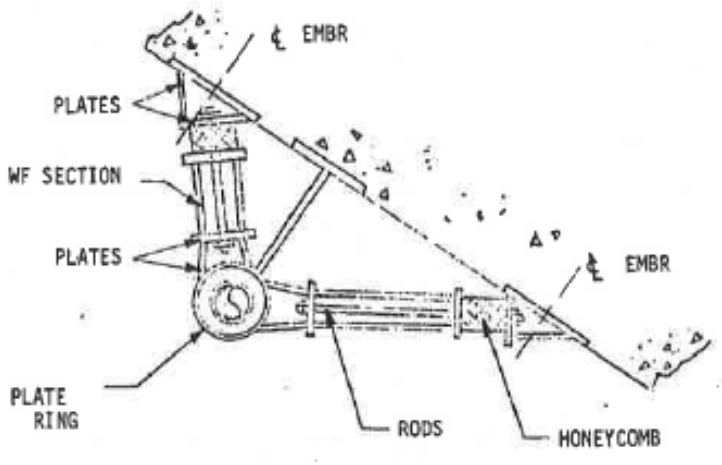

Fig III-6 (b)

Figure III-7. Typical Frame Restraints with Crush Blocks

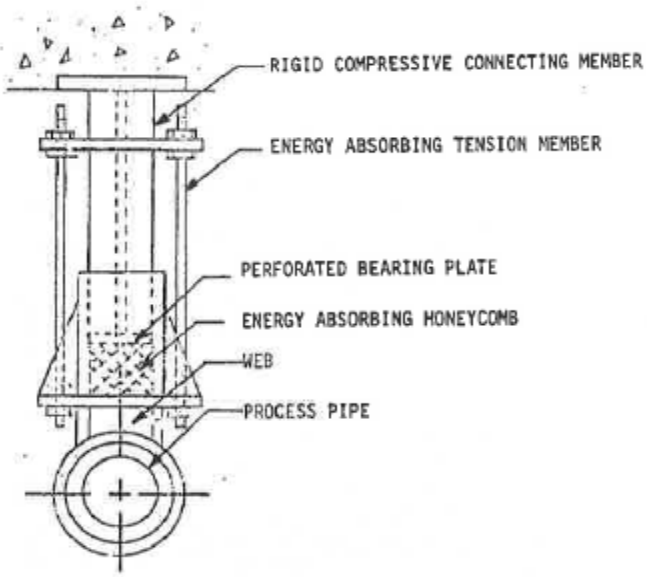

Figure III-8. Combination of Compression and Tension Energy Absorbing Device

III.6.1.4 Ring-bar Restraint

A ring bar restraint is shown in Figure III-9. The ring around the pipe restraints the pipe and the bars which connect the ring to the building structure absorb the pipe break energy by plastic deformation. This design is effective in all

directions and will function well if a pipe break occur. However, space requirements may prohibit the use of such restraint. Since mild steel bars are used as the yielding elements, relatively smaller ductility is available for energy absorption.

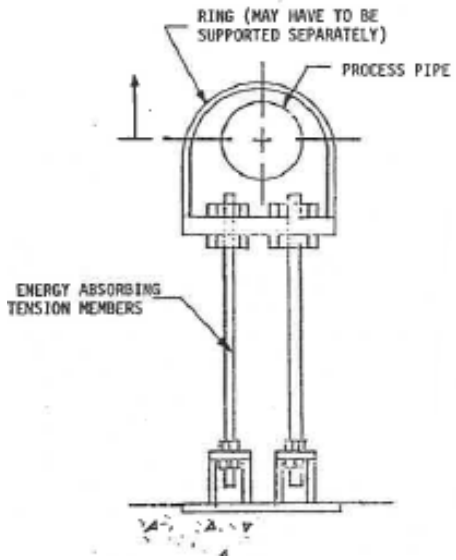

Figure III-9. Ring Bar Restraint

III.6.1.5 Pipe Crush Bumper

The pipe crush bumper (Figure III-10) is considered to be the most economical restraint design; the energy absorbing component is a standard pipe section. During a postulated rupture, the process pipe will impact the crush pipe causing indentation of the crush pipe, which thereby absorbs the impact energy. As the crush pipe is indented, it forms a well in which the process pipe is seated, causing the ends of the crush pipe to lift off the support, thus restraining sideway motions of the process pipe. The pipe crush bumper does not require precrushing and no special enclosures are required for the shipping, handling, storage or installation. The energy absorber (pipe) is far less sensitive to loading direction than many alternative devices. The assembly requires no supplemental or complicated structure and is assembled with relatively light weldment or bolting. The crush pipe utilizes up to 80 percent of its energy absorbing capability in compression.

Some of the advantages of the pipe crush bumper are:

- The fabrication and installation costs are much less than other systems.
- It simplifies in-service inspection of process pipe welds by its location and configuration.
- Material used are inexpensive and readily available.

The major disadvantages of this device is its bulkiness which allows its use only when space limitation is not a concern.

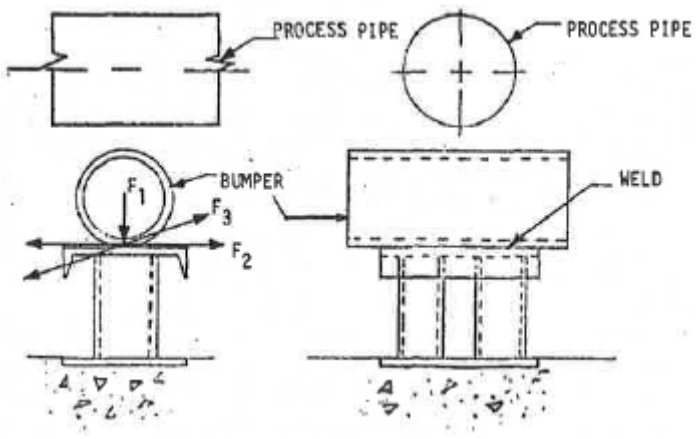

Figure III-10. Pipe Crush Bumper

III.6.2 Elastic Restraints

These are the restraints which are designed to stop the pipe without exceeding their elastic limit. Necessarily, the gap is small or zero (otherwise the dynamic load factor, DLF, would be large) and the resulting displacements are also small. Although this type of restraint is not very efficient, they have to be used where large pipe displacement cannot be tolerated or as required by the geometry and layout of the piping system.

III.6.2.1 Rigid Frame Restraints

These restraints were more commonly used in early projects; a typical rigid frame restraint is shown in Figure III-11.

Notable advantages of these type of restraints are as follows:

- It can be designed with sufficient lateral load capability, thus restraining the pipe in any direction.
- Resulting displacements are very small, thus limiting the break area and target area of the impinging jet.

On the other hand, it has several disadvantages:

- The restraint is usually too large, interferes with other systems and is more costly
- It is not flexible; once the restraint is installed, it is extremely difficult to remove it for in-service inspection.
- There is more heat loss possibility which reduces the plant efficiency and, at the same time, may create thermal problems in the supporting structure.
- The gap between the pipe and the restraint must be very small. The reason is that the DLF may become greater than 2.
- These restraints are highly rigid and thus may cause shearing and/or crushing of the impacting pipe which must be investigated.

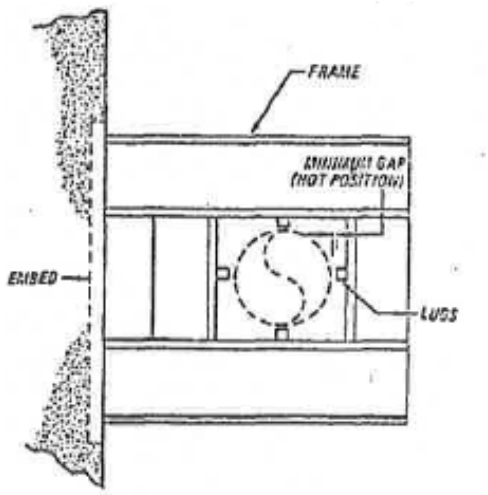

Figure III-11. Typical Rigid Frame Restraint

III.6.2.2 Cable Restraints

One of the earlier restraints designed is the cable restraint, as shown in Figure III-12. The behavior of this restraint is similar to those of the U-bar restraints except that the cable is intended to remain within the elastic range. This design is capable of containing the pipe regardless of the direction of the jet force. Since there is no gap between the cable and the pipe, the DLF in this system may be assumed to be 2. On the other hand, the cable has relatively less ductility, thus energy absorption capacity of the system is limited.

Figure III-12. Cable Restraint

III.7 U-bolt Design

Figure III-13 shows the standard U-bolt configuration and identifies the significant components and dimensions of the design. Each of the design dimensions must be selected within the specified limits so the results of the analysis are not invalidated. However, in some instances it is possible to deviate from the requirements if the effect can be shown to be negligible or if conservative design revisions can be incorporated.

III.7.1 Rod Diameter and Number of U-Bolts

For most designs the rod diameter and number of U-bolts it's established during initial sizing phase; however, sometimes inherent design conditions will negate the use of the specified number of U-bolts. A viable design solution can very often be worked out by increasing or decreasing the number; this can be accomplished without additional dynamic analysis if the change is accompanied by a corresponding change in the rod diameter. The only requirement is that the total rod cross-sectional area, remains unchanged so that the combined stiffness of the U-bolts is identical for both cases. An increase in the number of rods will dictate a decrease in the rod diameter, and viceversa.

III.7.2 U-Bolt Length

Experimental results have shown that the axial strain in the U-bolt rod is uniform along the straight portion and gradually decreases toward the bottom of the U portion.

Based on this observation, the effective length of the U-bolt, which is defined as an equivalent straight length of rod having identical cross-sectional area, material properties and stiffness, is taken conservatively as:

$L \leq L_1 + \frac{\pi}{4}R$

When rod splices are utilized in the design, an adjustment for the value of straight length, L_1, is necessary to account for the loss of effective length at the splice portion. The length from this equation must be at least as large as the value specified in the dynamic analysis.

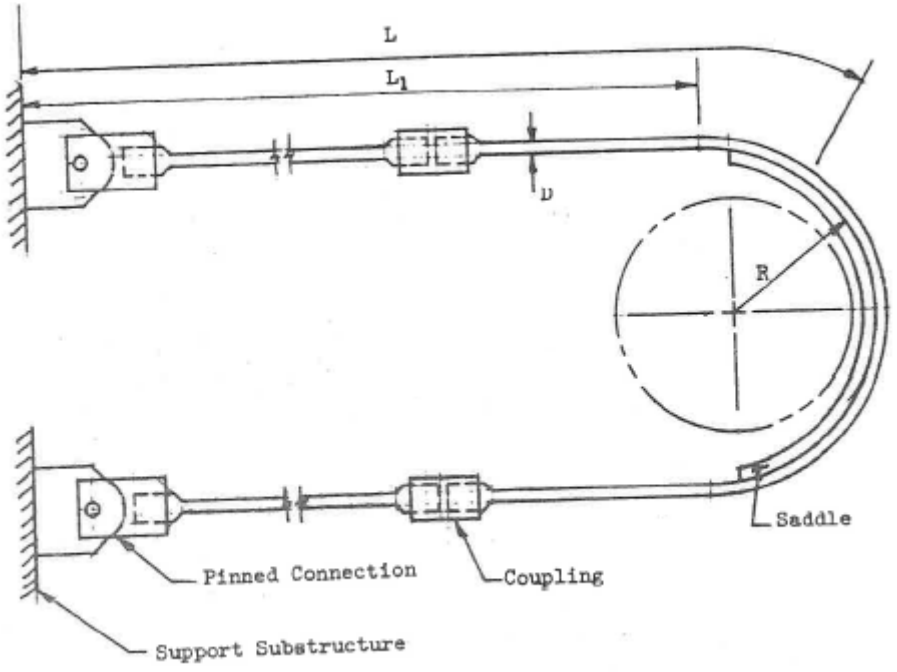

Figure III-13. Standard U-bolt configuration

III.7.3 U-Bolt Radius

The radius (R) of the U-bar is not specifically controlled by the design bases requirements, but it has an influence on the effective gap because it contributes to the take-up slack which is inherent in the U-bolt design. Therefore, the choice of this dimension must be consistent with the maximum effective gap (see III.3). Another primary consideration is to insure that the radius is large enough to allow uninhibited thermal movements of the pipe in all directions. Other considerations are pipe diameter, thickness of thermal insulation, tolerances, and design clearances. The following equation is used to determine the design radius:

$$R = OD/2 + C_t + T_i + T_s + \delta_t \qquad \text{Eq. 3.1}$$

The equation does allow some margin for deviations but does not guarantee that the effective gap requirement will be met. Installation and fabrication tolerances of ± 1/8'' has to be considered and accounted for in the determination of the design radius. Figure III-14 reports mentioned parameters.

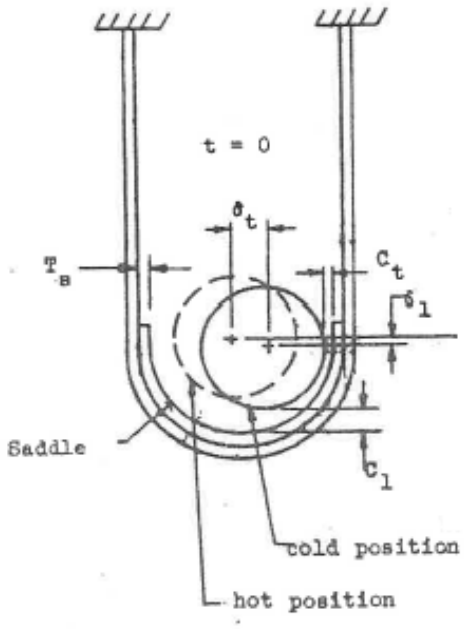

Figure III-14. Pipe and U-bolt Position

III.7.4 Rod attachment

The main requirements of the end attachments aside from transferring the rod loads are to provide longitudinal adjustment capability and freedom for end rotations. The U-bolt position relative to the pipe must be adjustable to account for fabrication and installation tolerances and to allow for inaccuracies of predicted pipe thermal movements and deviations of the exact pipe position. Rod ends must be free to rotate so, bending moments are not induced into the rods by angular changes which occur during take up of U-bolt slack. Rotations may also be caused by lack of perfect symmetry or by lack of parallelism between the blowdown force direction and the U-bolt line of action. End connection design has to be sized to transfer upper bound rod loads.

The basic elements of a pin connection for a U-bolt consist of an upset rod end, clevis, lug and pin. Restraint reaction loads are transferred to the support structure through

the upset end, clevis and lug, which is welded to the substructure. A typical arrangement of this type of connection is shown in Figure III-15.

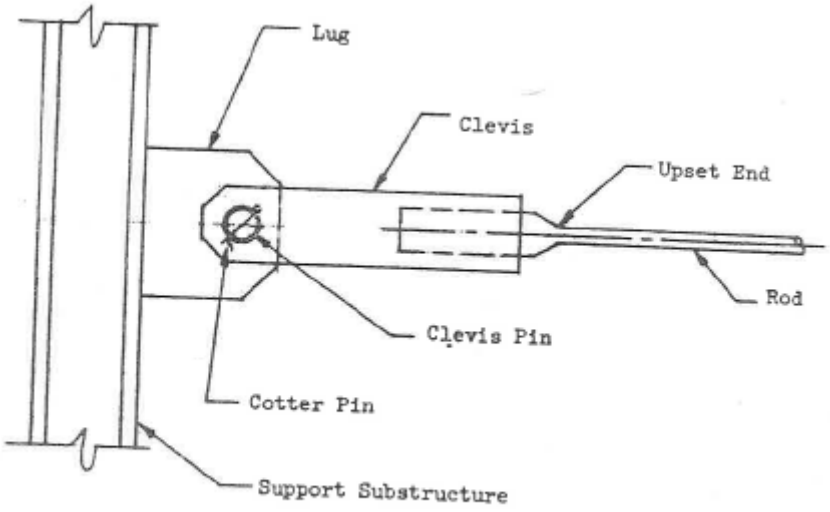

Figure III-15. End connection for U-bolt

III.7.5 Rod Splices

Because of rod availability and manufacturing limitations, field splices, may be necessary along the straight portion for some U-bolts. Also, splices may be required to facilitate installation where space limitations pose placement problems for single piece assemblies.

The use of cylindrical couplings provides a simple mechanical method for field splices. The coupling design loads are determined from upper bound rod loads. However, lower bound or guaranteed minimum coupling properties should be assumed for sizing purposes and the applied tensile stress should be kept below the material tensile yield. There is no special requirement to utilize 304 stainless steel; however if carbon steel is used, special precautions may be necessary to prevent corrosive action with the 304 rod material. The couplings are to be tapped and threaded to mate with the upset ends of the rods and should be at least four rod diameters long.

III.7.6 U-Bolt Saddles

A saddle, or pad, is usually provided at the pipe and U-bolt interface to distribute the loads on the pipe more uniformly, thereby preventing local collapse of the pipe. The saddles conform to the U-bolt contour and are attached to the rods with simple

clamps which are fabricated in the field from plate stock. Minimum width of the saddle is two times the rod diameter and minimum thickness is approximately one rod diameter. Since the saddle primarily supplies stiffness to the U-bar, the material selected need not be high strength; A36 carbon steel can be recommended.

Chapter IV: FE Model and Analysis

IV.1 Introduction

The study has been performed using ANSYS LS-DYNA; a general purpose nonlinear static and dynamic FEA program capable of analyzing highly explicit dynamic events and is appropriate for pipe whip and impact analysis. ANSYS LS-DYNA combines the LS-DYNA explicit finite element solver/program with the pre- and post-processing capabilities of the ANSYS program. The explicit method of solution used by LS-DYNA provides solutions for short-time, large deformation dynamics, quasi-static problems with large deformations and multiple nonlinearities, and complex contact or impact problems. Using this integrated feature, the whipping pipe and PWR structure can be modeled. In this thesis work a general ANSYS pre-processing tool has been used to model the whipping pipe and PWR structure, set loads and boundary conditions; LS-DYNA Solver to obtain the explicit dynamic solution, and the LS-Prepost post-processing tools to record the results. This interface between ANSYS and LS-DYNA seamlessly links the ANSYS pre- and post-processing software with the LS-DYNA explicit solver.

A series of pipe rupture tests has been performed at the Japan Atomic Energy Research Institute (JAERI) to demonstrate the safety of primary coolant circuits in the event of pipe rupture in nuclear power plants. Pipe whip tests and jet discharge tests have been conducted under boiling water reactor (BWR) and pressurized water reactor (PWR) loss-of-coolant accident (LOCA) conditions. (Ref. 9.)

The numerical study simulates two of these tests performed between 1979 and 1982 under BWR LOCA conditions for a 6” and 4” pipe (FRPC-II, RUN 5606 & 5501).

IV.2 RUN 5606 Test Condition, Input to the ANSYS FEM

A brief description of the test facility is reported in this section; the profile of the testing system is shown in Figure IV-1. Test pit and plant room are divided by a wall. An auxiliary connecting pipe which reduces the diameter of the 8 in. nozzle to the diameter of the 6 in. test pipe is attached to the nozzle of the pressure vessel. An electric heater and a pressure vessel are used to heat up water to BWR LOCA conditions, which are kept constant in a system by a circulating pump. The water level is set at the height of 4 m from the bottom of the pressure vessel just before the blowdown.

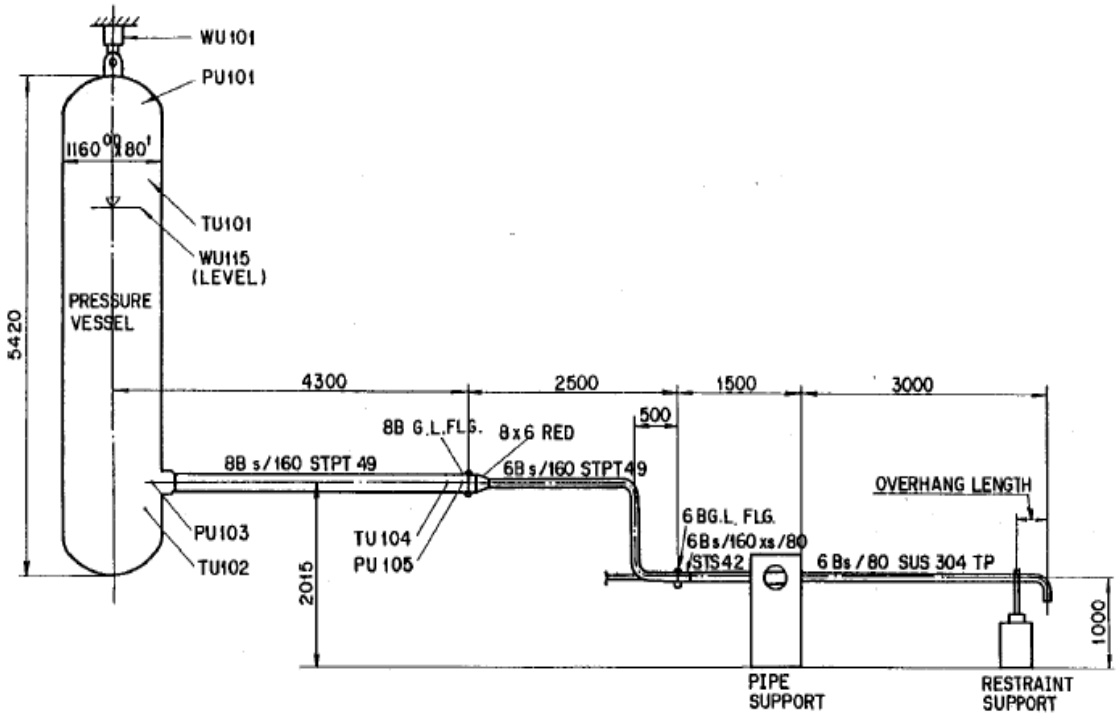

Figure IV-1. Pipe Line Layout of Pipe Whip Test

The test pipe is connected to the auxiliary connecting pipe and is 4500 mm in length and is fixed by the pipe support so that the length of the test section is 3000 mm.

Test conditions are summarized in Table IV-1. The test pipe is made of Type 304 stainless steel, and its outer diameter is 165.2 mm and its thickness is 11.0 mm. The restraints are made of Type 304 stainless steel, and its diameter is 16.0 mm. Two restraints were set on the restraint support with clearance of 100 mm.

The chemical composition and mechanical properties of the pipe and restraints are summarized in Table IV-2.

Run Number		[redacted]	5606
Test Number		[redacted]	6BW2
Date		[redacted]	'81.8.6
Pressure (MPa)		[redacted]	6.76
Temperature (℃)	Vessel	[redacted]	284.7
	Test Section	[redacted]	282.9
Diameter of Test Pipe		6B, sch 80	
Length of Test Section		3000 mm	
Restraint	Type	U – bar	
	Overhang (mm)	[redacted]	700
	Clearance (mm)	100	
	Diameter (mm)	16	
	Number	2	

Table IV-1. Test Condition

(a) Test Pipe (Room Temperature)

%

C	Si	Mn	P	S	Ni	Cr
0.05	0.47	1.50	0.029	0.005	9.30	18.40

Yield Strength	Tensile Strength	Elongation
264.6MPa	597.8MPa	66%

(b) Restraint (Room Temperature)

%

C	Si	Mn	P	S	Ni	Cr
0.04	0.46	0.89	0.032	0.025	8.10	18.30

Yield Strength	Tensile Strength	Elongation
287.1MPa	649.7MPa	61.8%

Table IV-2. Chemical Composition and Mechanical Properties

The details of the restraint are shown in Figure IV-2. The restraint is composed of a U-bar, bearing plate, clevis, bracket and pin. The clevis is screwed to the end of the U-bar and is used for fine adjustment of clearance. The bearing plate made of carbon steel is attached to the inner side of the circular part of the U-bar. The purpose of this plate is

to wrap around the test pipe to minimize pipe rebounds. Restraint assemblies are pinned to the bracket which is set on the restraint support.

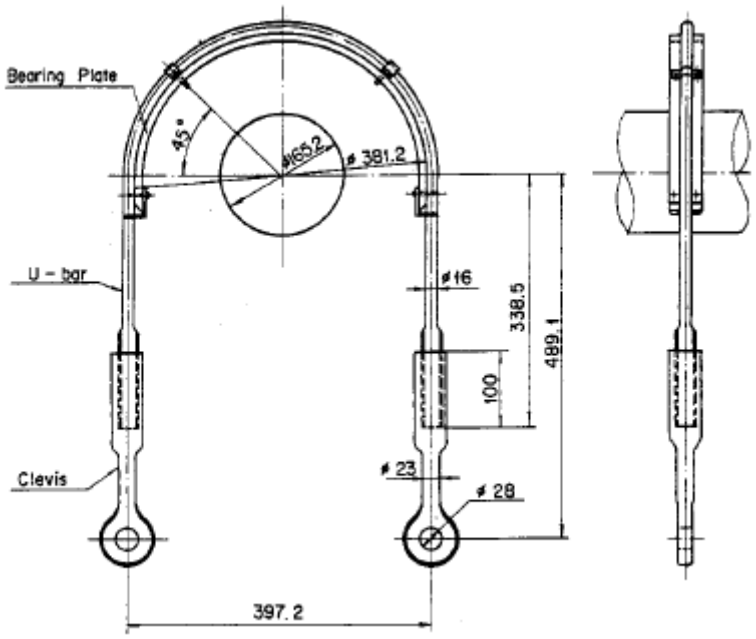

Figure IV-2. Details of Restraint

IV.3 Modeling RUN 5606. Theory and Implementation

The dynamic response of structural systems is the direct numerical integration of the dynamic equilibrium equation of motion which, is defined as mass times acceleration equals external forces minus internal force.

$$M \cdot \ddot{u} = P - I \qquad Eq.4.3$$

The explicit dynamic integration method is fundamentally involved with the solution of a set of linear equations at each time step to predict a solution at time "t+Δt" using a mathematical technique for integrating the dynamic equilibrium equation through time. The explicit methods are conditionally stable with respect to the size of the time step; therefore, a very small time step size is required to obtain a stable solution. The advantage of using an explicit dynamic analysis is for its ability to solve a highly discontinuous, high-speed dynamic problem without much iteration since no formal matrix factorization is necessary during each time step; while for these type of events an implicit solver would have been very time consuming.

The general purpose of the explicit dynamic finite element LS-DYNA Solver program is used to obtain the response characteristics of the pipe whip, pipe impact and PWR.

IV.3.1 Piping System and Pipe Whip Restraint

Meeting the input data presented before (piping layout, piping geometries, physical properties of the pipe, and pipe whip restraint detailed information) the following procedure was performed.

IV.3.1.1 Pipe Geometry

The pipe geometry was drafted using the solid modeling features of the ANSYS software (keypoint , lines and areas).

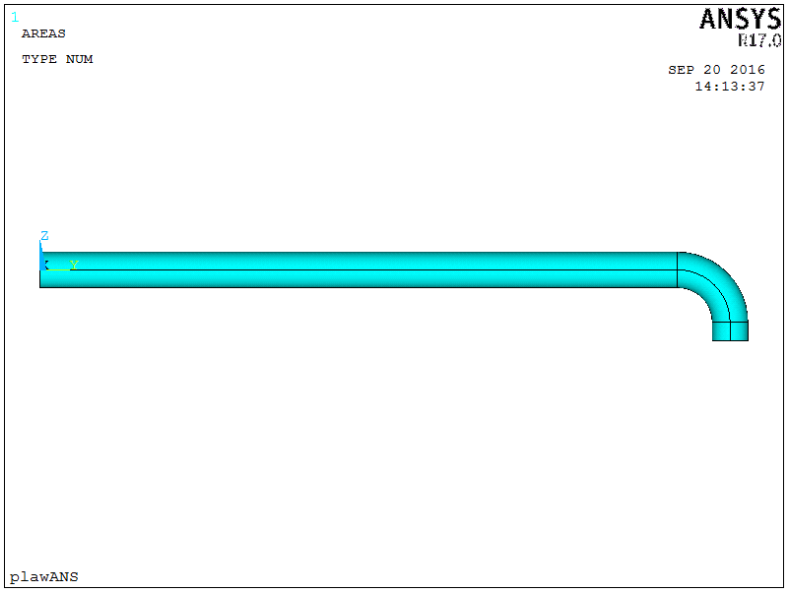

Figure IV-3. Pipe Geometry

IV.3.1.2 Element Type

SHELL163 element type was chosen for the pipe on the basis of the outside diameter to thickness ratio (D_o/t); it is a thin structural 4-node shell element with 12 degrees of freedom (6 displacement, 3 velocities, 3 accelerations) at each node. The integration points were set to 5 through the thickness; Figure IV-4 shows his geometry [Ref. 20].

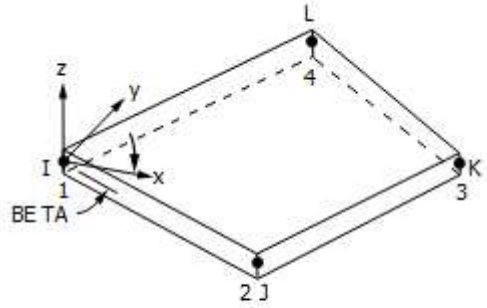

Note: x and y are in the plane of the element

Figure IV-4. Shell163 Geometry

Contrariwise BEAM161 element type has been chosen to model the U-bolts; the geometry, node locations and the coordinate system for this element are shown in Figure IV-5 [Ref.20].

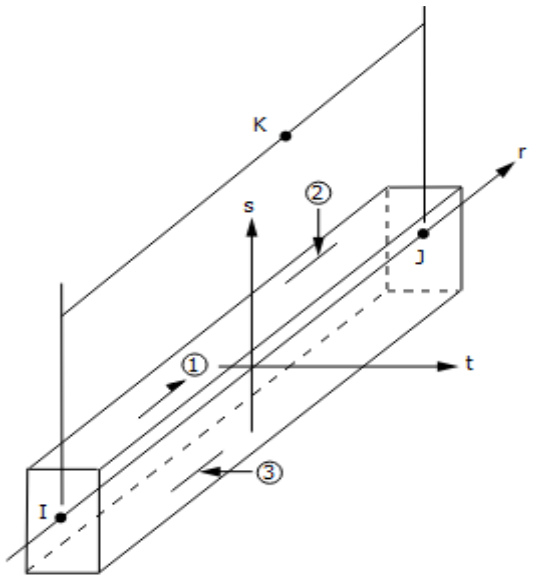

Figure IV-5. Beam161 Geometry

IV.3.1.3 Material Properties

Effort was needed to appropriately model the material behavior during the collision, under high strain rate conditions. Several tests were indeed performed with different stress-strain behavior; a piecewise linear plasticity law which takes into account for the strain rate dependency of the stress-strain curve after yielding of material has been finally implemented.

As reported in Ref. 17, the tensile test results of pipe and restraint materials are shown in Figure IV-6 to Figure IV-8 and are summarized in Table IV-3. Proof stress $\sigma_{0.2}$ and strain hardening modulus E_T are obtained from these stress-strain curves.

It's important to note that in order to take into account the weight of the fluid an equivalent density was added in the calculation:

$$\rho_{eq.} = \frac{\rho_{fluid} A_{fluid}}{A_{tot}} \qquad Eq.4.4$$

The parameters used in the analysis are reported in Table IV-4.

No.	Material	Temp.	$\sigma_{0.2}$	σ_u	ψ	E_T
1	Restraint	R. T.	30.2	75.0	60.9	162.5
2	Pipe	R. T.	23.0	62.6	57.0	242.5
3	Pipe	285℃	17.7	46.4	35.9	282.5

$\sigma_{0.2}$: Proof stress Kg/mm²

σ_u : Tensile strength Kg/mm²

ψ : Elongation %

E_T : Strain hardening modulus Kg/mm²

Material is Type 304 stainless steel

Table IV-3. Conditions and Results of Tensile Test

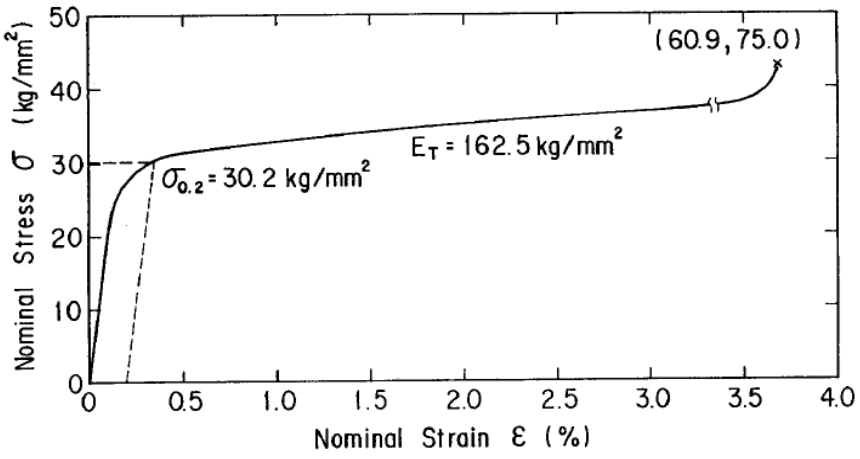

Figure IV-6. Tensile Test Result of Restraint Material's Specimen at R.T.

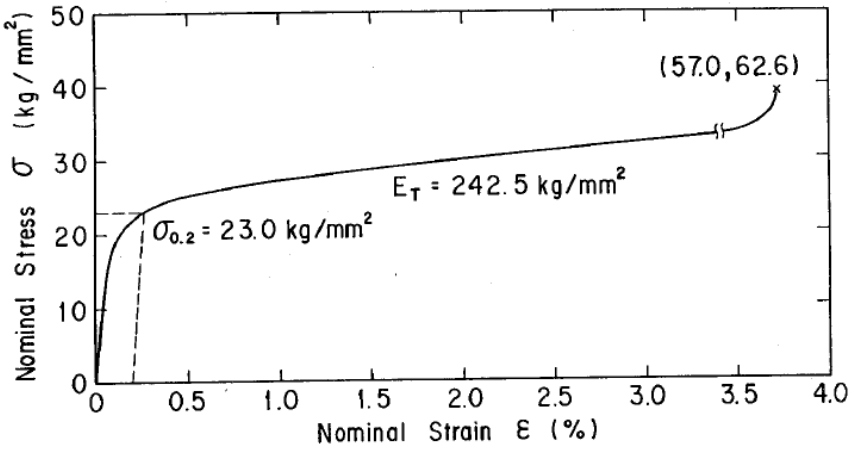

Figure IV-7. Tensile Test Results of 6 in. Pipe Material's Specimen at R.T

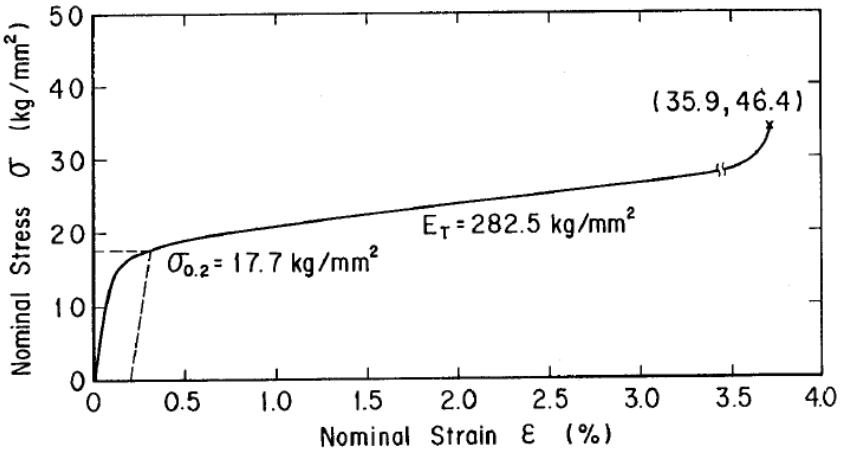

Figure IV-8. Tensile Test Results of 6 in. Pipe Material's Specimen at 285°C

Material properties used (SI units)		
E_{pipe}	178 e9	Pa
E_{restr}	195 e9	Pa
ρ_{eq}	594	Kg/m^3
ν	0.3	-
ρ_{fluid}	790	Kg/m^3
ρ_{steel}	7750	Kg/m^3
A_{fluid}	0.0161	m^2
A_{tot}	0.0214	m^2

Table IV-4. Implemented properties

In the following subsections a detailed description of the damping and the plasticity law chosen is reported.

IV.3.1.3.1 Damping

Damping is needed to minimize unrealistic oscillations in the response of a structure during transient dynamic analysis, both mass-weighted (alpha) and stiffness-weighted (beta) damping can be applied in ANSYS LS-DYNA using the EDDAMP or MP,DAMP command.

According to the US NRC Regulatory Guide 1.61 [Ref 18], its indicated that the damping ratio of 2-4% is acceptable for pressure vessel and/or piping (metal structures without joints). However 2% damping has been used to maintain conservatism. In ANSYS LS-DYNA, the only applicable regime is Rayleigh damping. This scheme applies a damping coefficient to the stiffness matrix and a separate damping coefficient to the mass matrix. A numerical method can be developed to determine the two Rayleigh damping coefficients as a function of the first and final mode using the damping ratio of 2%.

Alpha and Beta damping are the stiffness and mass proportional damping constants. The effective way to determine the damping coefficients is to use the lowest natural frequency and the highest frequency of interest and the corresponding damping ratios. For most of the engineering structures, the number of significant modes by which almost 95% of the mass has participated is usually around 3 at the minimum and about 25 at the maximum.

The structural damping, ζ_i, is then given as a function of frequency by the following formula:

$$\zeta_i(f) = \alpha/4\pi f + \pi\beta f$$

To verify the Rayleigh Equation is satisfied, meaning that all structural natural modes between frequencies f_1 and f_2 will have damping less than at modes f_1 and f_2 and that damping levels are appropriate, Figure IV-9 is provided.

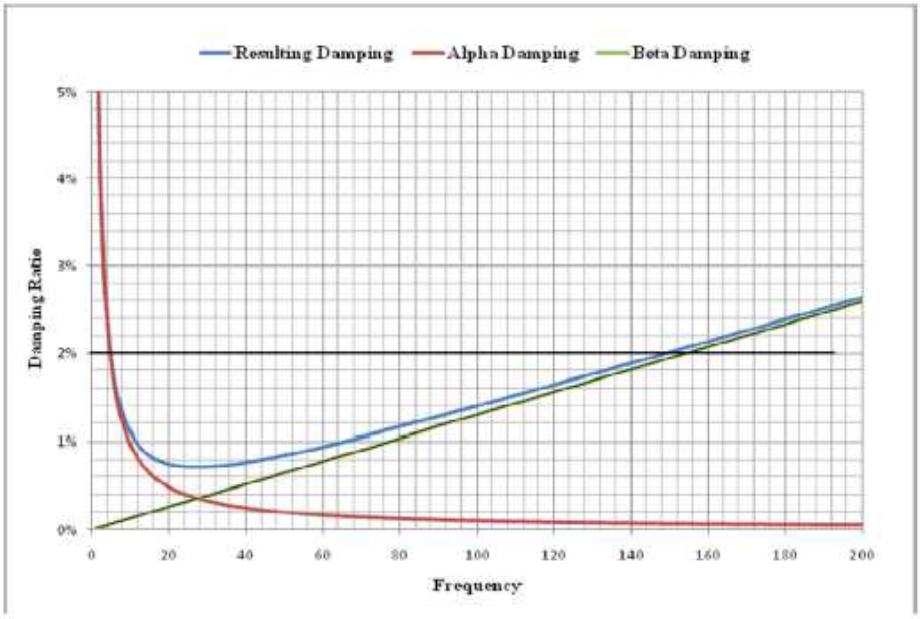

Figure IV-9. Resulting Rayleigh Damping as a Function of Frequency

The α and β damping coefficients are chosen to have a ζ = 2% damping for the frequencies f_1 = 5Hz and f_2 = 150 Hz: α = 1.22; β = 4.12e-5.

The modal analysis has been performed exploiting ANSYS capabilities, Figure IV-10 and Figure IV-11 (Appendix C). It has been observed that the first natural frequency of the modeled pipe is about 10.3 Hz, while for the restraint it has a value of about 73.0 Hz; these values are obtained placing an elastic BEAM188 element at pipe tip to better match the dynamic behavior of test pipe itself (initially the rigidity of the test pipe was greater than the model's one because of the presence of the pipe support at the beginning of the test section; placing this elastic element the modal behaviours were matched); these are very close to JAERI's experimental results, Table IV-5.

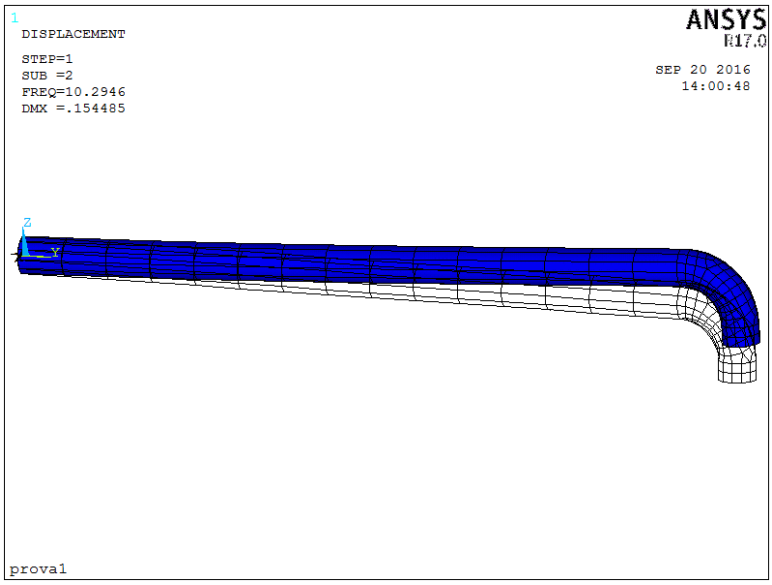

Figure IV-10. Natural Frequency of Test Pipe

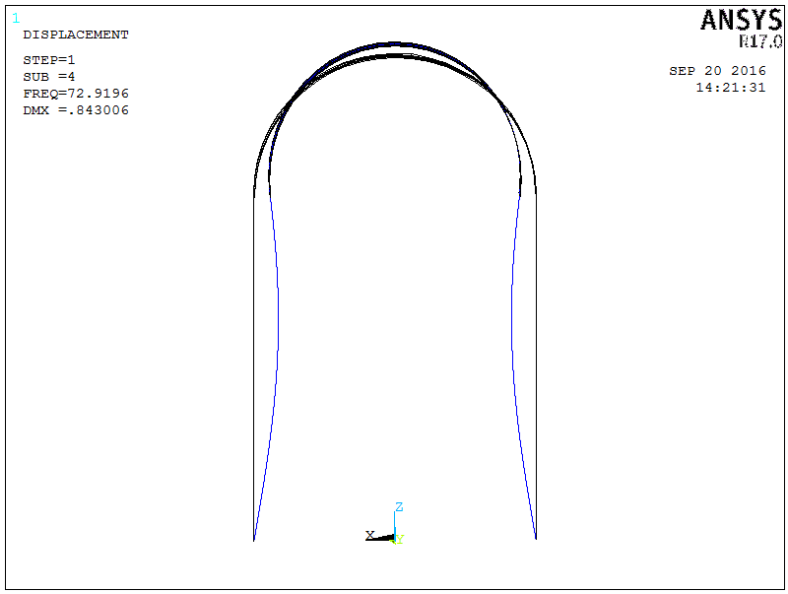

Figure IV-11. Natural Frequency of Restraint

	1	2	3	4
Restraint (Exp.)	10.5	74.0	235.0	630.0
Pipe (Exp.)	10.5	74.0	188.0	372.0
Pipe (Exp.)	16.8	105.8	294.9	578.0

Table IV-5. Natural Frequency of Pipe and Restraint

IV.3.1.3.2 Plasticity Law

Different tests were performed using divers material behavior; in particular the recommendations in 6.6.3 of Ref. 2 were exploited, together with a bilinear kinematic hardening trend of the stress-strain curve which was eventually found to be unrealistic, but finally the most accurate method with respect to the experimental results was the one which implements the Piecewise Linear Plasticity law below described.

As cited, modelling of material behavior under impact condition is crucial to catch the test results in terms of energy, displacements and strains; the Piecewise Linear Plasticity Law implemented provides a multi-linear elastic-plastic material option that allows stress vs. strain curve input and strain rate dependency.

This is a very commonly used plasticity law, especially for steel. Failure based on plastic strain can also be modeled with this material model.

The piecewise linear plasticity model provides different methods to account for the strain rate; the one exploited in this work utilizes the Cowper-Symonds model, which scales the yield stress as shown:

$$\frac{\sigma_{dyn}}{\sigma_{stat}} = 1 + \left(\frac{\dot{\varepsilon}}{D}\right)^{\frac{1}{p}} \qquad \text{Eq. 4.5}$$

Where $\dot{\varepsilon}$ is the effective plastic strain rate, and D and p are strain rate parameters. A sensitivity analysis has been performed on these two parameters and their influence in the Cowper-Symonds formula has been outlined (Appendix D). The chosen parameters are reported in Table IV-6. [Ref. 19].

	Pipe	Restraint
D	100	70000
q	10	3

Table IV-6. Cowper-Symonds Parameters

IV.3.1.4 Meshing

In ANSYS LS-DYNA element type, the specified mesh density in a FEM has great influence on the development and quality of the calculative result, especially the mesh density between two contact areas. If the mesh density is too coarse (small number of elements within a part), it's hard to satisfy the calculation accuracy. While if the mesh density is too fine (large number of elements within a part), it's possible to artificially increase the stiffness in local area of the model, and it is harder to astringe the result eventually. Therefore, it is important to choose a suitable mesh density which is not too coarse or too fine. A finer mesh density shall be used for the contact elements in comparison to the target elements or a uniform element size throughout the model can also be used for achieving appropriate and efficient results. Figure IV-12 reports the meshed pipe.

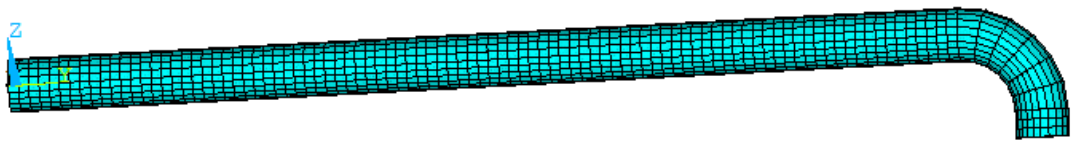

Figure IV-12. Meshed Pipe

Each individual discrete element defined by the mesh density also has an aspect ratio. The aspect ratio is defined as the ratio of the longest dimension to the shortest dimension of a discrete quadrilateral element. The aspect ratio of each discrete element also works in conjunction with the mesh density, as the aspect ratio increases, the accuracy of the solution decreases. As a general rule, the aspect ratio for each discrete element should be between one and three. Both the mesh density of the discrete elements creating a part and the aspect ratio of each individual discrete element are required to be coordinated to obtain an adequate and accurate FEM for solution. Shown in Figure IV-13 is the examples of a different aspect ratio.

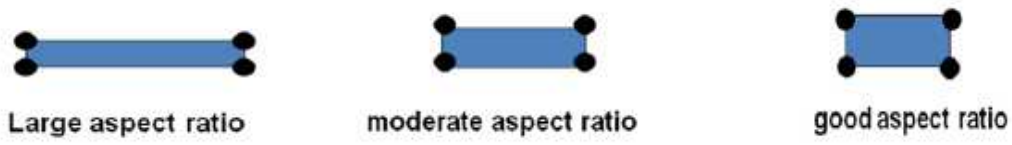

Figure IV-13. Aspect Ratio

IV.3.1.5 Hourglassing

Hourglassing is another important issue encountered during the analysis; it's a zero-energy mode of deformation that oscillate at a frequency much higher than the structure's global response. Hourglassing modes result in stable mathematical states that are not physically possible. They typically have no stiffness and are indicated graphically by a zigzag deformation appearance to a mesh. Figure IV-14 represents hourglassing due to mesh instability.

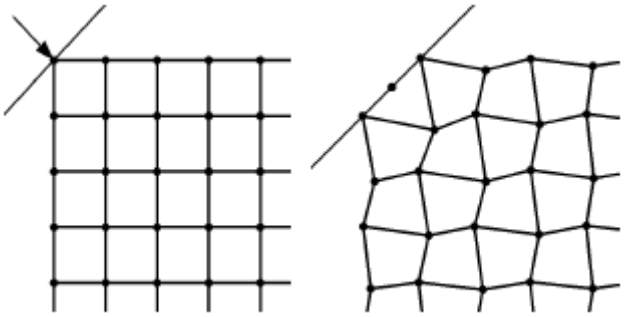

Figure IV-14. Illustration of Mesh Instability (Hourglassing)

Hourglassing should be checked, reduced/controlled and if is feasible or possible, it should be avoided by any available method. Two of the common hourglassing control methods are; 1) perform the analysis with an element formulation using a full integration method or 2) perform the analysis by using the hourglassing control element. The occurrence of hourglass deformations in the analysis can invalidate results. If the overall hourglass energy is more than 10% of the total internal energy of a model, there is likely a problem with the analysis in terms of mesh instability.

IV.3.1.6 Contact Definition and Algorithm

A contact is defined by identifying all possible locations that could come in contact (when an external surface of a body contacts with itself or the external surface of another body) and penetration that occur during the analysis. ANSYS LS-DYNA offers a large number of contacts types. Some types are for a certain specific application and others are suitable for more general use. In pipe whip impact and pipe whip restraint analysis, the appropriate contact type fall into the automatic single-surface type of contact algorithm. In pipe whip and pipe whip impact analysis, the deformations can be very large and predetermination of where and how contact will take place may be difficult to predict. The automatic single-surface algorithm options are recommended as these contacts are non-oriented which is more suitable for the pipe whip impact applications. For this reason the automatic contact family has been used to handle the beam-to-shell and shell-to-shell contact situation encountered. The automatic contact types takes into account for thickness offsets, hence appropriate gaps between PWR geometry and its plate have been counted in order to prevent the initial penetrations in the initial contact surfaces.

Figure IV-15 and Figure IV-16 show the final model of pipe and PWR in ANSYS and Ls-Prepost respectively.

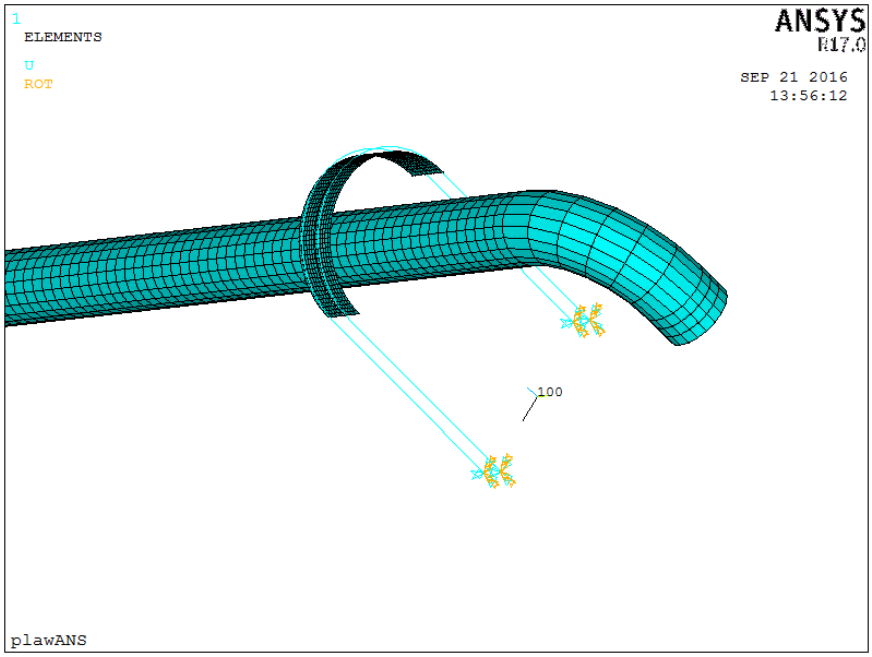

Figure IV-15. Pipe, PWR and Bearing Plate

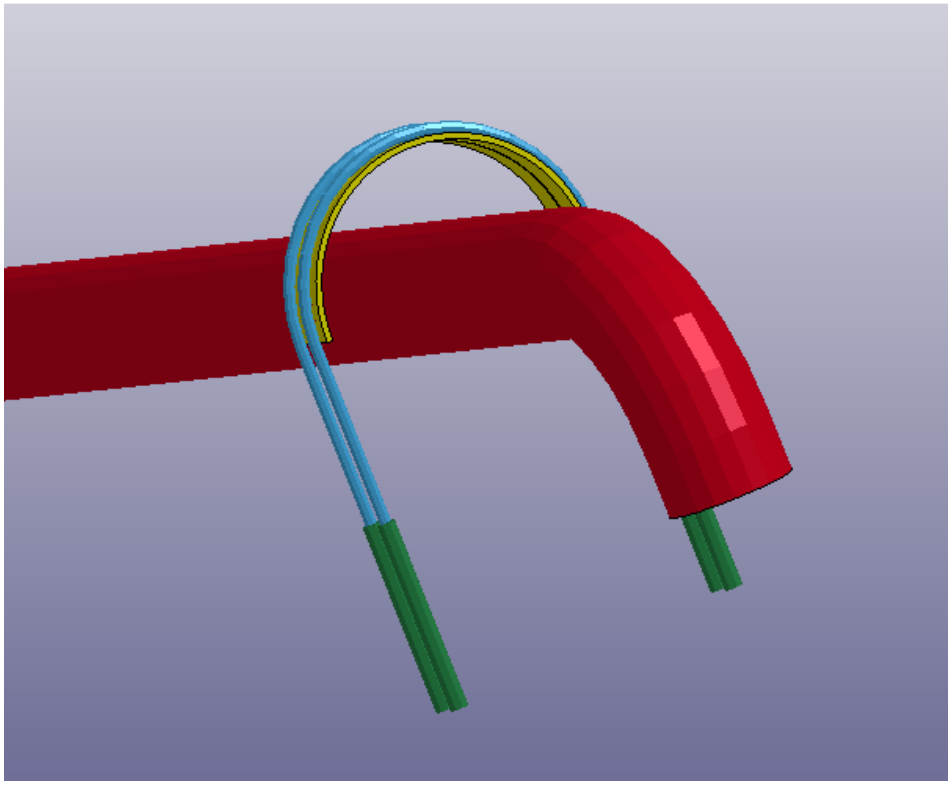

Figure IV-16. Pipe Whip Set-up Model

IV.3.1.7 Constraints

The pipe has been attached to an anchorage (all the 6 degrees of freedom are restrained). This anchorage is constrained as a “nodal rigid body” to the very first section of the pipe and is in turn fully constrained at its end; Figure IV-17.

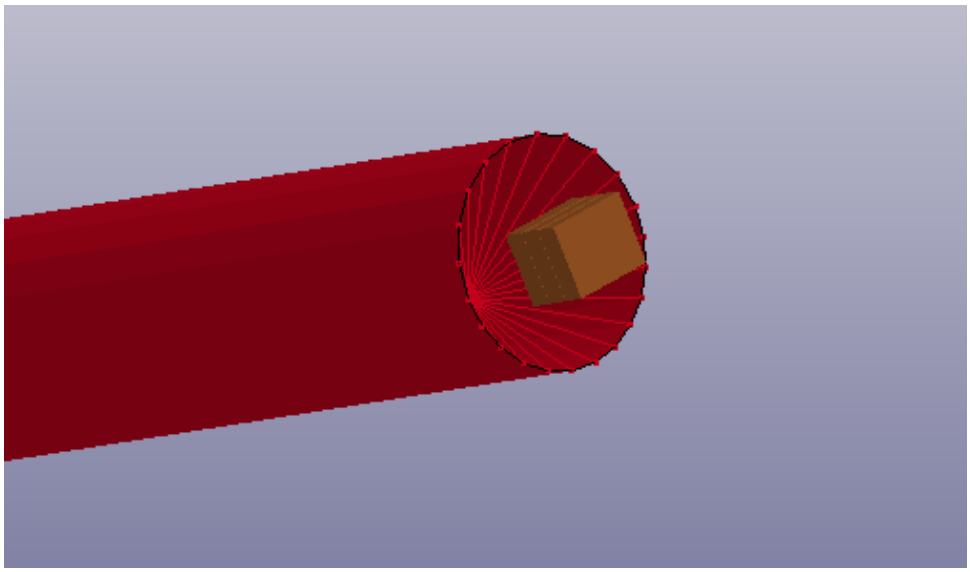

Figure IV-17. Anchorage

The PWR, as seen, is pinned to the bracket, so only one degree of freedom (y rot.) is available at its ends (all the other DOF are restrained). PWR and bearing plate are pinned together by means of several “rivet” components, Figure IV-18 and Figure IV-19.

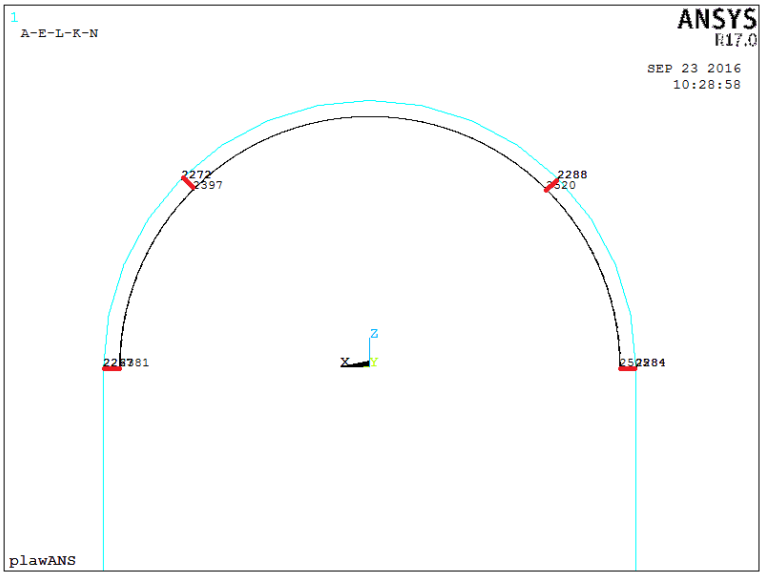

Figure IV-18. Rivets between PWR and Plate I

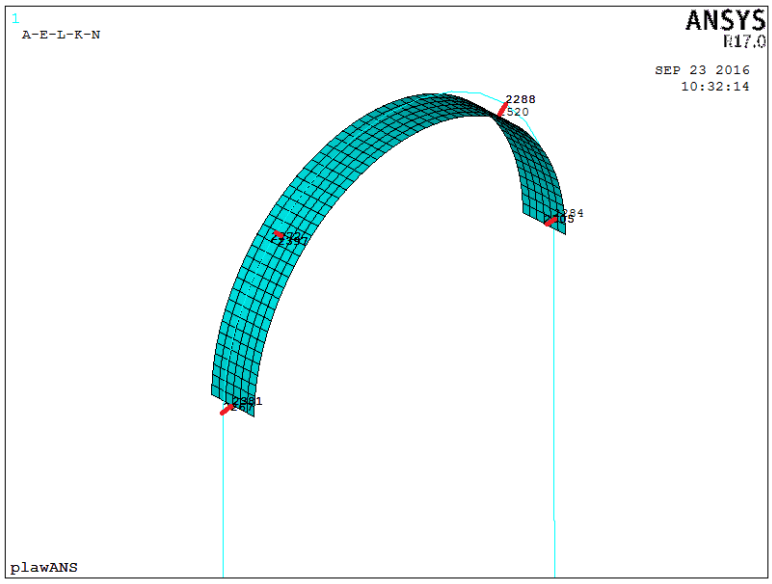

Figure IV-19. Rivets between PWR and Plate II

IV.3.2 Applied Force

Unlike an implicit static analysis , an explicit dynamic analysis must have all loads applied as a function of time. The applied load concept of many standard static ANSYS loading does not apply in ANSYS LS-DYNA. There is a unique procedure for applying loads in an explicit dynamic analysis using two array parameters. One array is for the time values and the other array is for the loading conditions.

The fluid thrust force time-history has been obtained from both a simplified method following ANS 58.2-88 (see II.2.3) and a more detailed decompression transient analysis derived from RELAP5 code. The thrust force has been applied to a massless node located at the center of pipe at the location of the pipe break plane; Figure IV-20. This node is connected to the structure with a nodal rigid body constraint.

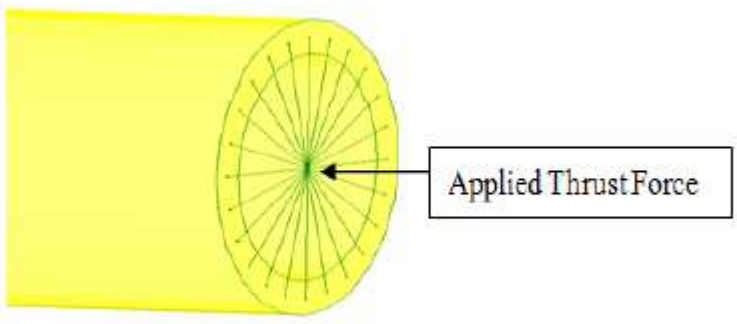

Figure IV-20. Applied Thrust Force for Circumferential Type Break

The thrust force representing a circumferential type break should be applied such that it follows the rotation of the pipe normal to the exit plane, Figure IV-21.

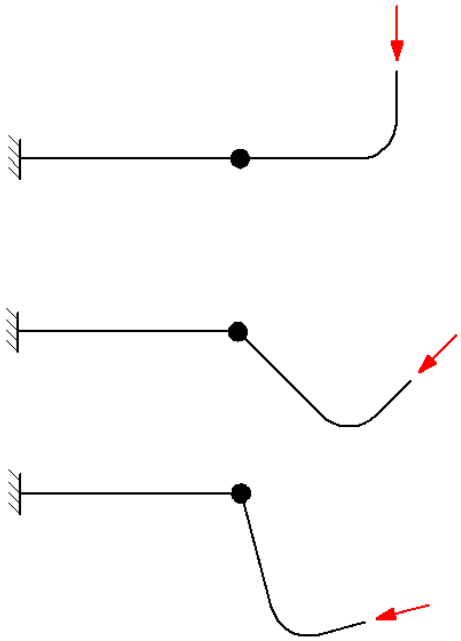

Figure IV-21. Follower Force

This concept is referred to as the "Follower Force". The follower force capability is not directly supported by ANSYS LS-DYNA interface. Therefore, in order to capture the effects of the follower force, the LS-DYNA keyword file (.k) has been directly modified under the *LOAD_NODE_SET command then solved explicit solution using LS-DYNA solver.

Following steps were performed to compute the thrust force.

IV.3.2.1 Thrust Coefficient, C_T

As shown in Section II.2.3 the thrust coefficient is used to determine the steady state force in accordance with ANS 58.2. Friction effects deriving from pipe geometry are to be taken into account for the analyzed test condition; the global friction coefficient can be calculated as follows:

$$f\frac{L_{pipe8"}}{D_{8"}} + f\frac{L_{pipe6"}}{D_{6"}} + 3K_{elbow} + K_{reduc} = 1.68 \qquad Eq.4.6$$

Table IV-7 is provided.

f	0.01
$L_{pipe8"}$	3.72 m
$D_{8"}$	0.2 m
$L_{pipe6"}$	7 m
$D_{6"}$	0.15 m
K_{elbow}	0.3
K_{reduc}	0.13

Table IV-7. Relevant Data

Knowing this value and the fluid stagnation enthalpy value (about 480 BTU/lb), Figure IV-22 can be exploited in order to obtain the thrust coefficient, C_T:

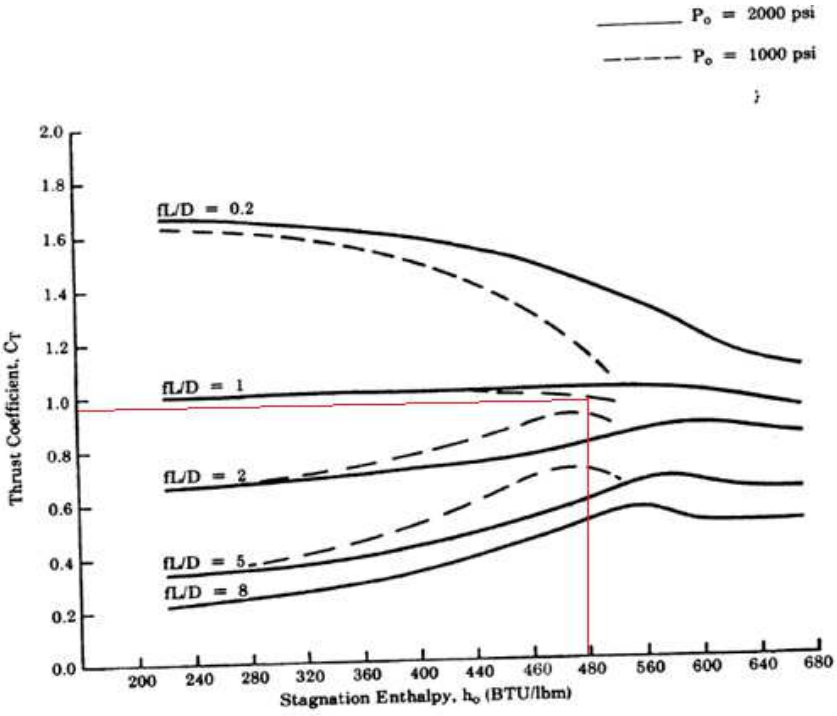

Figure IV-22. Subcooled Water Blowdown Thrust Coefficient as a Function of Stagnation Enthalpy and Pipe Friction

A value of about 0.97 is extracted which returns a thrust force of approximately 105.5 kN (Eq. 2.4); this is the steady state value of the thrust.

IV.3.2.2 Internal pressure

The experimental pressure trend has been implemented as internal load vector in ANSYS LS-DYNA, in fact it has been observed that it has an important effect limiting the ovalization of the cross section at the plastic hinge location. Figure IV-23 shows the internal pressure acting inside the pipe.

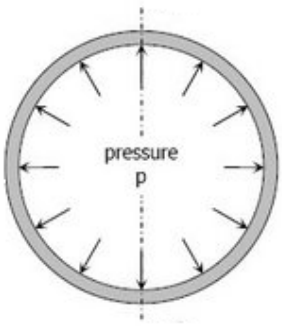

Figure IV-23. Internal Pressure

IV.3.2.3 RELAP5 Noding Scheme

A RELAP5 model was performed in order to have a more detailed time-history at the break location. A sketch of the model is shown in figure below which reproduce the 4 m^3 tank together with piping layout. Internal volumes and junctions in which the code solves mass, energy and momentum equations of the assigned problem are reported in the draft. Every junction has its own hydraulic loss coefficient as well as every pipe has its internal roughness. The surrounding (atmosphere) is represented by a time-dependent volume with theoretically infinite capacity (constant temperature and pressure).

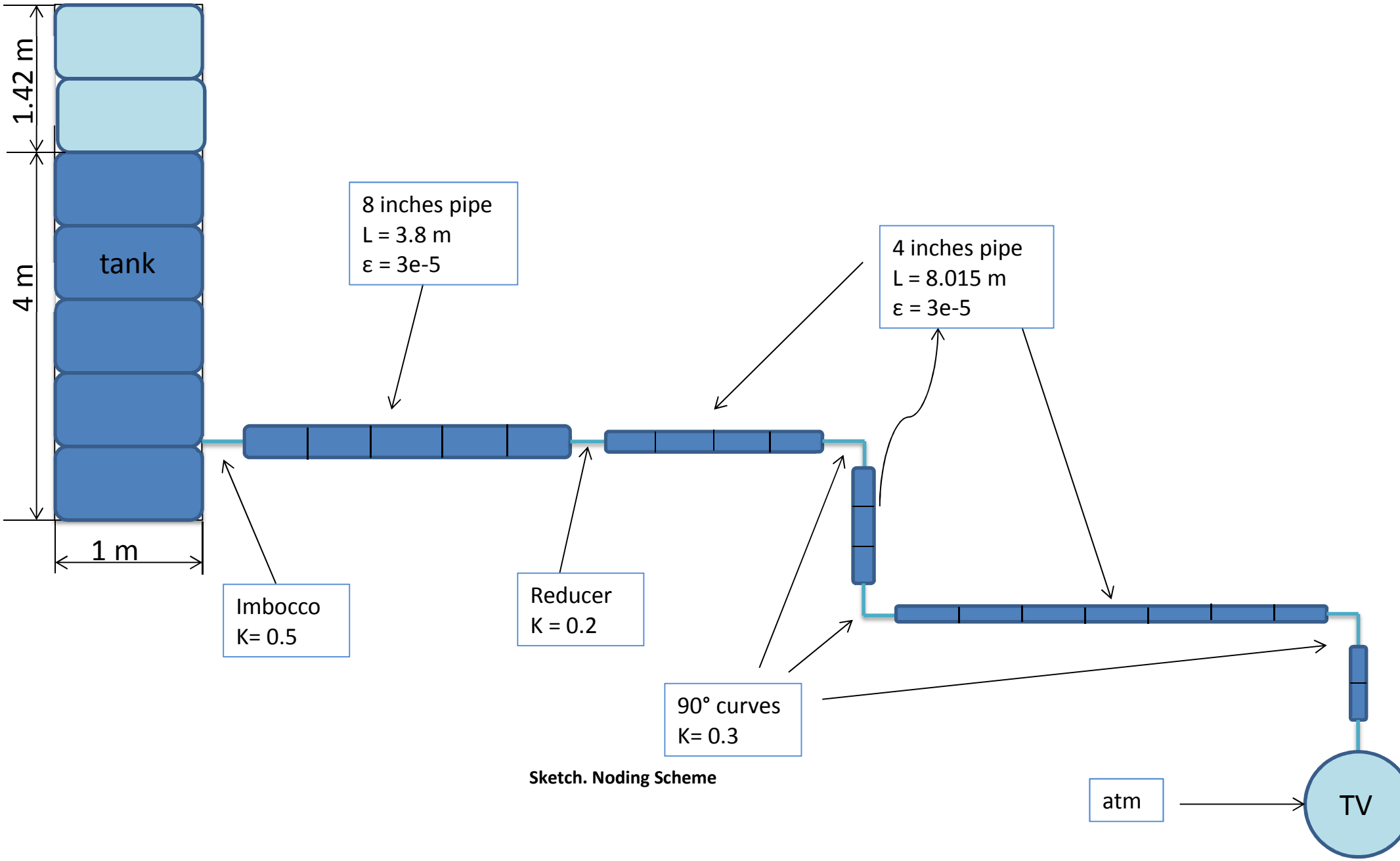

Sketch. Noding Scheme

IV.3.2.4 Discharge model

Various discharge models [Ref. 11] encoded within RELAP5 have been exploited in order to meet with more precision the depressurization trend given by test conditions. Henry-Fauske frozen homogeneous chocking model was chosen amongst the others as the more precise.

IV.3.2.5 Initialization

The initialization of the problem has also been changed from a pressure-temperature initial state to a pressure-quality condition defining the layout before opening occur. The two cases gave practically same results and the second was then adopted.

IV.3.2.6 Opening time

Another important parameter was the opening time of the motor valve junction mimicking the break point of test pipe. Following ANS 58.2 Section 6.2.3 [Ref.2] Standard recommendations the opening time has been varied from 1 ms up to 10 ms; the sensitivity analysis has suggested the 10 ms case as the more precise simulating the full opening of the rupture disk located at the end of the test pipe itself.

IV.3.2.7 Jet thrust

The simplified jet thrust formulation (Eq. 2.2) was finally implemented as a control variable inside the Code and the acting force was eventually plotted, Figure IV-24.

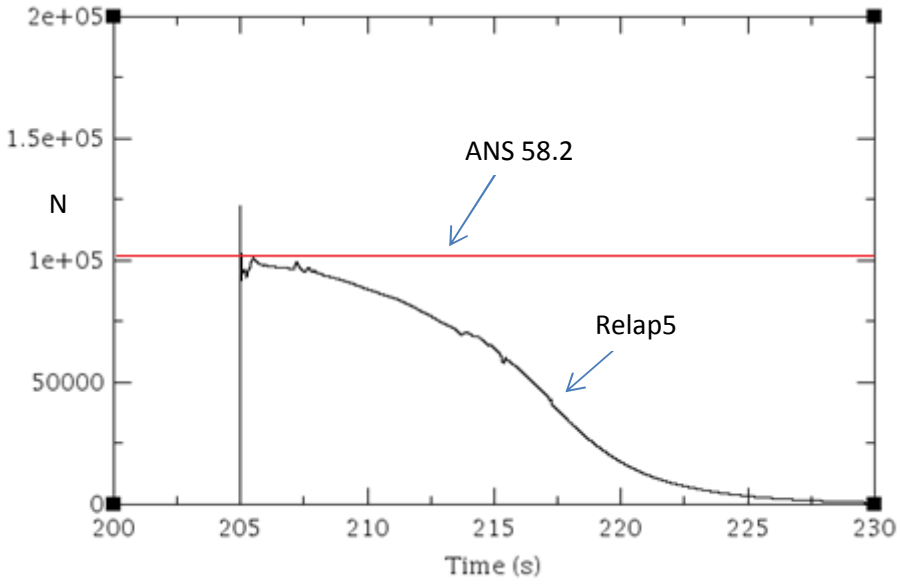

Figure IV-24. Thrust Force Trend, Run 5606 Simulation

It can be seen that there is a sharp peak just after the opening occur which is proved to be inversely proportional to the opening time of the valve and takes place in less than 2.4 ms.

These data have been imported in ANSYS LS-DYNA in order to compare the results with the preliminar analysis case (using Eq.2.4).

IV.4 RUN 5501 Test Equipment and Conditions

The profile of testing system is shown in Figure IV-25. the volume of the pressure vessel is about 4 m^3. An auxiliary connecting pipe which reduces the diameter of the 8 inch nozzle to the diameter of the 4 inch test pipe is attached to the nozzle of the pressure vessel. The 4 inch test pipe is 4500 mm in length and is fixed by the pipe support so that the length of test section is 3000 mm.

A detailed assembly of the test pipe and the restraint is shown in Figure IV-26. The test pipe is installed at a height of 1000 mm above the test bed. Four pipe whip restraints are sets on the restraint support. Clearance is the space between the pipe and the restraints and its value is 100 mm. The details of the restraint are shown in Figure IV-27. the restraint is composed of a U-bar, bearing plate, clevis, bracket and pin. The U-bar is made of Type 304 stinless steel and its diameter is 8 mm. The clevis is screwed to the

end of the U-bar and is used for fine adjustment of clearance. The bearing plate made of carbon steel is attached to the inner side of the circular part of the U-bar. The purpose of these plate is to wrap around the test pipe to minimize pipe rebound. Restraint assemblies are pinned to the bracket which is set on the restraint support. There were four restraints in this test.

The chemical composition and mechanical properties of a pipe and restraints are summarized in Table IV-8. Both material are Type 304 stainless steel.

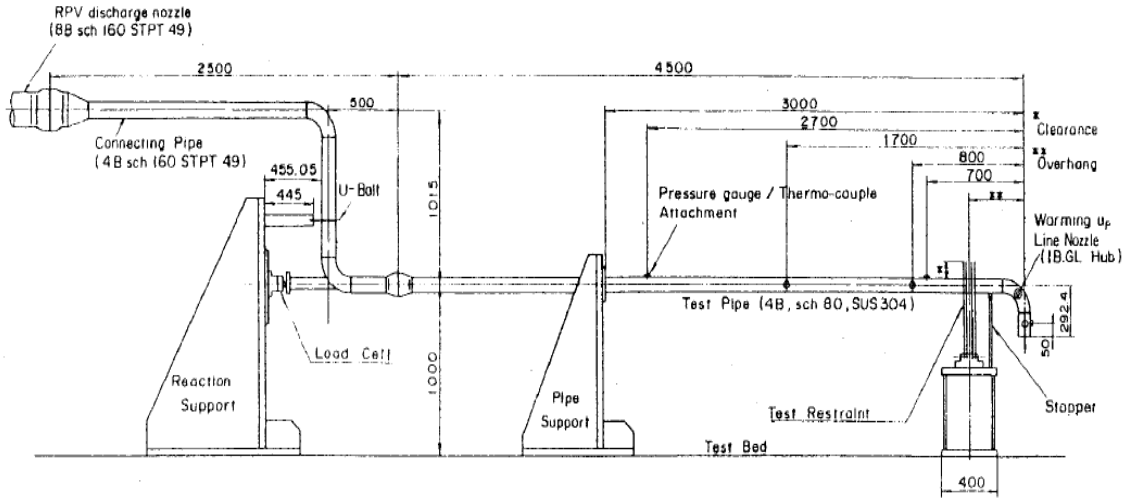

Figure IV-25. Arrangement of Test Section

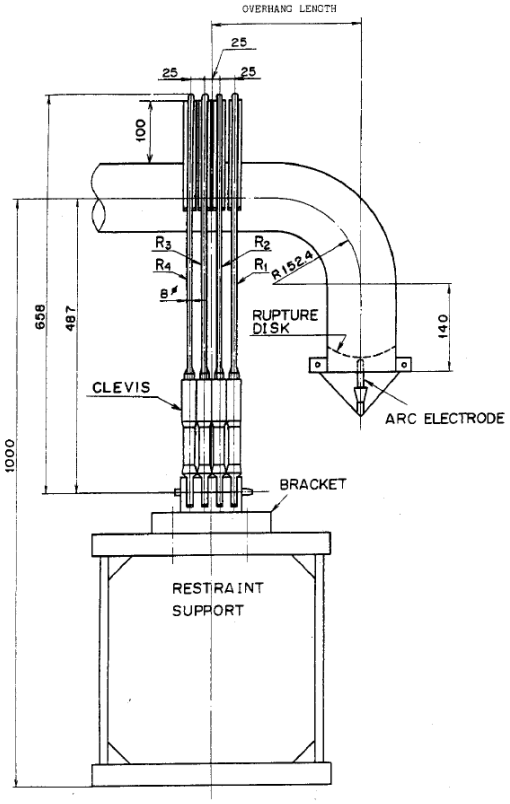

Figure IV-26. Details of Test Pipe

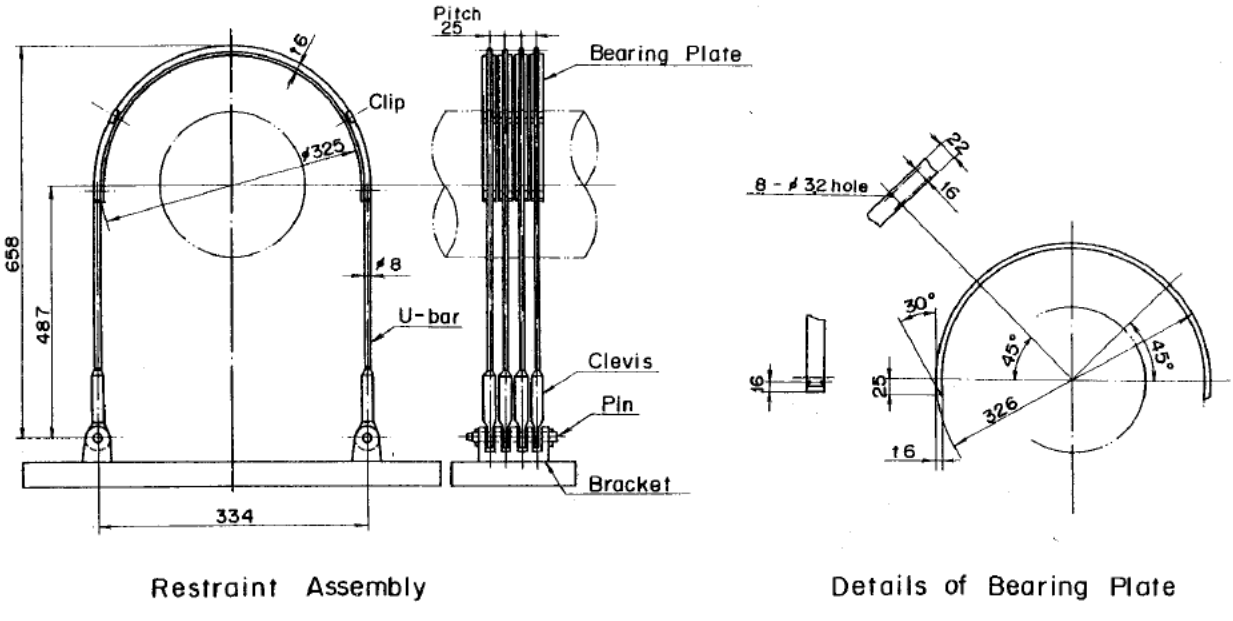

Figure IV-27. Restraint Configuration

Test conditions are summarized in Table IV-9. As can be seen from the table, the test was conducted under BWR operating conditions with 6.8 MPa pressure and 285 ℃ temperature of the primary coolant water. The temperature near the free end of pipe decreases a few degrees because of the heat radiation. Run 5501 is the test number, and the overhang length is 250 mm.

(a) Test Pipe (Room Temperature)

C	Si	Mn	P	S	Ni	Cr
0.5	0.47	1.43	0.026	0.03	9.20	18.35

Yield Strength	Tensile Strength	Elongation
24.8	61.4	56.8

(b) Restraint (Room Temperature)

C	Si	Mn	P	S	Cr	Ni
0.05	0.56	1.57	0.027	0.005	18.33	9.51

Yield Strength	Tensile Strength	Elongation
33.4	61.9	64.9

Table IV-8. Chemical Composition and Mechanical Properties

Run Number		5501
Pressure (MPa)		6.8
Temperature (℃)	Vessel	285
	Test Section	281
Diameter and Thickness of Test Pipe		4B, sch 80
Length of Test Section		3000 mm
Restraint	Type	U-bar
	Overhang (mm)	250
	Clearance (mm)	100
	Diameter (mm)	8
	Number	4

Table IV-9. Test Condition

IV.5 FE Model - RUN 5501

The procedure previously adopted, described in Section IV.3, has been repeated for the new test condition.

Figure IV-28 and Figure IV-29 show the final model of pipe and PWR in ANSYS and Ls-Prepost respectively.

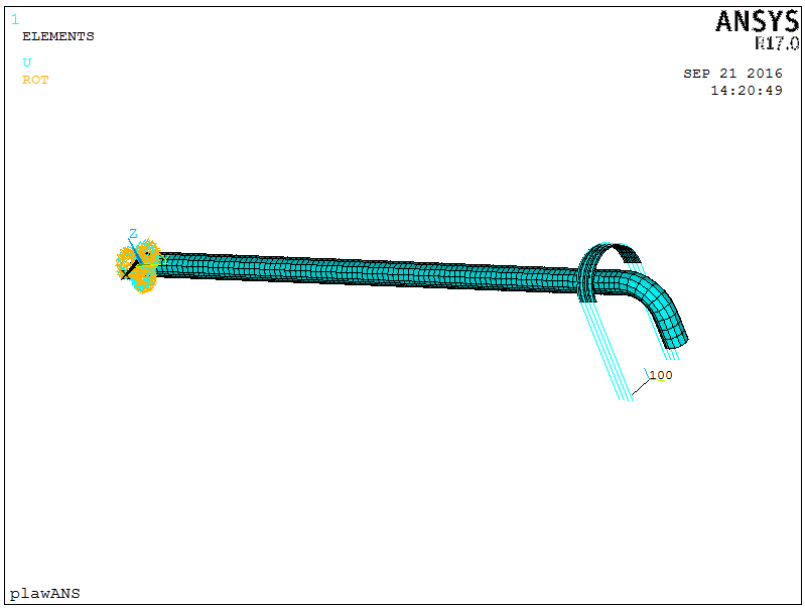

Figure IV-28. 4” Pipe and PWRs Model (a)

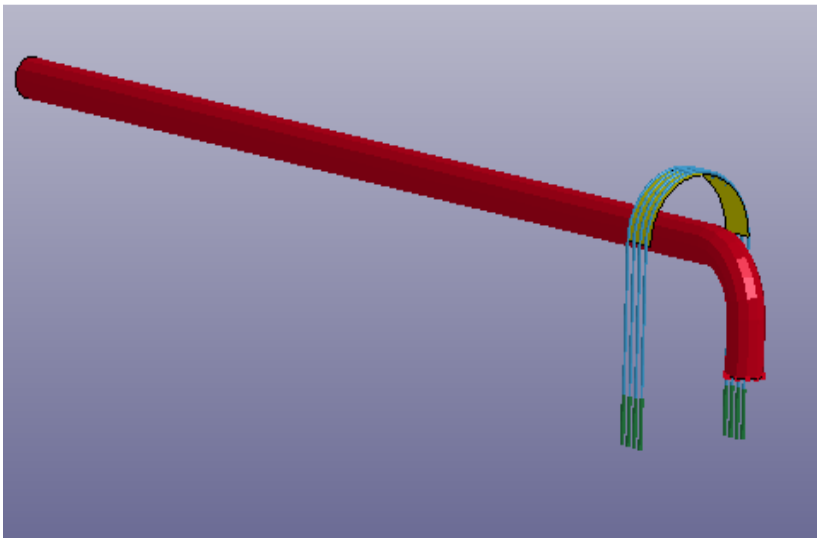

Figure IV-29. 4” Pipe and PWRs Model (b)

IV.5.1 Material Properties

The tensile test results of pipe material's specimen at 285 °C is shown in Figure IV-30. Proof stress $\sigma_{0.2}$ is 19.6 kg/mm^2 and strain hardening modulus is 380.6 kg/mm^2 from this stress-strain curve.

The tensile test result of restrain material's specimen at room temperature is shown in Figure IV-31. Proof stress $\sigma_{0.2}$ of restraint materials is about 37.0 kg/mm^2 from these two stress-strain curves.

These tensile test results are summarized in Table IV-10 [Ref. 21].

No.	Material	Temp.	$\sigma_{0.2}$	σ_u	ψ
1	Pipe	R.T.	29.3	62.8	45.7
2	Pipe	285°C	19.6	46.8	33.5
3	Restraint	R.T.	35.7	60.7	64.2
4	Restraint	R.T.	38.0	60.7	62.2

Note $\sigma_{0.2}$: Proof Stress kg/mm^2

σ_u : Tensile Strength kg/mm^2

ψ : Elongation %

Table IV-10. Conditions and Results of Tensile Test

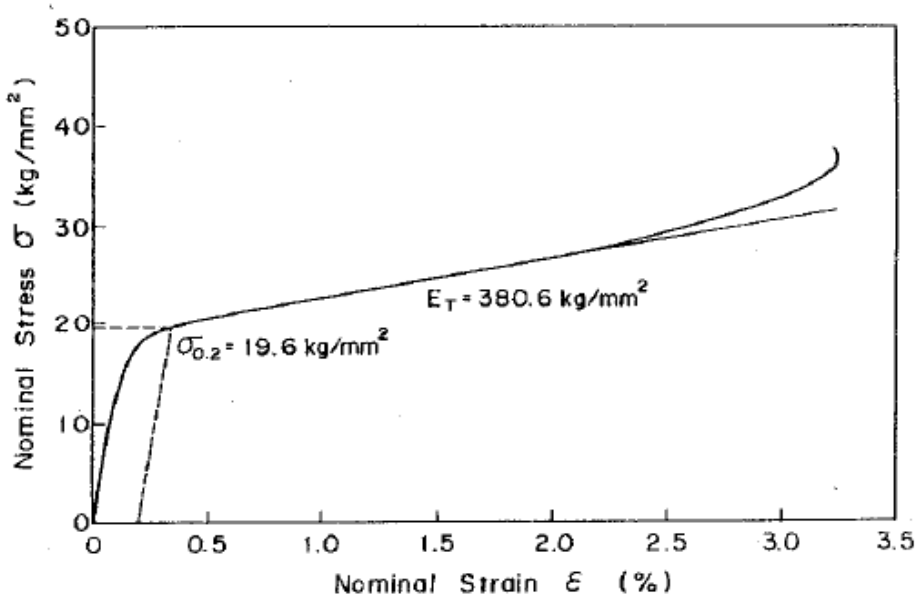

Figure IV-30. Tensile Test Result of Pipe Material's Specimen at 285°C

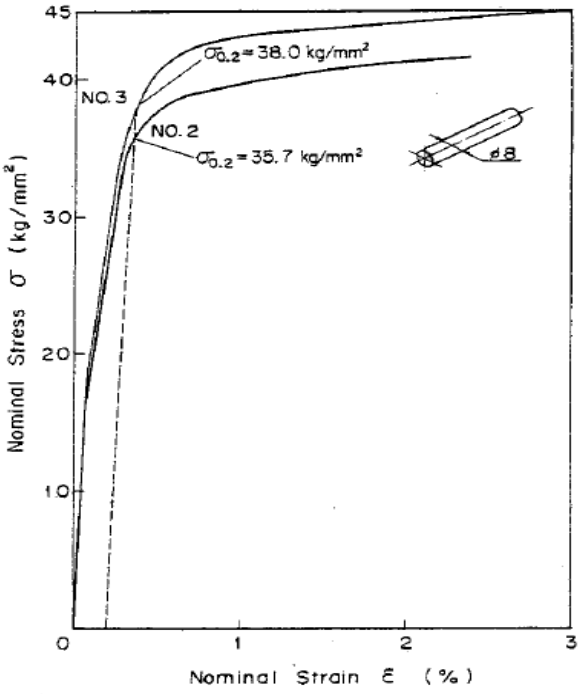

Figure IV-31. Tensile Test Results of Restraint Material's Specimen at R.T

Other material's properties are the same as previously depicted for RUN 5606.

IV.5.2 Applied Force

The fluid force has been computed following the proven procedure; the conservative analysis returns a value of approximately 45 kN (C_T of 0.9), while blowdown analysis gives the following trend, Figure IV-32 :

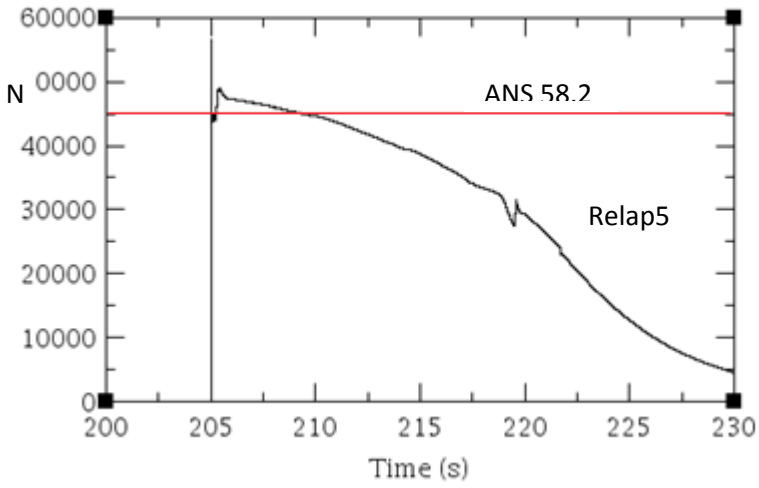

Figure IV-32. Thrust Force Trend, Run 5501 Simulation

IV.6 Analysis of Results.

The post-processing procedure, using LS Prepost, provides to the user those main characteristic parameters of the analysis such as strain of pipe and restraints, displacement of pipe-end, kinetic energy of whipping pipe and elongation of U-bars (for RUN 5606 & 5501).

IV.6.1 RUN 5606

From the simulation it can be seen that the instant of impact is 0.012 s; at this instant in time the kinetic energy of the whipping pipe is around 15 kJ, Figure IV-33, as hand calculation of Appendix B confirms. Subsequently this energy becomes plastic deformation energy of restraints; in about 0.037 s the whipping phenomenon takes place.

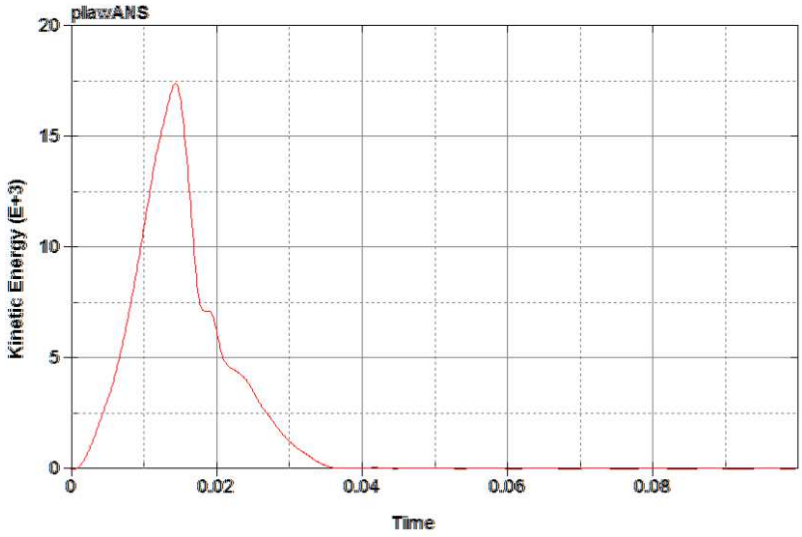

Figure IV-33. Kinetic Energy of Whipping Pipe, RUN 5606

The pipe clearly undergoes plastic deformation, generating a plastic hinge at about 1.3 m from its tip; Figure IV-34.

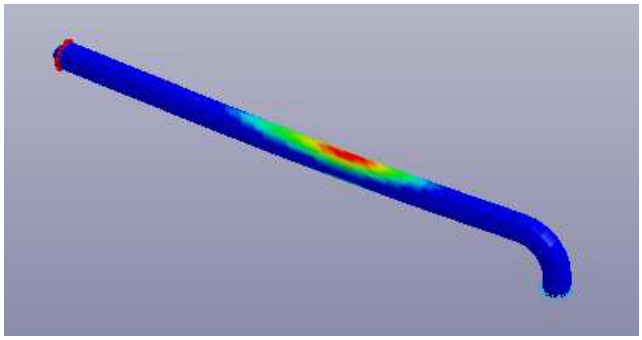

Figure IV-34. Hinge Generation

The restraints loads are reported in Figure IV-35; analyzing this figure it comes out that the simulation anticipates and differs from the experimental results (Fig 4.10 of Ref. 17), this is attributable to the faster rise of the computed force with respect to real one (see Ref. 22).

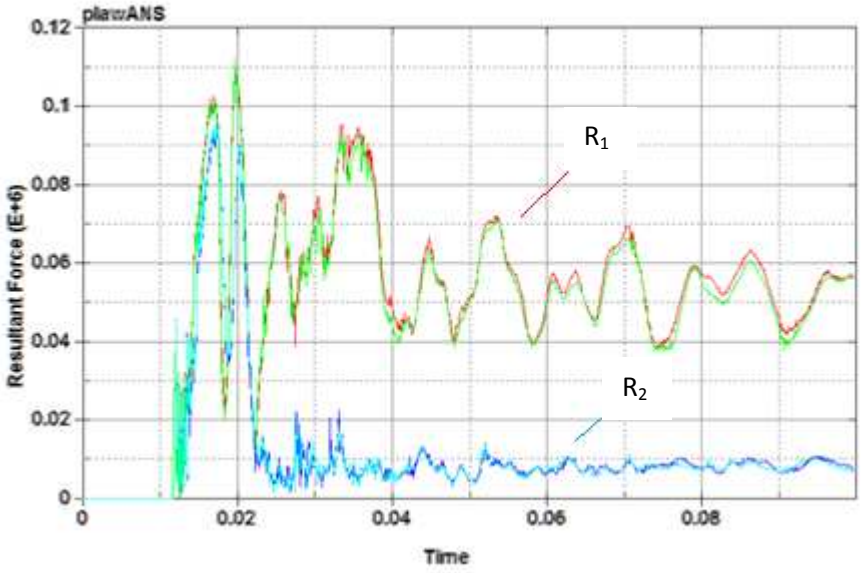

Figure IV-35. Loads on Restraints

It can be observed that some of the output parameters (Figure IV-35, Figure IV-36, Figure IV-37) are not consonant to the experimental results reported in JAERI's documents (M 83-020 and M 82-022 respectively), but on the other hand impact values are very close to preliminary hand calculations (Appendix B); Table IV-11 is provided.

	Data	Experimental	Numerical	ε %
RUN 5606	Vertical Displacement	700 mm	690 mm	1.4
	Kin. Energy	15 kJ	15 kJ	/
	Change in length of PWR	2.5 cm	2.4 cm	4

Table IV-11. Experimental vs Numerical Data, RUN 5606

Few of the output parameters are reported in Figures below; their magnitude is in SI units.

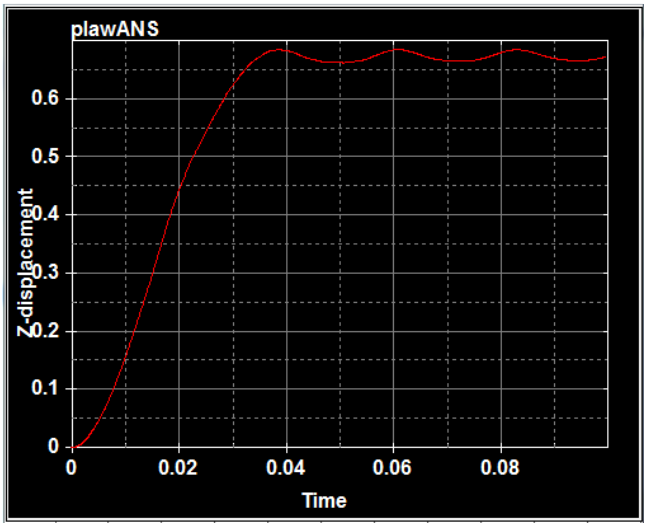

Figure IV-36. Vertical Displacement of pipe-end, RUN 5606

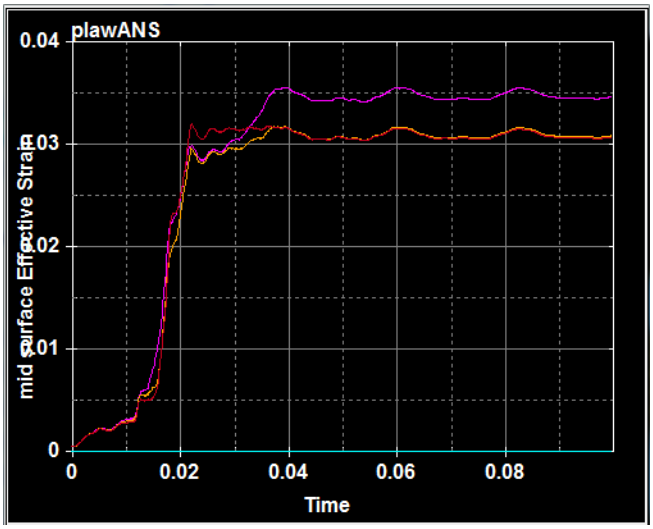

Figure IV-37. Strain of Pipe Elements under Restraints, RUN 5606

Following is an overview of the simulation before and after the impact between the pipe and its restraints, Figure IV-38 .

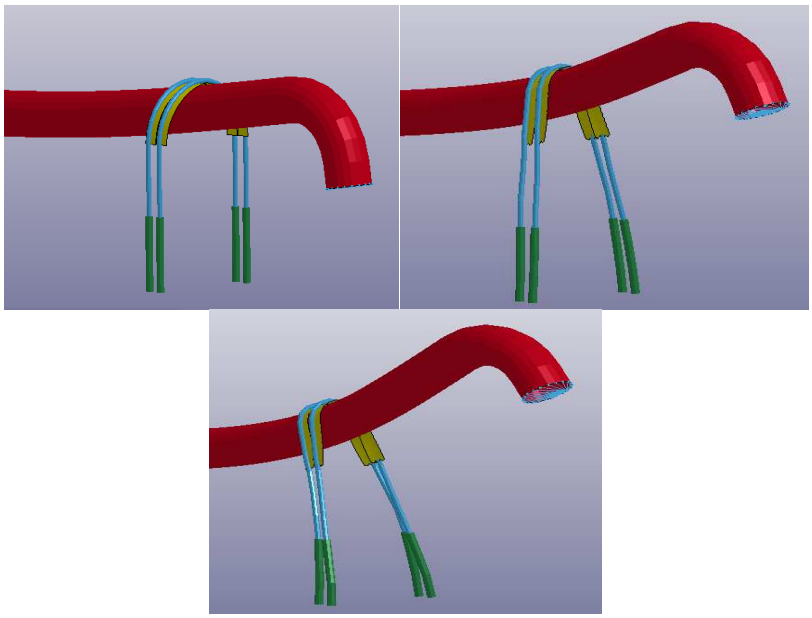

Figure IV-38. Run 5606 Simulation at three different instants

IV.6.2 RUN 5501

Similar considerations can be made for the 4 inch pipe, except for the fact that in this case it is experienced pipe rebound phenomenon after first impact; in fact kinetic energy decreases after first peak and then oscillate up to about 1kJ for the rest of the simulation, Figure IV-39.

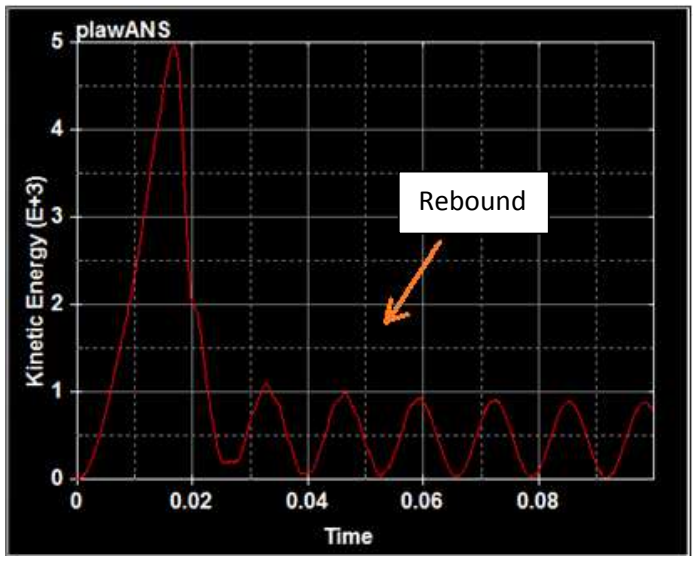

Figure IV-39. Kinetic Energy of Whipping Pipe, RUN 5501

Few of the output parameters are reported in Figures below; their magnitude is in SI units.

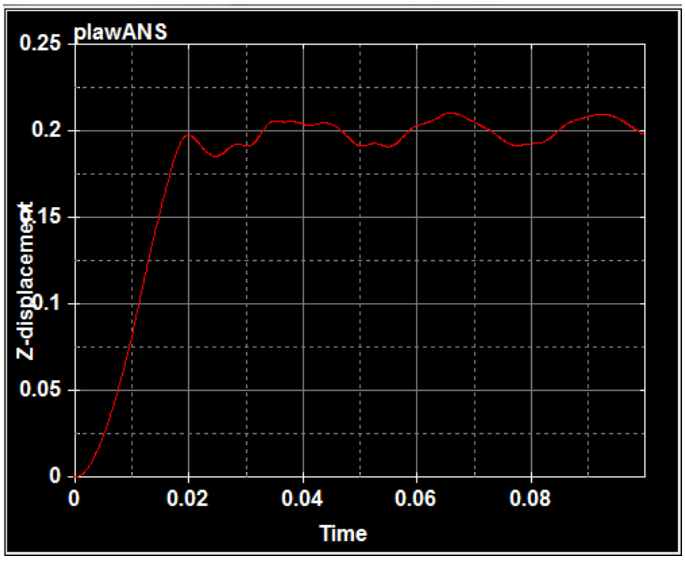

Figure IV-40. Vertical Displacement of pipe-end, RUN 5501

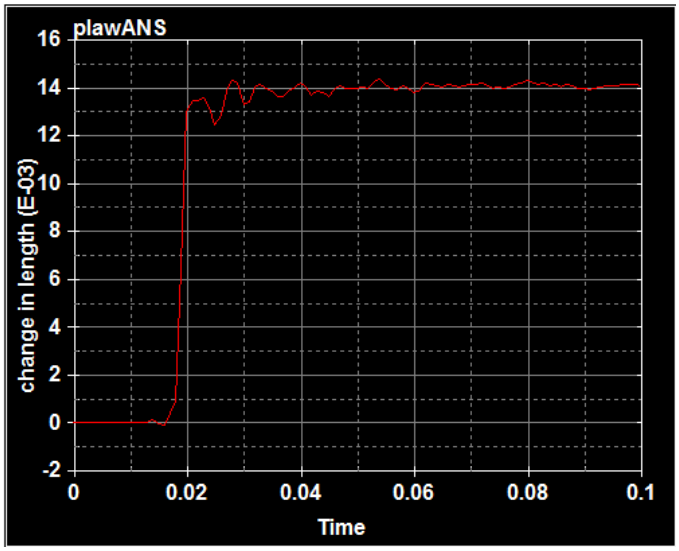

Figure IV-41. Change in Length of Straight Part of U-bolt, RUN 5501

Table IV-12 is provided.

	Data	Experimental	Numerical	ε %
RUN 5501	Vertical Displacement	300 mm	200 mm	33
	Kin. Energy	5 kJ	4.9 kJ	2
	Change in length of PWR	1.5 cm	1.4 cm	6.6

Table IV-12. Experimental vs Numerical Data, RUN 5501

An overview of the simulation before and after the impact between the pipe and its restraints is reported in Figure IV-42.

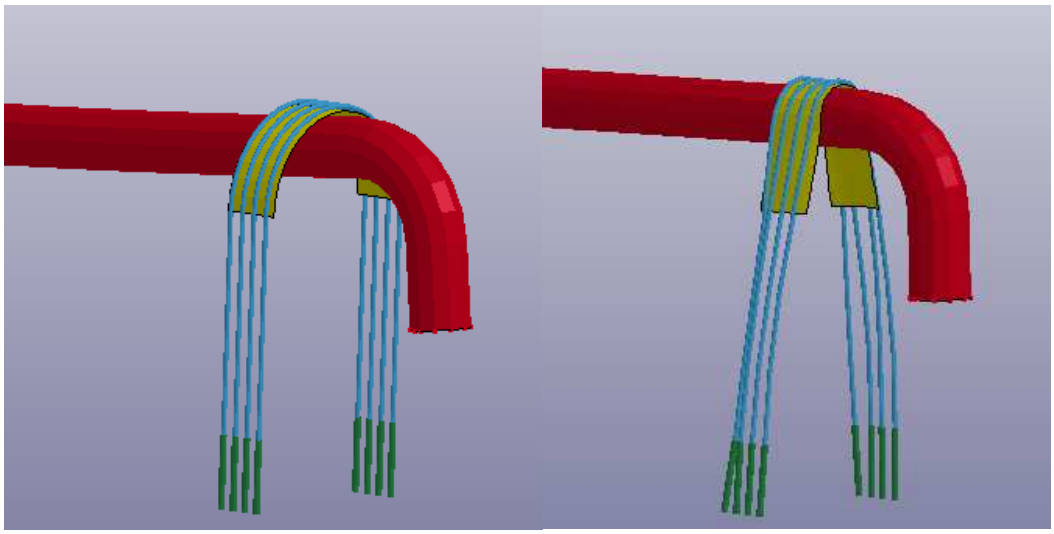

Figure IV-42. Run 5501 Simulation at two different instants

IV.6.3 Considerations

Modelling HEPB phenomena covers deep accuracy in sizing components and structures involved; their stiffness and mass, thicknesses and mostly material properties. The study analyzes different material behaviors under impact starting from ANS 58.2 [Ref.2] recommendations (Section 6.6.3 in conjunction with 6.6.2), and furtherly exploiting different properties embedded within ANSYS LS-DYNA such as the bilinear kinematic stress-strain trend and finally the multi-linear plasticity law, suggested as the most suitable. A sensitivity analysis of several important parameters was performed and values which give the best results are reported. The use of these values is suggested in the design of PWR components.

The other important aspect is that of inputting to the Code a well-defined thrust force trend; this has been done following the regulations and later on with a transient blowdown analysis using RELAP5 Code. The two are proven to be consonant but mainly too conservative specially in the rise time of the force (see Ref. 9.); deeper information about the opening of the rupture disk should be provided. Anyway a procedure to deal with HEPB phenomena has been built and tested and will be practiced for a further analysis.

Chapter V: Application to a real case

V.1 Introduction

The current reference case reports the analysis of a piping system that belongs to the Emergency Core Cooling System of a VVER440; the layout includes valves and supports together with the PWR required for accident mitigation, his position has been previously determined on the basis of pipe break location analysis. The break has been postulated in correspondence of a valve where pressure difference is present; the pipeline is made of stainless steel, has an external diameter of 273 mm (thickness 28.5 mm) and is classified ASME Class I.

This Chapter presents the whole model built in ANSYS and the final simulation using LS-Prepost.

V.2 Piping Layout

Pipeline geometry definition is the first step of modelling procedure; isometric drawings have been exploited to construct lines and areas for element assignment.

It has been reputed suitable to model most of piping layout as tubular BEAM161 elements whilst the region affected to plastic deformation and hinge as a SHELL163 element; this is done for computation reasons. Following is the geometry definition, already meshed, in ANSYS environment.

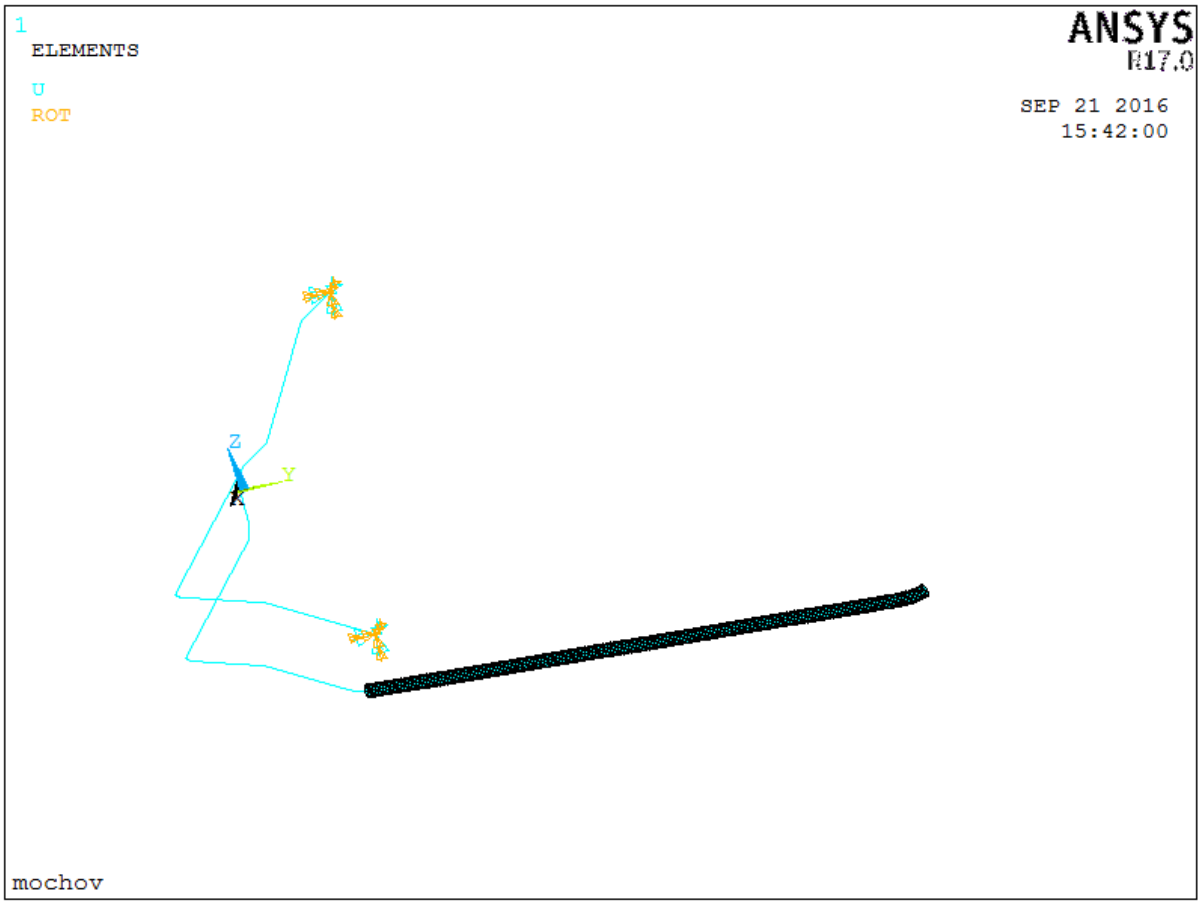

Figure V-1. Geometry Definition and Meshed Pipes

Figure V-1 reports the two constrained ends of the pipeline; one corresponding to a wall penetration and the other to an anchorage. Those two constraints largely confine the break affected range under analysis.

The beam-to-shell connection has been realized by means of a nodal rigid body constraint as previously depicted for the force application (IV.3.2).

A MASS166 element has been added along a branch in order to simulate the presence of a valve, his mass is 690 kg. Furtherly, eight vertical supports are reported in the model together with the main PWR support structure, modelled using two BEAM161 HEM300 profile; following is the complete ANSYS model of the reference line, PWR and support structures.

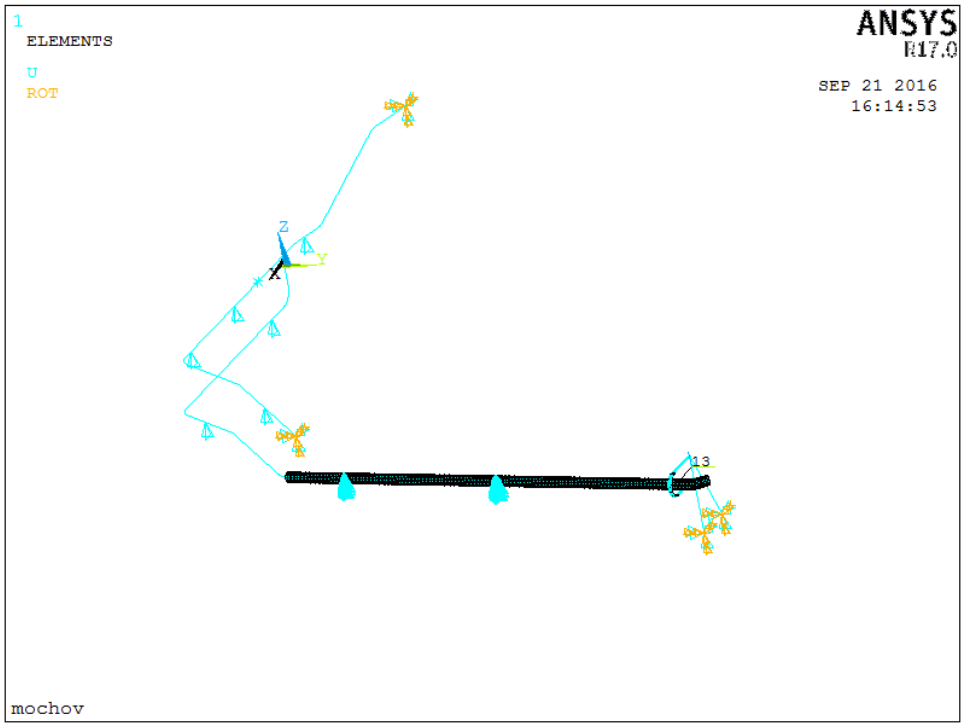

Figure V-2. ANSYS Final Model

V.3 Relevant Data

Following are reported design and operating data of the line under consideration, piping material properties and thermal insulation data, Table V-1. The pipe material is A-312 TP 321.

Design Press. [MPa]g	14	Operating Press. [MPa]g	12.26
Design Temp. [°C]	335	Operating Temp. [°C]	295
Young's Modulus [MPa]	180000		
Yield Point Rp 0.2 [MPa]	177		
Insulation Weight [Kg/m]	36.58		

Table V-1. Relevant Data

V.3.1 Calculation of the Force in the PWR device

The thrust force and the location of the plastic hinge come from the free-whip analysis already described in previous Chapters; it is:

T_0	448.6 kN
T_{ss}	358.8 kN
L_h	3.11 m

Table V-2. Relevant Data II

the enthalpy of the fluid is about 560 (BTU/lb) and the discharge coefficient C_D comes out to be 0.8 for the layout under investigation; check by Figure V-3.

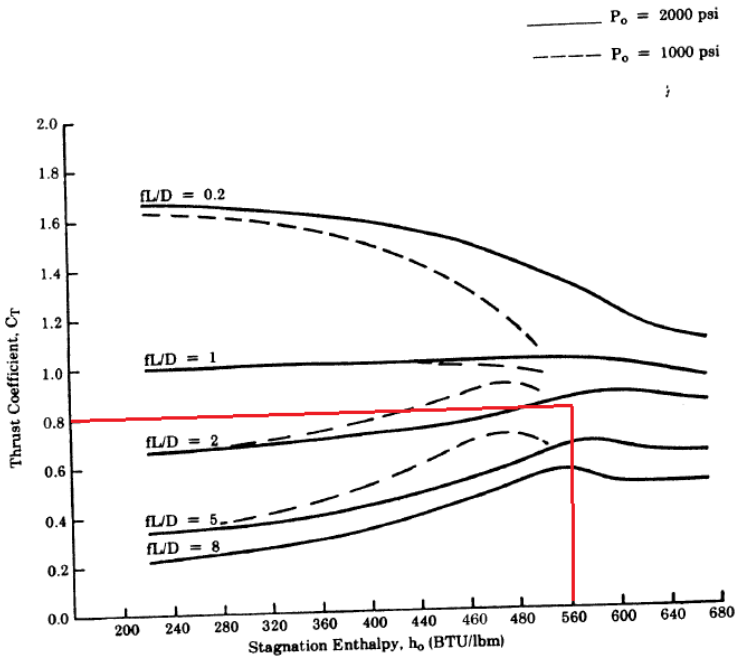

Figure V-3. Discharge Coefficient

V.3.2 Design of the Stainless Steel U-Bar Restraint

In this section the design of the restraint is developed; noting that a reduced insulation thickness has been taken into account to limit the displacement of the pipe before the activation of restraint.

13 mm	Bearing plate thickness
955 mm	U-bolt straight length
575 mm	U-bolt internal diameter
273 mm	Pipe external diameter
3 mm	tolerance
70 mm	Thermal displacement
60 mm	Seismic displacement
3 mm	installation
0 mm	Insulation thickness

Table V-3. Relevant Data III

The section required for the PWR U-Bolts can be calculated knowing the maximum elongation, ε_m (50% of ε_u); the PWR is composed by 8 U-bolts, 20 mm in diameter. Detail of the PWR is reported in Figure V-4.

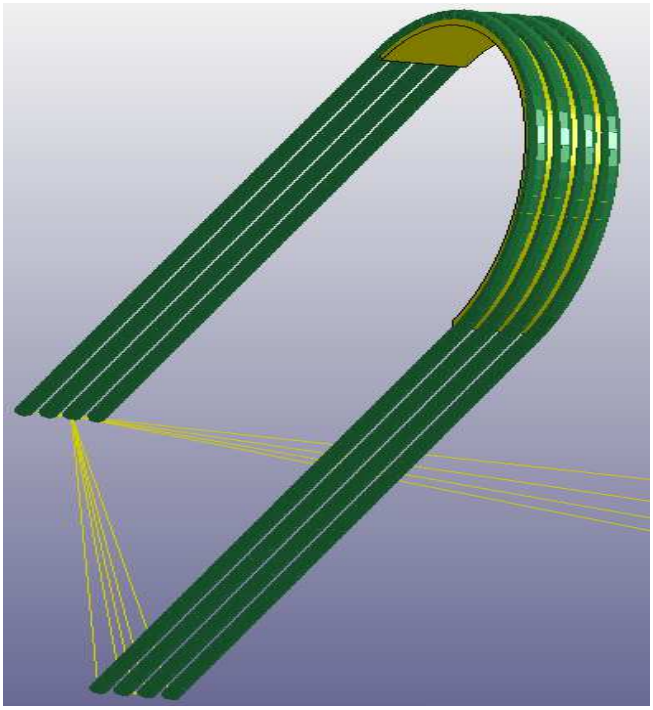

Figure V-4. Detail of PWR

V.3.3 Design of the PWR Support

As mentioned in V.2 the PWR support structure is composed of two beams HEM300 profile; the vertical one 1995 mm in length, the other 2079 mm, the material is S235JR. Figure V-5 reports the model of the support structure.

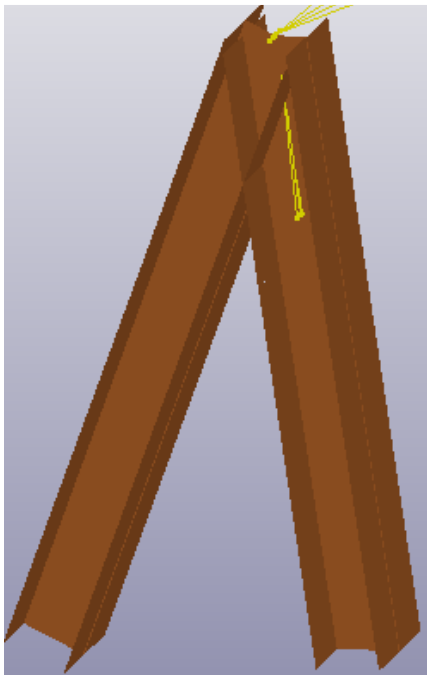

Figure V-5. Detail of PWR Support

V.4 Impact Simulation

Following is reported the complete model dynamic simulation at different instants in time.

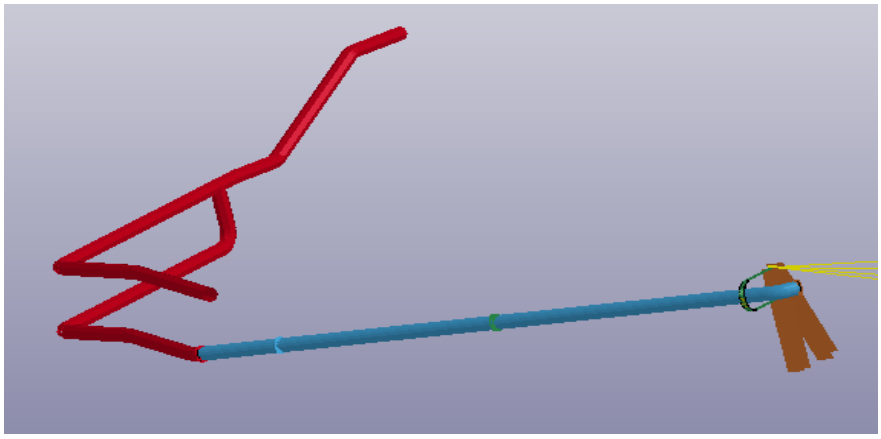

Figure V-6. Model at t=0

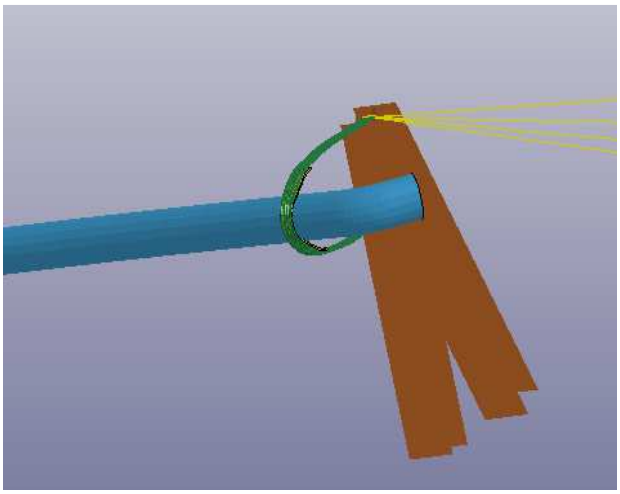

Figure V-7. Detail at t=0.012

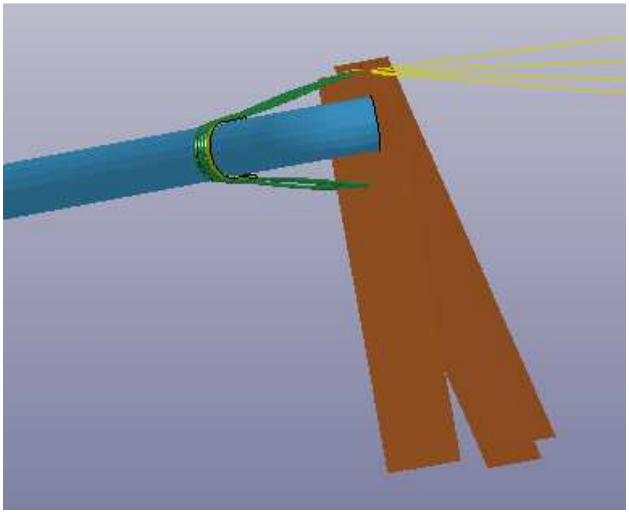

Figure V-8. Detail at t=0.035

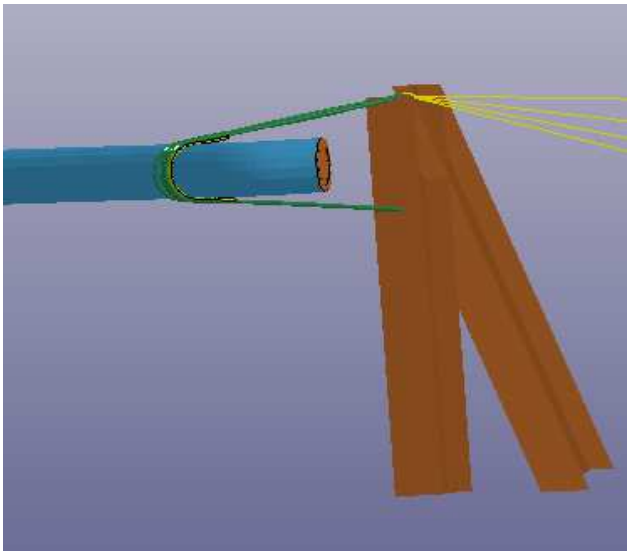

Figure V-9. Detail at t=0.1

V.5 Conclusions

Real case analysis introduces those main design features fundamental in HEPB phenomena: gap determination (clearance), force evaluation, PWR location and design of U-bolts.

For the case under investigation clearance and PWR location were assigned, thus simplifying the calculations; while force has been estimated with the proven procedure and U-bolts have been dimensioned using the 50% of ε_u criterion.

Maximum plastic deformation of U-bars is about $\varepsilon_p = 0.15$, Figure V-10.

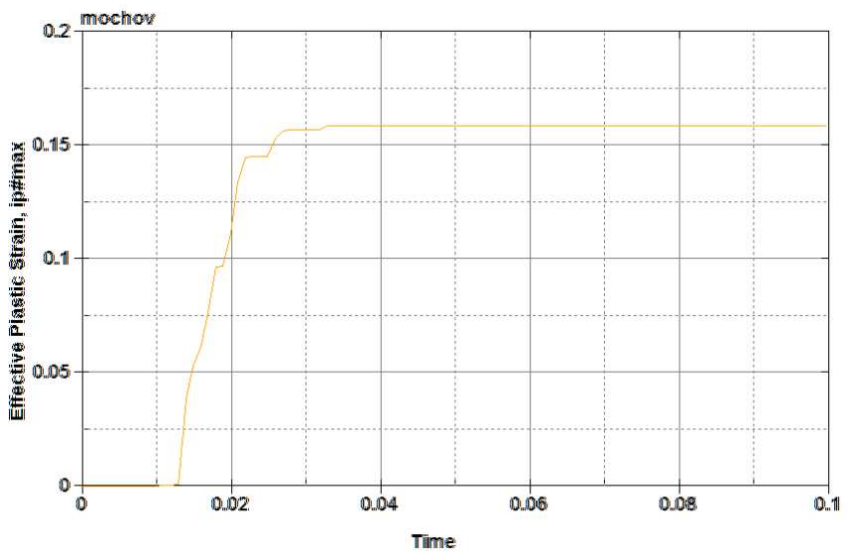

Figure V-10. Maximum Plastic Strain

Moreover it can be seen that the PWR support structure maintains its elasticity and the maximum Von Mises stress is in the order of 200 MPa; loads on basement plates are reported in Figure V-11.

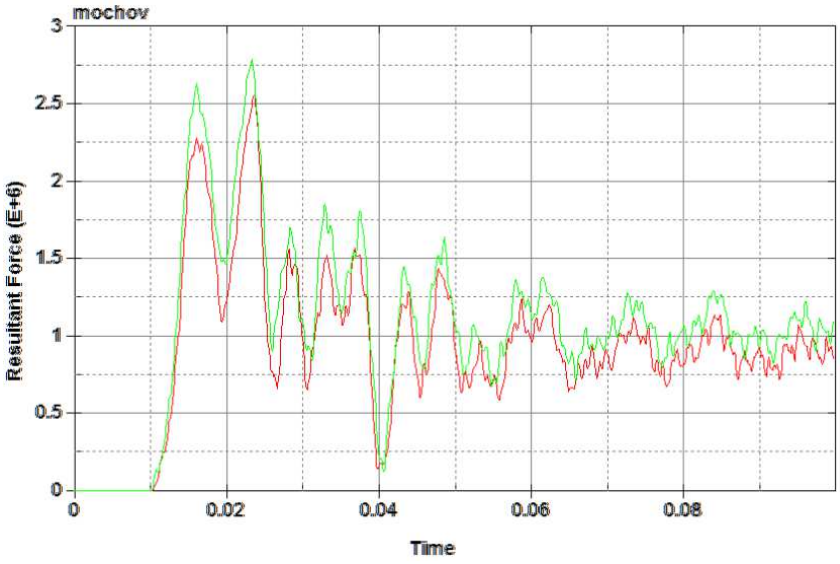

Figure V-11. Force on Basement

Ls-Prepost therefore allows to confirm the elastic field of deformation of the piping system and of all the support structures except made for the shell component, which as expected undergoes plastic deformation.

Appendix A – Location of pipe ruptures

Fig. A.1 shows a principal flow-chart for procedure that could be implemented for location of postulated piping ruptures according to ANSI/ANS – 58.2 Standard. To perform such evaluation the following stages of analyses should be done for High-Energy piping systems:

- Static analysis (deadweight and thermal expansion);
- Dynamic (seismic) analysis.

Static analysis is carried out under gravity loads due to dead and live weights (i.e. pipe material, insulation, fluid medium) and design pressure. Thermal expansion analyses of piping systems are performed for all designated sets of piping operational conditions for evaluation of correspondent ASME BPVC equations and performing of fatigue analysis.

In frame of dynamic analysis piping internal forces and moments should be calculated under seismic input corresponding to OBE level.

The following set of ASME Class 1 equations are considered according to ANSI/ANS – 58.2 Standard and ASME BPVC NB-3600:

- Satisfaction of Primary Plus Secondary Stress Intensity Range under the combination of loadings for which either Level A or Level B service limit have been specified (Equation N 10, NB-3653.1):

$$S_n = C_1 \frac{P_0 D_0}{2t} + C_2 \frac{D_0}{2I} M_i + C_3 E_{ab} \times |\alpha_a T_a - \alpha_b T_b| \leq \begin{cases} 2.4 S_m \\ 1.2 S_m \end{cases} \qquad (1)$$

Nomenclature for this and following equations corresponds to the terminology from ASME BPVC.

According to presented flow chart, if condition $S_n < 1.2 * S_m$ is satisfied, then no piping rupture is postulated in the given location.

In opposite case, an additional investigation is performed:

Check of Equation 12 (ASME NB-3653.6):

$$S_e = C_2 \frac{D_0}{2I} M_i^* \leq \begin{cases} 2.4 S_m \\ 1.2 S_m \end{cases} \qquad (2)$$

And Equation 13:

$$S = C_1 \frac{P_0 D_0}{2t} + C_2 \frac{D_0}{2I} M_i + C_3' E_{ab} \times |\alpha_a T_a - \alpha_b T_b| \leq \begin{cases} 2.4 S_m \\ 1.2 S_m \end{cases} \quad (3)$$

If stress value calculated according Equations (2) and (3) are higher than 2.4*S_m, then piping break is postulated in the considered location. If stress values calculated according Equations (2) and (3) are less than 2.4*S_m, but higher than 1.1*S_m, then through-wall crack is postulated in the considered location. In opposite case no piping ruptures are postulated.

An additional condition that should be checked in the frame of performed analysis is the value of cumulative usage factor U (NB-3653.5).

To define this value the following stresses should be calculated (Equation (11), NB-3653.2):

$$S_p = K_1 C_1 \frac{P_0 D_0}{2t} + K_2 C_2 \frac{D_0}{2I} M_i + \frac{1}{2(1-\nu)} K_3 E\alpha |\Delta T_1| + K_3 C_3 E_{ab} |\alpha_a T_a - \alpha_b T_b| + \frac{1}{1-\nu} E\alpha |\Delta T_2| \quad (4)$$

and Equation (14), NB-3653.2:

$$S_{alt} = \frac{S_p}{2} \quad (5)$$

According to ANSI/ANS – 58.2: a piping break is postulated if U > 0.4, a through-wall crack is postulated if 0.2 < U < 0.4, and no piping ruptures are postulated in the given location if U < 0.2. it should be noted, that in this part ANSI/ANS approach still differs from the US NRC position [4], that use more severe acceptance criteria for fatigue: no piping breaks are postulated if the cumulative usage factor U < 0.1.

For piping system classified as Class 2, the following set of equations should be accessed:

Equation (9), NC-3653.1 $$S_{OL} = B_1 \frac{P_{max} D_0}{2t_n} + B_2 \frac{(M_A + M_B)}{Z} \quad (6)$$

Equation (10),NC-3653.2: $$S_E = \frac{i * M_C}{Z} \quad (7)$$

For location of postulated pipe rupture the following equation is checked:

$$S_{OL} + S_E > \begin{cases} 0.8(1.8 S_h + S_a) \\ 0.4(1.8 S_h + S_a) \end{cases} \quad (8)$$

If stress value $S_{OL} + S_E$ is less than $0.4(1.8 S_h + S_a)$ no piping ruptures are postulated.

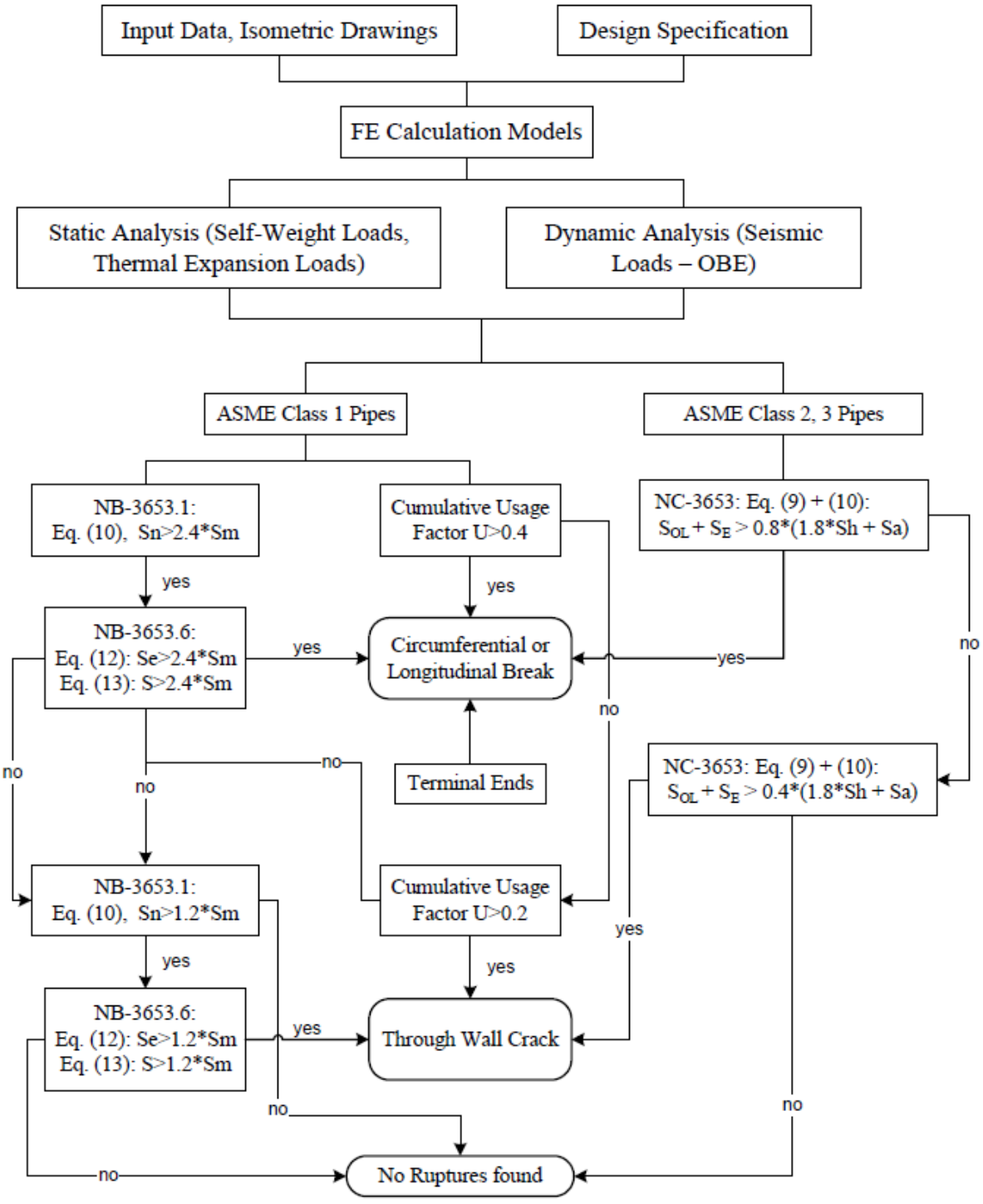

Fig A.1. Logical Diagram for Postulation of Ruptures in High Energy Lines.

Appendix B – Representative parameters

Several parameters characterizing the phenomenon were previously evaluated by hand in order to have confirmation from the analytical model set-up; respectively for RUN 5606 and 5501.

RUN 5606:

$T_{ss} = C_T P_0 A$

C_T	1		
P_0	6.76E+06	N/m²	
A	0.016	m²	
T_{ss} =	1.08E+05	N	
---	---	---	---

calcolo della cerniera plastica:

$L_h = 3M_p/2F_b*(1+(1+8LF_b/3M_p)^1/2)$

M_p =	4.48E+04	Nm	
$F_b = T_{ss}$ =	1.08E+05	N	
L =	7.94E-02	m	
L_h =	1.39E+00	m	
---	---	---	---

kinetic energy of impacting pipe:

$E_{kin} = (F_b*L_h - M_p)*\theta$

θ =	0.144904	rad	
E_{kin} =	15216.2	J	

---

allungamento U-bar dopo l'impatto (tratto rettilineo)

$E_a = \sigma_s * 2 * S_v * \Delta l$

S_v = area sezione totale delle barre 8.00E-04 m²

σ_s = 3.02E+08 N/m²

Δl = 3.15E-02 m

RUN 5501:

$T_{ss} = C_T P_0 A$

C_T	1	
P_0	6.80E+06	N/m²
A	0.0074	m²
T_{ss} =	5.03E+04	N

---

calcolo della cerniera plastica:

$L_h = 3M_p/2F_b * (1+(1+8LF_b/3M_p)^{1/2})$

M_p =	2.70E+04	Nm
$F_b = T_{ss}$ =	5.03E+04	N
L =	1.40E-01	m
L_h =	1.85E+00	m

---

kinetic energy of impacting pipe:

$E_{kin} = (F_b * L_h - M_p) * \theta$

θ = 0.074545 rad

E_{kin} =	4937.875	J
---	---	---

allungamento U-bar dopo l'impatto (tratto rettilineo)

$E_a = \sigma_s * 2 * S_v * \Delta l$

S_v = area sezione totale delle barre	4.00E-04	m^2
σ_s =	3.57E+08	N/m^2
Δl =	1.73E-02	m

Appendix C – Modal Analysis

File modalPipe.txt and modalPWR.txt for RUN 5606 are below reported.

```
finish
/clear
/title,prova1
/vup,,z
/units,mks

/prep7

pigreco=3.14159

!!!!!!
!PIPE!
!!!!!!

k,1,0,0,0
k,2,0,3,0
k,3,0,3,-.308

l,1,2
l,2,3

lfillt,1,2,.2286

circle,1,.1652/2-.0055,2,3
adrag,4,5,6,7,,,1,3,2

mp,dens,1,7850
mp,ex,1,2E11
mp,nuxy,1,0.33

et,1,281
sectype,1,shell
secdata,0.011,

type,1
mat,1
secnum,1
amesh,all


k,1001,0,-.05,0
l,1001,1

allsel,all

et,2,188
sectype,2,beam,rect
```

```
secdata,.05,.06

type,2
mat,1
secnum,2
lmesh,32

nsel,s,loc,y,0
cerig,1101,all,all

nsel,s,loc,y,-.05
d,all,all

/SOLU
ANTYPE,MODAL
MODOPT,LANB,10
EQSLV,SPAR
MXPAND,10, , ,0
LUMPM,0
PSTRES,0
solv
```

```
finish
/clear

/vup,,z
/units,mks

/prep7

et,1,beam188
mp,dens,1,7850
mp,ex,1,1.51E11
mp,nuxy,1,0.33
sectype,1,beam,csolid
secdata,.008


k,101,.1986,0,0
k,102,-.1986,0,0
k,103,.1986,0,.4891
k,104,-.1986,0,.4891
k,105,0,0,.4891
k,107,0,0,.4891+.3972/2
larc,103,107,105,.3972/2
larc,104,107,105,.3972/2
l,101,103
l,102,104

type,1
mat,1
secnum,1
```

```
lesize,all,0.025
lmesh,all

nsel,s,loc,z,0
d,all,ux,0,,,,,uy,uz,rotx,rotz

allsel

k,110,0,.024,.4891+.3972/2
k,111,0,-.024,.4891+.3972/2

l,110,111

ldiv,5,,,2

adrag,5,6,,,,,1
adrag,5,6,,,,,2

et,2,281
sectype,2,shell
secdata,0.008

type,2
mat,1
secnum,2
amesh,all
nummrg,node


/SOLU
ANTYPE,MODAL
MODOPT,LANB,10
EQSLV,SPAR
MXPAND,10, , ,0
LUMPM,0
PSTRES,0
solv
```

Appendix D – Cowper-Symonds Formula

The Cowper-Symonds equation varying the p and D parameters:

$$\frac{\sigma_{dyn}}{\sigma_{stat}} = 1 + \left(\frac{\dot{\varepsilon}}{D}\right)^{\frac{1}{p}}$$

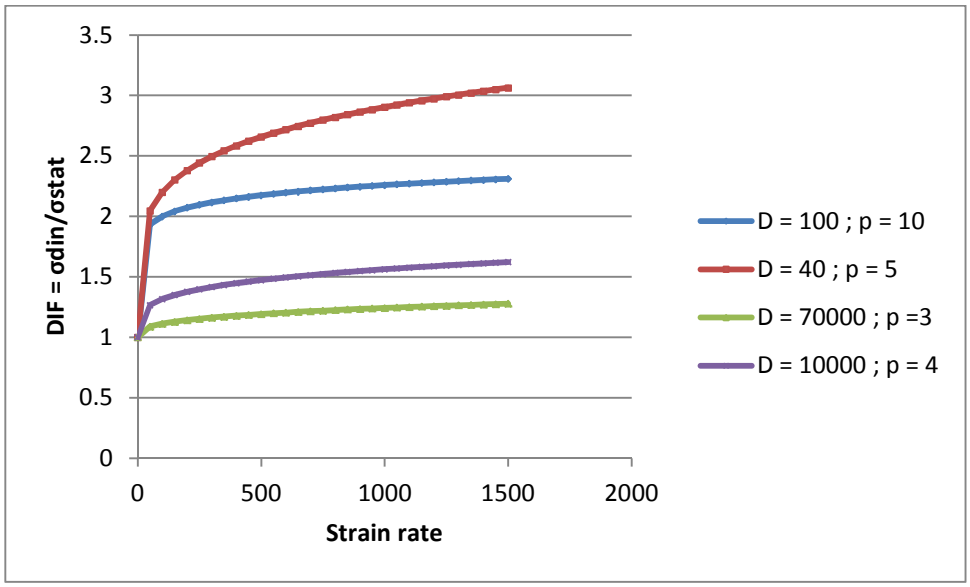

The strain rate in the analysis conducted was in the order of 350-500 s^{-1}.

Appendix E – LS-Dyna and Relap5 input files

Input File for RUN 5606; 6 in. pipe.

```
finish
/clear
/title,plawANS
/vup,,z
/units,mks

/prep7

!!!!!!
!PIPE!
!!!!!!

k,1,0,0,0
k,2,0,3,0
k,3,0,3,-.308

l,1,2
l,2,3

lfillt,1,2,.2286

circle,1,.1652/2-.0055,2,3
adrag,4,5,6,7,,,1,3,2

et,1,163
keyopt,1,1,0
r,1,5/6,5,.011

mp,ex,1,178e9
mp,nuxy,1,.3
mp,dens,1,8344
mp,damp,1,4.12E-5
tb,plaw,1,,,8
TBDATA,1,177e6,2.825e9,.464,100,10

asel,s,,,2,3
aesize,all,.03
amesh,all

asel,s,,,1,12
```

```
aatt,1,1,1
mshk,2
amesh,all

esel,s,,,1,2046
cm,tube,elem


!!!!!
!PWR!
!!!!!

Epl=1.625e9
mp,ex,2,195e9
mp,nuxy,2,.3
mp,dens,2,7750
mp,damp,2,4.12E-5
tb,plaw,2,,,8
tbdata,1,302e6
tbdata,2,Epl
TBDATA,3,.75  ! Failure strain
TBDATA,4,70000  ! C (strain rate parameter)
TBDATA,5,3 ! P (strain rate parameter)



et,2,161
keyopt,2,5,1
r,2,,.016,.016


local,100,0,0,2.3,-.4891
k,101,.1986,0,0
k,102,-.1986,0,0
k,103,.1986,0,.4891
k,104,-.1986,0,.4891
k,105,0,0,.4891
k,107,0,0,.4891+.3972/2
larc,103,107,105,.3972/2
larc,104,107,105,.3972/2
l,101,103
l,102,104
lgen,2,32,35,,,.026
lgen,2,32,35,,,-.026

k,50000,50000,0,0
```

```
ldiv,42,.512,7000
ldiv,38,.512,7001
ldiv,39,.512,7002
ldiv,43,.512,7003

lsel,s,,,36,41
lsel,u,,,38,39
lesize,all,0.0416

r,4,,.025,.025

lsel,s,,,38,43
lsel,u,,,40,41
latt,2,4,2,,50000

lsel,s,line,,36,47
lsel,u,,,38,39
lsel,u,,,42,43
latt,2,2,2,,50000

lsel,s,,,36,47
lmesh,all

nsel,s,loc,z,0
d,all,ux,0,,,,,uy,uz,rotx,rotz

esel,s,,,2245,2300
cm,restr,elem
allsel

!!!!!!!!!
!!plate!!
!!!!!!!!!

k,110,0,.026+.024,.6757
k,111,0,.026-.024,.6757
k,112,0,-.026-.024,.6757
k,113,0,-.026+.024,.6757
l,110,111
l,112,113

k,115,.1866,0,.4891
k,116,-.1866,0,.4891
k,117,0,0,.6757
larc,115,117,105,.1866
larc,116,117,105,.1866
lgen,2,50,51,,,.026
```

```
lgen,2,50,51,,,-.026

ldiv,48,,,2
ldiv,49,,,2

adrag,52,53,,,,,48
adrag,52,53,,,,,56
adrag,54,55,,,,,57
adrag,54,55,,,,,49

mp,ex,3,2e11
mp,nuxy,3,.3
mp,dens,3,7750
TB,BKIN,3
TBDATA,1,425e6 !(yield stress)
TBDATA,2,8.8e8 !(tangent modulus)

r,3,,5,.008

asel,s,,,13,20
aesize,all,0.01
aatt,3,3,1
amesh,all

edcnstr,add,rivet,2288,2520
edcnstr,add,rivet,2335,2947
edcnstr,add,rivet,2272,2397
edcnstr,add,rivet,2319,2824
edcnstr,add,rivet,2267,2381
edcnstr,add,rivet,2314,2808
edcnstr,add,rivet,2284,2505
edcnstr,add,rivet,2331,2932

edcgen,assc,,,0.1,0.1

!!!!!!!!!!!!!
!!ancoraggio!!
!!!!!!!!!!!!!
csys,0

k,1001,0,-.05,0
l,1001,1

allsel,all


et,161,161
```

```
keyopt,161,2,2

r,161,,.06,.06,.05,.05
mp,ex,161,400e9
mp,nuxy,161,.3
mp,dens,161,7850

lsel,s,line,,78

latt,161,161,161,,50000
lmesh,all

nsel,s,loc,y,-.05
d,all,all,0

nsel,all

nsel,s,loc,y,0
cm,iplane,node

allsel,all
edlcs,add,10,1,0,0,0,1,0,0,0,1
edcnstr,add,nrb,iplane,,10

!!!!!!!!!!!!!
!Thrust Force!
!!!!!!!!!!!!!

csys,0

nkpt,30000,3

allsel,all

nsel,s,node,,30000
cm,endnode,node

nsel,all

nsel,s,loc,z,-.308
nsel,r,loc,y,2.5,3.5

cm,endplane,node
allsel,all
edlcs,add,10,1,0,0,0,1,0,0,0,1
edcnstr,add,nrb,endplane,,10
```

```
*dim,time,,6
*dim,tforce,,6
*dim,inpres,,6

time(1)=0,0.001,0.0175,0.02,0.07,0.1
tforce(1)=0,108.8e3,108.8e3,108.8e3,108.8e3,108.8e3
inpres(1)=-6.76e6,-6.76e6,-6.76e6,-4.76e6,-5.76e6,-5.7e6
edload,add,fz,,endnode,time,tforce
edload,add,press,1,tube,time,inpres,2

/solu

time,0.1
allsel,all
outpr,all

edhist,tube
EDHIST,endnode
edhist,restr
EDOPT,ADD,,BOTH
EDOUT,GLSTAT
EDOUT,MATSUM
EDOUT,SPCFORC
EDOUT,RCFORC
EDOUT,NODOUT
EDOUT,RBDOUT
edout,elout
edwrite,both

save

solve
```

Input file for RUN 5501; 4 in. pipe.

```
finish
/clear
/title,plawANS
/vup,,z
/units,mks

/prep7


!!!!!!
```

```
!PIPE!
!!!!!!

k,1,0,0,0
k,2,0,3,0
k,3,0,3,-.2924

l,1,2
l,2,3

lfillt,1,2,.1524

circle,1,.0504,2,3
adrag,4,5,6,7,,,1,3,2

et,1,163
keyopt,1,1,0
r,1,5/6,5,.0135

mp,ex,1,178e9
mp,nuxy,1,.3
mp,dens,1,8344
mp,damp,1,4.12E-5
tb,plaw,1,,,8
TBDATA,1,196e6,3.806e9,.335,100,10


asel,s,,,2,3
aesize,all,.03
amesh,all

asel,s,,,1,12
aatt,1,1,1
mshk,2
amesh,all

esel,s,,,1,1710
cm,tube,elem


!!!!!
!PWR!
!!!!!

Epl=1.625e9
mp,ex,2,195e9
mp,nuxy,2,.3
```

```
mp,dens,2,7850
mp,damp,2,4.12E-5
tb,plaw,2,,,8
tbdata,1,365e6
tbdata,2,Epl
TBDATA,3,.63  ! Failure strain
TBDATA,4,70000  ! C (strain rate parameter)
TBDATA,5,3 ! P (strain rate parameter)


et,2,161
keyopt,2,5,1
r,2,,.008,.008


local,100,0,0,2.75,-.487
k,101,.167,0,0
k,102,-.167,0,0
k,103,.167,0,.487
k,104,-.167,0,.487
k,105,0,0,.487
k,107,0,0,.487+.167
larc,103,107,105,.167
larc,104,107,105,.167
l,101,103
l,102,104
lgen,2,32,35,,,.0125
lgen,2,32,35,,,-.0125
lgen,2,32,35,,,.0375
lgen,2,32,35,,,-.0375

k,50000,50000,0,0

ldiv,42,.25,7000
ldiv,38,.25,7001
ldiv,39,.25,7002
ldiv,43,.25,7003
ldiv,46,.25,7004
ldiv,47,.25,7005
ldiv,50,.25,7006
ldiv,51,.25,7007

lsel,s,,,36,49
lsel,u,,,38,39
lsel,u,,,42,43
lsel,u,,,46,47
lesize,all,0.03
```

```
r,4,,.011,.011

lsel,s,,,38,51
lsel,u,,,40,41
lsel,u,,,44,45
lsel,u,,,48,49
latt,2,4,2,,50000

lsel,s,line,,36,59
lsel,u,,,38,39
lsel,u,,,42,43
lsel,u,,,46,47
lsel,u,,,50,51
latt,2,2,2,,50000

lsel,s,,,36,59
lmesh,all

nsel,s,loc,z,0
d,all,ux,0,,,,,uy,uz,rotx,rotz

esel,s,,,1891,1992
cm,restr,elem
allsel

!!!!!!!!!
!!plate!!
!!!!!!!!!

k,110,0,.0485,.487+.167-.007
k,111,0,-.0485,.487+.167-.007
l,110,111


adrag,60,,,,,,44
adrag,60,,,,,,45

mp,ex,3,2e11
mp,nuxy,3,.3
mp,dens,3,7750
TB,BKIN,3
TBDATA,1,425e6 !(yield stress)
TBDATA,2,8.8e8 !(tangent modulus)

r,3,,5,.006
```

```
asel,s,,,13,14
aesize,all,0.01
aatt,3,3,1
amesh,all

edcnstr,add,rivet,2044,2163
edcnstr,add,rivet,1993,2157
edcnstr,add,rivet,2063,2262
edcnstr,add,rivet,1910,2256
edcnstr,add,rivet,2045,2144
edcnstr,add,rivet,1994,2138

csys,0
edcgen,assc,,,0.1,0.1

nsel,s,loc,y,0
d,all,all,0

!!!!!!!!!!!!!
!Thrust Force!
!!!!!!!!!!!!!

csys,0

nkpt,30000,3

allsel,all

nsel,s,node,,30000
cm,endnode,node

nsel,all

nsel,s,loc,z,-.2924
nsel,r,loc,y,2.5,3.5

cm,endplane,node
allsel,all
edlcs,add,10,1,0,0,0,1,0,0,0,1
edcnstr,add,nrb,endplane,,10

*dim,inpres,,6
*dim,time4,,3001
*dim,force4,,3001
*CREATE,ansuitmp
*VREAD,time4,'Time4','txt',' ',IJK,3001,1,1, ,
(1F10.4)
```

```
*END
/INPUT,ansuitmp

*CREATE,ansuitmp
*VREAD,force4,'Force4','txt',' ',IJK,3001,1,1, ,
(1F10.0)
*END
/INPUT,ansuitmp
inpres(1)=-6.76e6,-3.5e6,-5.5e6,-3.5e6,-3.5e6,-3.5e6
edload,add,fz,,endnode,time4,force4
edload,add,press,1,tube,time4,inpres,2

/solu

time,0.3
allsel,all
outpr,all

edhist,tube
EDHIST,endnode
edhist,restr
EDOPT,ADD,,BOTH
EDOUT,GLSTAT
EDOUT,MATSUM
EDOUT,SPCFORC
EDOUT,RCFORC
EDOUT,NODOUT
EDOUT,RBDOUT
edout,elout
edwrite,both

save
solve
```

Input File for Relap5 depressurization transient.

```
=JAERI TEST
*
100  new transnt
*
201  205. 1.0-7  1.0-2  07   1000   1000    1600
202 210. 1.0-7  1.0-5  07   10   10    160
203 240.0 1.0-7  3.0-4  07   10   10    160
*
*-----------------------------------
```

```
* Trip Variable
500   time   0  ge   null  0  205.   l
501   time   0 ge   null   0  1000.   l
*=========================================================
component 080
*
*       name      type
*0800000 presBC    tmdpvol
*         area    lung    vol    horz   vert   delz    rug    hyd
tlpvbfe
*0800101   1.05    1.42    0.0     0.0     0.0    0.0    0.0    0.0
0000010
*       ebt
*0800200 002
*       time   press     qual
*0800201 0.0    6.86e6     1.0
*
*=============================================================
== component 080
*
*       name     type
0800000 tank     pipe
*       n.vol
0800001  7
*       area               v.no.
0800101   .75                7
*       area               j.no.
0800201   0.0                 6
*       length             v.no.
0800301   .71                 2
0800302   0.8                  7
*       volume             v.no.
0800401   0.0                  7
*       v-ang              v.no.
0800601   -90.                 7
*       elevation          v.no.
*0800701   0.0                7
*       rough    dhy       v.no.
0800801 3e-5    0.0         7
*       fflc   rflc         j.no.
0800901   0.    0.            6
*       tlpvbfe            v.no.
0801001 0000000              7
*       jefvcahs           j.no.
0801101 0000000              6
*       ebt   pres   qual          v.no
0801201 002   6.86e6  1. 0. 0. 0.  2
```

```
0801202 003   6.86e6  556.65 0. 0. 0.  7
*        Boron Con.   v.no
*0802001   0           7
*       i.c.
0801300  1
*       flowf  flowg  velj  j.no.
0801301 0.0    0.0     0.0   6
*       dhy    flood  g.int slope   j.no.
*0801401 0.429   0.0   1.0    1.0     10
*===============================================================
== component 005
*
*       name      type
0050000 imbocco    sngljun
*       from      to        area    fflc   rflc   jefvcahs
0050101 080060004 010010001  0.0      .5    .5       0
*       ctl   flowf   flowg     int.v
0050201  1      0.0     0.0       0.
*===============================================================
== component 010
*
*       name     type
0100000 eightint     pipe
*       n.vol
0100001  5
*       area               v.no.
0100101  0.02              5
*       area               j.no.
0100201   0.0               4
*       length             v.no.
0100301  .744              5
*       volume             v.no.
0100401   0.0                5
*       v-ang              v.no.
0100601   0.0                5
*       elevation          v.no.
0100701    0                 5
*       rough    dhy       v.no.
0100801 3e-5  0.1812        5
*       fflc   rflc        j.no.
0100901  0.0    0.0          4
*       tlpvbfe            v.no.
0101001 0000000             5
*       jefvcahs           j.no.
0101101 0000000            4
*       ebt   pres   qual          v.no
0101201 003   6.86e6 556.65  0. 0. 0.    5
```

```
*        Boron Con.   v.no
*0102001  0.0           5
*       i.c.
0101300  1
*       flowf  flowg  velj  j.no.
0101301 0.0    0.0     0.0   4
*       dhy    flood  g.int slope   j.no.
*0101401 0.429   0.0   1.0    1.0     10
*===============================================================
== component 015
*
*       name      type
0150000  reduc    sngljun
*       from      to        area    fflc   rflc   jefvcahs
0150101 010050002 020010001  0.0     .2    .2      0
*       ctl   flowf   flowg     int.v
0150201  1     0.0      0.0        0.
*===============================================================
== component 020
*
*       name     type
0200000 sixint   pipe
*       n.vol
0200001  4
*       area               v.no.
0200101  .0074               4
*       area               j.no.
0200201  0.0                 3
*       length             v.no.
0200301   .5                  4
*       volume             v.no.
0200401   0.0                  4
*       v-ang              v.no.
0200601   0.0                 4
*       elevation          v.no.
0200701    0.                 4
*       rough    dhy       v.no.
0200801 3e-5   .1432         4
*       fflc   rflc         j.no.
0200901   0.0   0.0             3
*       tlpvbfe            v.no.
0201001 0000000             4
*       jefvcahs           j.no.
0201101 0000000            3
*       ebt   pres   qual          v.no
0201201 003  6.86e6   556.65 0. 0. 0.    4
*        Boron Con.   v.no
```

```
*0202001  0.0           4
*       i.c.
0201300  1
*       flowf  flowg  velj  j.no.
0201301 0.0    0.0     0.0   3
*       dhy    flood  g.int slope   j.no.
*0201401 0.429   0.0   1.0    1.0     10
*===============================================================
== component 025
*
*       name      type
0250000 firstc   sngljun
*       from      to        area    fflc   rflc   jefvcahs
0250101 020040002 030010001  0.0      .3      .3      0
*       ctl   flowf   flowg     int.v
0250201  1      0.0     0.0        0.
*===============================================================
== component 030
*
*       name     type
0300000 sixint   pipe
*       n.vol
0300001  3
*       area               v.no.
0300101   .0074               3
*       area               j.no.
0300201 0.0                2
*       length             v.no.
0300301   .338              3
*       volume             v.no.
0300401   0.0                3
*       v-ang              v.no.
0300601   -90.                  3
*       elevation          v.no.
0300701     -0.338                3
*       rough    dhy       v.no.
0300801 3e-5  .1432         3
*       fflc   rflc        j.no.
0300901   0.     0.             2
*       tlpvbfe            v.no.
0301001 0000000             3
*       jefvcahs           j.no.
0301101 0000000            2
*       ebt   pres   qual          v.no
0301201 003   6.86e6   556.65 0. 0. 0.  3
*        Boron Con.   v.no
*0302001  0.0           3
```

```
*       i.c.
0301300  1
*       flowf  flowg  velj  j.no.
0301301 0.0    0.0     0.0   2
*       dhy    flood  g.int slope   j.no.
*0301401 0.429   0.0   1.0    1.0     10
*=================================================================
== component 035
*
*       name      type
0350000 secondc    sngljun
*       from      to        area    fflc   rflc   jefvcahs
0350101 030030002 040010001   0.0    .3      .3        0
*       ctl   flowf   flowg     int.v
0350201  1     0.      0.         0.
*=================================================================
== component 040
*
*       name     type
0400000 sixint  pipe
*       n.vol
0400001  7
*       area               v.no.
0400101  .0074                 7
*       area               j.no.
0400201  0.0                   6
*       length             v.no.
0400301   .714                 7
*       volume             v.no.
0400401   0.0                  7
*       v-ang              v.no.
0400601    0.0                 7
*       elevation          v.no.
0400701    0.0                 7
*       rough    dhy       v.no.
0400801 3e-5  .1432         7
*       fflc   rflc        j.no.
0400901   0.    0.            6
*       tlpvbfe            v.no.
0401001 0000000             7
*       jefvcahs           j.no.
0401101 0000000            6
*       ebt   pres   qual          v.no
0401201 003   6.86e6   556.65 0. 0. 0.  7
*        Boron Con.   v.no
*0402001  0.0           7
*       i.c.
```

```
0401300  1
*       flowf  flowg  velj  j.no.
0401301 0.0    0.0     0.0   6
*       dhy    flood  g.int slope   j.no.
*0401401 0.429   0.0   1.0    1.0     10
*============================================================
== component 045
*
*       name      type
0450000 thirdc    sngljun
*       from      to        area    fflc   rflc   jefvcahs
0450101 040070002 050010001  0.0     .3      .3       0
*       ctl   flowf   flowg     int.v
0450201  1      0.      0.        0.
*============================================================
== component 050
*
*       name     type
0500000 sixint     pipe
*       n.vol
0500001  2
*       area               v.no.
0500101  .0074                   2
*       area               j.no.
0500201  0.0                  1
*       length             v.no.
0500301   .154                 2
*       volume             v.no.
0500401   0.0                  2
*       v-ang              v.no.
0500601   -90.                 2
*       elevation          v.no.
0500701   -.154                 2
*       rough    dhy       v.no.
0500801 3e-5  .1432         2
*       fflc   rflc        j.no.
0500901  0.    0.           1
*       tlpvbfe            v.no.
0501001 0000000             2
*       jefvcahs           j.no.
0501101 0000000             1
*       ebt   pres   qual          v.no
0501201 003   6.86e6 556.65 0. 0. 0.    2
*        Boron Con.   v.no
*0502001  0.0          2
*       i.c.
0501300  1
```

```
*       flowf  flowg  velj  j.no.
0501301 0.0    0.0     0.0   1
*       dhy    flood  g.int slope   j.no.
*0501401 0.429   0.0   1.0    1.0     10
*=============================================================
== component 055
*
*       name      type
*0550000  break     sngljun
*       from      to        area    fflc   rflc   jefvcahs
*0550101 050020002 060010001  0.0     1.      1.      0
*       ctl   flowf   flowg     int.v
*0550201  1     0.0     0.0        0.
*=================================== component 055
*
*       name    type
0550000 break    valve
*       from      to          area   fflc  rflc   jefvcahs
0550101 050020002 060010001    0.0074     1.       1.    00002100
1.0   10000.0
*       ctl flowf  flowg  int.v
0550201  1   0.0    0.0    0.0
*       type
0550300 mtrvlv
*       Ton/off
0550301 500   501   100.   0.
*
*=========================================================
component 060
*
*       name      type
0600000 atm    tmdpvol
*         area    lung    vol    horz   vert   delz    rug    hyd
tlpvbfe
0600101   1.e3      0.0   1.e6   0.0     0.0    0.0    0.0    0.0
0000010
*       ebt
0600200 002
*       time   press     qual
0600201 1.e5     1.e5      1.0
*
20500000   9999
*-------------------------------------------------
* tank level computation
*        name     type  s.fact.  init. ctl
20500800 tanklvl  sum      1.      0.   1
*         A0     A1     name  parameter
```

```
20500801  0.   .8      voidf 080030000
20500802       .8      voidf 080040000
20500803       .8      voidf 080050000
20500804       .8      voidf 080060000
20500805       .8      voidf 080070000
*-----------------------------------------------
* thrust computation
*
20511310  mflowj  sum   1.  0.  1  0
20511311  0.  0.5  mflowj 050010000  0.5  mflowj  050010000
20511312  1.   mflowj 050010000
*
20511320  length  div  1.  0.  1  0
20511321    avol  050010000
20511322     vvol  050010000
*
20511330   del_re   delay   1.  0.  1  0
20511331   cntrlvar  1131  0.001   2
*
20511340  int_di  sum   1.  0.  1  0
20511341  0.   1.   cntrlvar   1131
20511342     -1.  cntrlvar  1133
*
*******cntrlvar 1140
* wave force
*
20511400  F_wav  mult   -1000.  0.  1   0
20511401       cntrlvar   1134
20511402       cntrlvar   1132
*
*
20519910  thr-ra  mult  0.0074  0.  1  0
20519911     voidgj   055000000
20519912     rhogj    055000000
*
20519920  thr-r1  mult  0.0074   0.  1  0
20519921      voidfj   055000000
20519922      rhofj    055000000
*
20519930  thr-r2   sum  1.  0.  1  0
20519931  0.   1.   cntrlvar  1991
20519932       1.   cntrlvar  1992
*
20519940  thr-r2  mult   0.0074   0.  1  0
20519941     cntrlvar  1993
*
20519950  pref-1   mult  1.  0.  1 0
```

```
20519951     mflowj  055000000
20519952     mflowj  055000000
*
20519960  pref-2   div  1.  0.  1 0
20519961      cntrlvar  1994
20519962      cntrlvar  1995
*
20519970   thrust-1  sum   1.  0.  1  0
20519971   0.  1.   p  050020000
20519972      -1.   p  060010000
20519973       1.  cntrlvar  1996
*
20519980   forF-1  mult   0.0074  0.  1  0
20519981          cntrlvar    1997
*
20520000   F-out   mult  -1.   0.  1  0
20520001         cntrlvar   1998
*
*
20530000   Ftot  sum  1.  0.  1  0
20530001  0.  1.  cntrlvar   1140
20530002      1.  cntrlvar   1998
*
20540000  Fout  tripunit  1.  0.  1  0
20540001   -500
*
20540010  const constant  0.
*
20540020  per   mult  1.  0.  1  0
20540021   cntrlvar  4000  cntrlvar  4001
*
20540030   Fout  tripunit  1.  0.  1  0
20540031   500
*
20540040   per1  mult  1.  0.  1  0
20540041   cntrlvar  4003  cntrlvar  3000
*
20540050   final  sum  1.  0.  1  0
20540051   0.   1.   cntrlvar  4004
20540052      1.   cntrlvar   4002
.
```

REFERENCES

1. STANDARD REVIEW PLAN. BTP 3-3. Protection against postulated piping failures in fluid systems outside containment.

2. ANSI/ANS 58.2-1988. Design basis for protection of light water nuclear power plants against the effects of postulated pipe rupture.

3. STANDARD REVIEW PLAN. BTP 3-4. Postulated rupture locations in fluid system piping inside and outside containment.

4. ABWR Design Control Document/Tier 2, Sec. 3.6. Protection Against Dynamic Effects Associated with the Postulated Rupture of Piping.

5. Westinghouse AP 1000 Design Control Document Rev. 19 –Tier 2 Chapter 3 – Design of Structures, Components, Equip. & Systems – Section 3.6 Protection Against the Dynamic Effects Associated with the Postula.

6. IAEA-TECDOC-710; Applicbility of the leak before break concept.

7. Igli Micheli, Piero Zanaboni, An Analytical Validation of Simplified Methods for the Assessment of Pipe Whip Characteristics.

8. Nuclear Engineering and design, Experimental and analytical studies of pipe whip tests under PWR LOCA conditions, R. Kurihara, S. Ueda and S. Miyazono.

9. Nuclear Engineering and design, On finite elements analysis of pipe whip problems, S.M. Ma and K.J. Bathe.

10. Nuclear Engineering and design, Pipe whip analysis for nuclear reactor applications, N.Bisconti, L. Lazzeri and P.P. Strona.

11. Todreas Kazimi Nuclear Systems V.1, 11.7.3.2 Thermal Nonequilibrium Models.

12. Caruso Gianfranco. Esercitazioni di Impianti Nucleari.

13. ASME Boiler and Pressure Vessel Code (BPVC).

14. GDC 4 of 10 CFR 50 Appendix A.

15. ASTM A20. Standard Specification for General Requirements for Steel Plates for Pressure Vessel.

16. F. Cioli, G. Forasassi, B. Guerrini, F. Veroni. Experimental Analysis of Dynamic Behaviour of Pipe Restraints Under Pipe Whip Accident Conditions.

17. JAERI-M-83-020. Pipe rupture test results; 6 in. pipe whip test under BWR LOCA conditions.

18. US NRC Regulatory Guide 1.61. Damping Values for Seismic Design of Nuclear Power Plants.

19. Ezio Cadoni, Luigi Fenu, Daniele Forni. Strain rate behaviour in tension of austenitic stainless steel used for reinforcing bar.

20. Mechanical APDL Reference Guide.

21. JAERI –M-82-022. Pipe rupture test results; 4 in. pipe whip test under BWR LOCA conditions.

22. Nuclear Engineering and Design; Test results of jet discharge from a 4 inch pipe under BWR LOCA conditions, T. Isozaki, T. Yano, N. Miyazaki, R. Kurihara, S. Ueda and S. Miyazono.